UNIVERSITÀ DI PISA

PhD School of Engineering "Leonardo da Vinci"

PHD COURSE IN APPLIED ELECTROMAGNETISM IN ELECTRICAL AND BIOMEDICAL ENGINEERING, ELECTRONICS, SMART SENSORS, NANO-TECHNOLOGIES

PhD Thesis

Development and Experimentation of Magnetostrictive Sensors for Inspection and Monitoring of Piping Systems

Author:

Florin Octavian Turcu

Supervisor:

Prof. Marco Raugi

2008

ACKNOWLEDGEMENTS

I wish to express my gratitude to my supervisor, Prof. Marco Raugi for offering me his support to pursue this research activity towards my PhD and for assisting me in the elaboration of this thesis.

I would like also to address my special thanks to Dr. Francesco Bertoncini for constantly helping and encouraging me throughout my 3 years of work as a PhD student.

Last but not least, I want to thank my brother, Gabriel for offering me his moral support and encouraging me to carry on my studies abroad.

ABSTRACT

Nondestructive Evaluation – NDE, is an important aspect of the integrity management of industrial plants, where pipe systems are the dominant component. During the last decade Ultrasonic Guided Waves (UGW), have started to be used as a useful instrument for on-stream long range inspection of pipes. Various procedures and systems have been proposed for the generation and detection of UGW. Presently, they are based on piezoelectric (PZT) or magnetostrictive (MT) transducers or electromagnetic acoustic transducers (EMAT).

It is generally known that PZT based systems have elevated diagnostic capacities due to their high transduction efficiency. However, the elevated costs of installation of such devices make their use for long-term monitoring of piping systems quite improbable.

On the other hand, the MT based systems have the advantage of the reduced costs of the composing materials, simplicity of attaching it to the pipe wall and flexibility regarding the diameters of the pipes that can be inspected. Still, its single-element configuration limits the capacity to characterize the detected discontinuities in terms of geometry, thus being unable to distinguish between possible flaws from symmetrical features, normally located on pipes, like welds or flanges. Furthermore, its reduced capability to geometrically characterize flaws makes the classification of their severity particularly difficult.

The improvement of the diagnostic capacity of MT based systems in order to make practically possible and economically convenient its use in monitoring applications is the main purpose of this thesis.

In this dissertation multiple laboratory and field experiments are described and the magnetostrictive technology is evaluated. Furthermore, a new magnetostrictive transducer for UGW acquisition is presented. It allows step-by-step data acquisition around the pipe circumference revealing important information on the geometry and circumferential position of flaws.

The new sensor was validated by computer simulations as well as further laboratory and field tests. The resulting data was used as input for various digital signal processing techniques to describe geometrically the features detected in the acquired signal.

The final results outline the potential of MT based long-range inspection to reach also a good sensitivity and a good defect sizing and classification with respect to conventional techniques, making it an important candidate for monitoring activities for the integrity management of industrial plants.

TABLE OF CONTENTS

ACKNOWLEDGEMENTS ..... **III**

ABSTRACT ..... **V**

TABLE OF CONTENTS ..... **VII**

ACRONYMS ..... **XI**

CHAPTER 1 INTRODUCTION **1**

1.1 Application field and objectives 1

1.2 Thesis layout and organization 1

CHAPTER 2 CHALLENGES IN NONDESTRUCTIVE EVALUATION OF PIPE SYSTEMS **3**

2.1 On-stream inspection 6

2.1.1 On-stream inspection challenges in industrial plant and distribution *7*

2.1.2 On-stream inspection challenges in transmission lines *7*

2.2 Monitoring 9

2.3 Defect identification and classification 10

CHAPTER 3 LONG RANGE UGW TECHNIQUES FOR PIPE INSPECTION – THE STATE OF THE ART **13**

3.1 Ultrasonic Guided Waves – U.G.W. 13

3.2 UGW Inspection Systems 22

3.2.1 Piezoelectric transducers *25*

3.2.2 Magnetostrictive transducers *27*

3.3 Benefits and limitations 28

3.3.1 Advantages of UGW inspection *28*

3.3.2 Limitations 30

CHAPTER 4 GUIDED WAVES AND MAGNETOSTRICTIVE SENSORS 35

4.1 Magnetostriction 35

4.2 Magnetostrictive Strip sensor – MsS® 37

4.2.1 Hardware 39

4.2.2 Signal processing features 41

CHAPTER 5 EXPERIMENTATION WITH U.G.W. USING AN MSS TYPE TRANSDUCER . 45

5.1 Laboratory and field tests 45

5.1.1 Artificial defects 45

5.1.2 Sensitivity analysis 48

5.1.3 Inspection Range 52

5.1.4 Monitoring potential 59

5.2 Conclusions 63

5.2.1 Advantages of the MsS® guided-wave technology 63

5.2.2 Limitations 64

CHAPTER 6 NUMERICAL SIMULATIONS OF UGW AND DEVELOPMENT OF SIGNAL PROCESSING ALGORITHMS 67

6.1 Simulations 67

6.1.1 Validation of the simulation software 67

6.1.2 Test settings 69

6.1.3 Results 73

6.1.4 Conclusions 75

6.2 Signal processing algorithms for the UGW signal averaged over the circumference in the same pipe-wall cross-section 75

6.2.1 Time domain analysis: axial extent estimation 75

6.2.2 Fourier domain analysis 77

6.2.3 Wavelet analysis 79

6.2.4 Conclusions 79

6.3 Signal processing algorithms for sets of local UGW signals corresponding to the same pipe-wall cross-section..... 80

6.3.1 Simulations 80

6.3.2 Neural network approach for defect characterisation 81

6.3.3 Phase diagram and Magnitude profile..... 83

6.3.4 Asymmetry coefficient..... 90

6.3.5 Conclusions 91

CHAPTER 7 DEVELOPMENT OF NEW MAGNETOSTRICTIVE SENSORS FOR UGW ACQUISITION 93

7.1 Background..... 93

7.2 Guided Ultrasonics Local Acquisition System 95

7.3 Development of dedicated software for signal acquisition and processing..... 98

7.3.1 Representation of results..... 99

7.3.2 Denoising..... 100

7.3.3 Discrimination between symmetrical and asymmetrical features..... 102

7.4 Graphical user interface..... 106

7.5 Inspection procedure 107

7.6 Field Test 109

7.7 Conclusions 111

CHAPTER 8 FURTHER DEVELOPMENTS 113

8.1 Pipeline monitoring applications 113

8.2 Extreme temperature applications..... 114

REFERENCES..... 115

ACRONYMS

CBM	Condition-Based Maintenance
CUI	Corrosion Under Insulation
EC	Eddy Current
ECNDT	European Conference on NDT
EMAT	Electro-Magnetic Acoustic Transducer
ILI	In-Line Inspection
IMP	Integrity Management Plan or Program
LRGW	Long Range Guided-Wave
LRUT	Long-Range Ultrasonic Testing
MFL	Magnetic Flux Leakeage
MPI	Magnetic Particle Inspection
MsS	Magnetostrictive strip Sensor
MT	Magnetostrictive Transducer
NDE	Non-Destructive Evaluation
NDT	Non-Destructive Testing
OD	Outer Diameter
PIG	Pipeline Inspection Gauges
PoD	Probability of Detection
PZT	Piezoelectric Transducer
RCM	Reliability Centred Maintenance
SCC	Stress Corrosion Cracking
SHM	Structural Health Monitoring
SWRI	South-West Research Institute
UGW	Ultrasonic Guided Waves
UT	Ultrasonic Testing

CHAPTER 1 INTRODUCTION

1.1 Application field and objectives

In recent years, Ultrasonic Guided Waves – UGW, have gained an increasingly importance in the field of non-destructive evaluation of pipe systems – NDE, as a part of the integrity management plans for the industrial plants.

Design of new components to improve the sensitivity of instruments able to generate and detect UGW and to render UGW a method that is applicable and economically convenient for pipe monitoring is the main objective of this thesis.

More detailed, the goals of this work can be divided as it follows:

- *theoretical study of ultrasonic guided waves* and their applications to NDE of pipe systems. The study was based on literature and computer simulations.
- *experimental evaluation of the guided wave technology*, using magnetostrictive sensors for their generation and detection.
- design and development of a new magnetostrictive sensor for UGW detection
- development of signal processing methods for flaw detection and classification.

1.2 Thesis layout and organization

After a short description of the main issues concerning the field of non-destructive evaluation of pipe systems, namely the on-stream techniques, the attention is focused on the experiments conducted on UGW generated by a magnetostrictive system. The thesis concludes with the description of an innovative system for the acquisition and interpretation of UGW echoes generated by flaws.

The thesis comprises 7 chapters.

Chapter 2 makes a short description of the main challenges that characterize the NDE of pipe systems: on-stream inspection, condition monitoring, identification and classification of flaws.

Chapter 3 discusses the long-range techniques and instrumentation for on-stream inspection of pipes: pipeline inspection gauges – P.I.G. and the ultrasonic guided waves and the available systems for their generation and detection.

Chapter 4 focuses on the magnetostrictive sensors as instruments based on UGW for the NDE of pipe systems. Particularly, the Magnetostrictive Strip – MsS® sensor is described together with its signal processing features.

Chapter 5 deals with experiments conducted on dismounted pipes in laboratory as well as field tests on various types of pipes found in different conditions: water and gas pipes, buried or suspended, coated or uncoated, at high or low temperature. The goal of these tests was to evaluate the sensitivity of this technique as well as the inspection range for multiple test conditions.

Chapter 6 presents the results of the research activity finalized with the development of an innovative guided wave local acquisition system. This section begins with the description of the research background in this field and continues with the new sensor and its particularities concerning the hardware, signal processing and inspection procedure. In addition, a procedure for defect identification and characterization is explained. Simulated results are backed by experimental tests conducted on real pipelines with artificial defects.

Chapter 7 discusses possible improvements to the technology.

CHAPTER 2 CHALLENGES IN NONDESTRUCTIVE EVALUATION OF PIPE SYSTEMS

Pipes are important components of petrochemical, nuclear and electrical power generation industrial plants and for the distribution of water and gas [1]. Moreover [2] a vast network of pipelines transports large volumes of energy products as oil and gas over long distances from production wells to processing and consumption sites.

Therefore, inspection to check the corrosion and the presence of flaws in the pipes is an essential aspect for the safety and continuity of operation of industrial plants and in the distribution of energy.

The wide variety of flaws implies different inspection techniques to be used. Typical pipeline flaws and anomalies are listed in Table 2-1 and partially shown in [3], [4].

Table 2-1 Typical pipeline anomalies

Category	Typical examples	Description
Geometric anomalies	Dent, Bukles, Ovality etc.	Dents are depressions in the pipe surface, and buckles are a partial collapse of the pipe due to excessive bending or compression
Metallurgic anomalies	hard spots, laminations, slivers, scabs, inclusions, and various other imperfections and defects	Hard spots are local regions that have a considerably higher hardness than the bulk hardness of a pipe. Hard spots result from uneven cooling or quenching during the manufacture of the steel plate or skelp; cracks, which can lead to failure, can form in hard spots when atomic hydrogen is present. Laminations are internal metal separations that are generally parallel to the surface of a

		pipe. Slivers and scabs are pieces of metal that have been rolled into the surface; scabs are usually due to casting defects while slivers are introduced during rolling. Inclusions are foreign or non-metallic particles that are trapped during steel solidification.
Metal Loss	General corrosion, localized corrosion, pittings, gauging, narrow axially corrosion	Corrosion is wastage or thinning of the pipe wall due to a chemical or electrochemical attack. Common forms of corrosion include external, internal, pitting (internal or external), selective seam corrosion, and stress corrosion cracking. Gouging is the mechanical removal of metal from a local area on the surface of a pipe.
Cracks	Fatigue cracks, laminations, weld cracks, SCC, HIC, Hook Crack	Cracks are not common in pipelines, but when they occur, they are due to fatigue, stress corrosion, and weld defects.

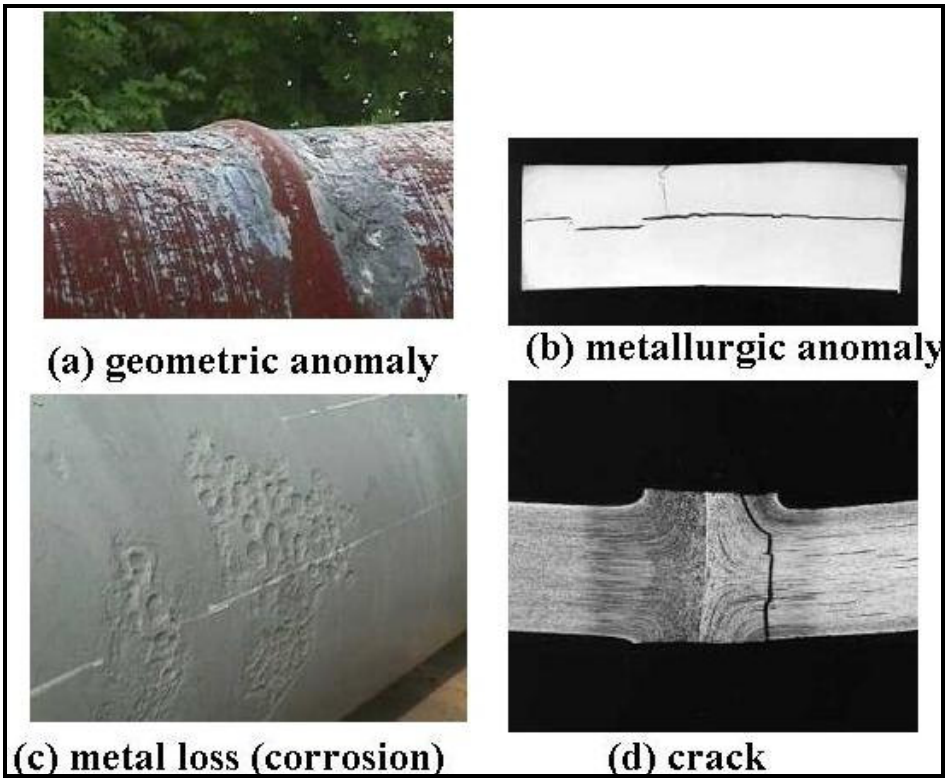

Figure 2-1 Imperfections and defects that are commonly found in gas-transmission pipelines

The inspection is usually carried out by means of non-destructive testing –NDT whose role becomes more and more important for pipeline condition assessment and to optimise maintenance management and safety. The large number of journals and international conferences dedicated to this subject testifies the importance of these techniques in engineering applications. Many NDT methods and techniques are available, each having particular advantages and disadvantages, the proper one having to be chosen on the basis of the particular pipe operating condition. The most popular and experienced techniques use sensors that are able to assess the integrity of a pipe only in a small area close to the sensor. The inspection of a long pipe can be very time consuming or dangerous since the pipe needs to be fully accessible to the operator carrying the sensor. Otherwise, the insertion of a PIG (Pipeline Inspection Gauge) has to be possible. This devices, themselves, or carrying intelligent sensors – smart PIG, travel inside the pipe and store the measured data. Recently, great interest has been manifested for the possibility of adopting a technique based on low frequency

UGW that allows the inspection of pipelines over long distances from the point of application of the sensor.

Whatever the technology used, the challenges in NDT inspection of pipeline systems can be summarized as:

- *on-stream inspection*: to be economically convenient inspection should be carried during the normal service of the plant.
- *monitoring*: by periodically examining the structure using installed probes and comparing the test data, changes in the structural condition with time can be tracked cost effectively for assessing its safety and determining an appropriate course of action for operation and maintenance/inspection.
- *defect characterization*: while data acquisition from NDT inspection is not in general a complex task, the analysis and defect size reconstruction require more sophisticated methods that quickly convert characteristic signal feature into measures for flaw depth, length and width. Up till now a full 3D reconstruction of the flaw geometry is rarely possible.

These challenges are discussed in the following sections.

2.1 On-stream inspection

Pressure vessels and piping are used widely in various industries, including electric power, refining, chemical and petrochemical, and transmission pipelines [5]. Corrosion and defects in pipelines are a major problem: their failures not only cause disruption of operation and associated revenue loss, but also safety hazards. If the failure is catastrophic, it could result in enormous property damage and loss of life. Maintaining their structural integrity and safety is therefore very important to the operators of these structures as well as to the public. Moreover, the inspection to check for the corrosion and the presence of defects in pipes is an essential aspect for the safety and continuity of operation of industrial plants.

To be economically convenient these inspection operations should be carried out during the normal service of the plant – *on-stream* inspection.

Several challenges characterize on-stream inspection in industrial plants and in transmission lines.

2.1.1 On-stream inspection challenges in industrial plant and distribution

Since a significant portion of industrial pipelines are insulated, this means that even external corrosion cannot readily be detected without the removal of the insulation, which in most cases is prohibitively expensive. Furthermore, a technique capable to perform in-service inspection would be as useful for continuous cycle plants as for the petro-chemical ones [6]. Moreover, the problem is severe also for water and gas distribution systems because in that case the pipelines are disposed under ground and often across the roads in urban environments. In the last case, the excavation for visual or conventional ultrasonic inspection can be very expensive and severely affects the traffic. There is therefore an urgent need for the development of a quick, reliable method for the detection of corrosion and defects of not accessible pipes. Testing of large structures using conventional techniques is slow because the test region is limited to the area immediately surrounding the transducer. Therefore, scanning is required if the whole structure is to be tested.

Ultrasonic guided waves potentially provide an attractive solution to this problem because they can be excited at one location on the structure and will propagate for several meters. The returning echoes will point out the presence of corrosion or other discontinuities.

2.1.2 On-stream inspection challenges in transmission lines

A pipeline network of over four million kilometres spans the world and is growing every year, being used for the transportation of oil, oil products and natural gas [7]. It is of greatest importance to ensure the safety, efficiency, environmental integrity and regulatory compliance of the worldwide pipeline infrastructure. Achieving this objective entails the need for effective inspection technologies, incorporating the accuracy and reliability required for optimized maintenance strategies. Figure 2-2 shows key requirements regarding the operator's needs and operational issues.

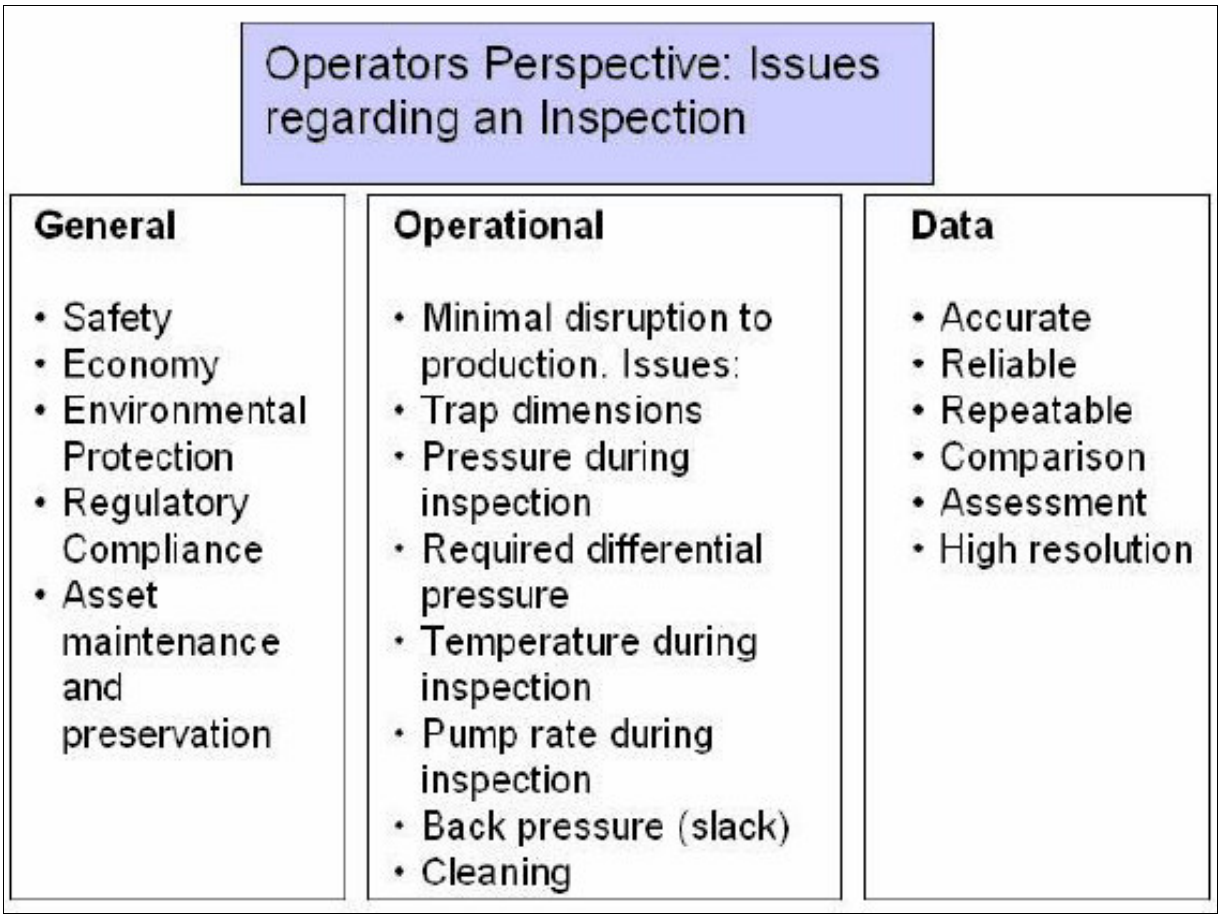

Figure 2-2 Issues regarding inspection

In-line inspection (ILI) equipment [2] is commonly used to examine a large portion of the long distance transmission pipeline system that transports energy products from well gathering points to local distribution companies. A piece of equipment that is inserted into a pipeline and driven by product flow is called a PIG. Pigs that are equipped with sensors and data recording devises are called "*smart pigs*". Pipelines that cannot be inspected using intelligent pigs are deemed *unpiggable*. But many factors affect the passage of a pig through a pipeline, or the *piggability*. The concept of piggability of a pipeline extends well beyond the basic need for a long round hole with a means to enter and exit. An accurate assessment of piggability includes consideration of pipeline length, attributes, pressure, flow rate, deformation, cleanliness, and other factors as well as the availability of inspection technology. All factors must be considered when assessing the appropriateness of in-line inspection to assess specific pipeline threats.

Moreover advanced in-line inspection tools are required. For instance until recently [7] the inspection of a pipeline regarding metal loss and cracks not only constituted the need for two separate inspection runs but also the use of two separate tools.

A new generation of electronics and an entirely new design of sensor-carrier have been developed to enable metal loss- and crack inspection surveys to be performed with a single tool in a single run.

Inspection tool developers are challenged to implement sensitive measurement technology on a platform that must survive the pipeline environment.

2.2 Monitoring

An effective way to maintain structural integrity and safety of any primary load-bearing component is to monitor its health condition periodically at relatively short intervals to track and assess structural degradation with time and, before it fails, to implement appropriate maintenance measures to prevent potential failure [5]. In order for the structural health monitoring (SHM) and condition-based maintenance (CBM) to be applicable in practice, its implementation cost must be reasonable. Therefore, to make SHM viable for large structures such as pipelines and pressure vessels, means are necessary that can provide comprehensive structural condition information quickly, cost-effectively, and on-stream, allow structural integrity to be assessed and an appropriate course of action for operation and maintenance/inspection to be determined.

An emerging technology that can quickly survey a large area of a structure for defects and provide comprehensive condition information is the long-range ultrasonic guided-wave technology. By using relatively low-frequency (typically in the range of kHz) guided-waves in the pulse-echo testing mode, this technology performs 100-percent volumetric examination of a large area of a pipe and detects and locates both internal and external defects in the sections around the test position. In aboveground pipes, for example, the test range for detecting 2- to 3-percent defects is typically more than 30 m [8] in one direction from the test position (here, percent refers to the circumferential cross-sectional area of defect

relative to the total pipe-wall cross-section). This technology is now widely used for testing piping networks in processing plants such as refineries and chemical plants.

2.3 Defect identification and classification

Advanced data processing systems are required to extract the proper information from acquired signals during inspection. In particular it is fundamental to develop identification methods that are able to:

Detect and localize defects along the inspected pipeline;

Identify and size the defect.

The first task needs to discriminate echoes generated by defects from noise or echoes generated by joints, welds, elbow branches and other geometric features found along the pipe.

The second task requires the geometrical reconstruction of the flaw. Since this operation is inverse compared to traditional mechanical design tasks, the problem is called an inverse problem. Several methods are known in NDT evaluation. Their application to specific techniques and data is still an area of active research and everyday performance improvement.

The inverse problem solving methods can be subdivided [9] in two categories. There are *heuristic methods* that neglect the underlying physical phenomenon and *physical models* that use physical theory for the solution.

The heuristic methods can be further divided in two groups: the first group is based on calibration methods that map the signal using signal processing methods and use an analytical regression method. The second group uses more advanced methods of regression like neural networks.

For the physical models it is possible to distinguish between direct inversion methods and iterative approaches that use a forward solution.

The following table provides an overview of inversion methods.

Table 2-2- Overview of inversion methods

Calibration This is the most widely used method and at the same time is the simplest one. Artificial defects are placed onto a pipe. The set of defects should comprehend all the shapes that are expected, i.e. deeper and shallower ones as well as internal and external defects. They need to have a well defined size such that an actual length, width and depth can be determined. Areas of general corrosion are thus not suitable for the calibration. The signals are recorded and calibration curves of signal versus defect size are set up. The benefit of this method is, that a full scale system test is performed at the same time. Often these tests are repeated regularly to check the performance of the tool. Neural Networks The problem of mapping the signal onto the actual defect size is a regression problem. We have some bins given by the artificial defects and need to find the defects geometries for all other defects with a somehow similar but different signal. Since the mapping is given by an a-priori unknown function and any closed form equations are usually falling short of the underlying complexity of the problem, other means of regression are considered. Among those ones the use of neural networks for regression has been proposed. Different types of neural networks can be considered. In the learning process that network is set up by minimizing the difference between the output of the artificial defects and their corresponding actual size. For the prediction the signal of an unknown defect is fed into the network and the output delivers an estimated defect size. Direct Inversion The signal received from the measurement is considered to be a convolution of the actual defect shape and a transfer function. The nature of the transfer function is unknown. However, the results from direct measurement can be used to determine a possible transfer function. Naturally the lack of uniqueness typical for inverse problems does not fully determine the actual transfer function. However, the

determination of the defect shape and some heuristic assumption on the defect would reduce the size determination to a de-convolution problem.

Iterative Inversion

The defect can be modelled to calculate the signal based on the actual geometry. For instance, with reference to magnetic flux leakage –MFL inspection, the faces of the defect are modelled with magnetic dipoles of various size and dipole moment to describe the magnetic charge density. The stray field can be calculated on the dipole field distribution. One of the most popular forward methods is finite element modelling. A certain starting geometry is assumed. The forward method is used to calculate the expected MFL-signal. The geometry is then iteratively adapted to generate a field distribution that best fits to the actually measured signal.

CHAPTER 3 LONG RANGE UGW TECHNIQUES FOR PIPE INSPECTION – THE STATE OF THE ART

NDE techniques can be classified as detail or local techniques and long-range inspection techniques.

The detailed inspection techniques can be summarized as it follows:

- Ultrasonic Testing (UT) using piezoelectric transducers (PZT) or electromagnetic acoustic transducers (EMAT);
- Magnetic Flux Leakage (MFL)
- Eddy Current (EC)
- Radiography Testing (RT)

Sensors used for detailed inspection are often integrated on special devices that travel inside the in-service pipelines (the so-called In-Line Inspection-ILI) [2] to provide long-range inspection.

There are several particular cases when ILI cannot be performed. In these cases, the inspection can be accomplished by using Ultrasonic Guided Waves.

In the further sections of this chapter, the long-range techniques will be discussed.

3.1 Ultrasonic Guided Waves – U.G.W.

The ultrasonic guided waves (UGW) are structure-borne elastic waves that propagate along the length of a structure, guided by and confined in its geometric boundaries. UGW exist in many different types and modes, depending on particle displacement : longitudinal (L) , torsional (T), flexural (F), Lamb waves, shear-horizontal (SH) , surface waves, etc. Their properties (velocity, displacement pattern) vary significantly with the geometric shape and size of the structure and wave frequency; in contrast, bulk waves used in conventional UT depend only on the structure's material.

The wave types and modes differ by wave's particle displacements, considering the three orthogonal directions: axial (along the length of the pipe), radial (along the pipe radius) and circumferential (along the pipe circumference) as shown in Figure 3-1. The various types and modes of UGW are briefly described below [12], [13].

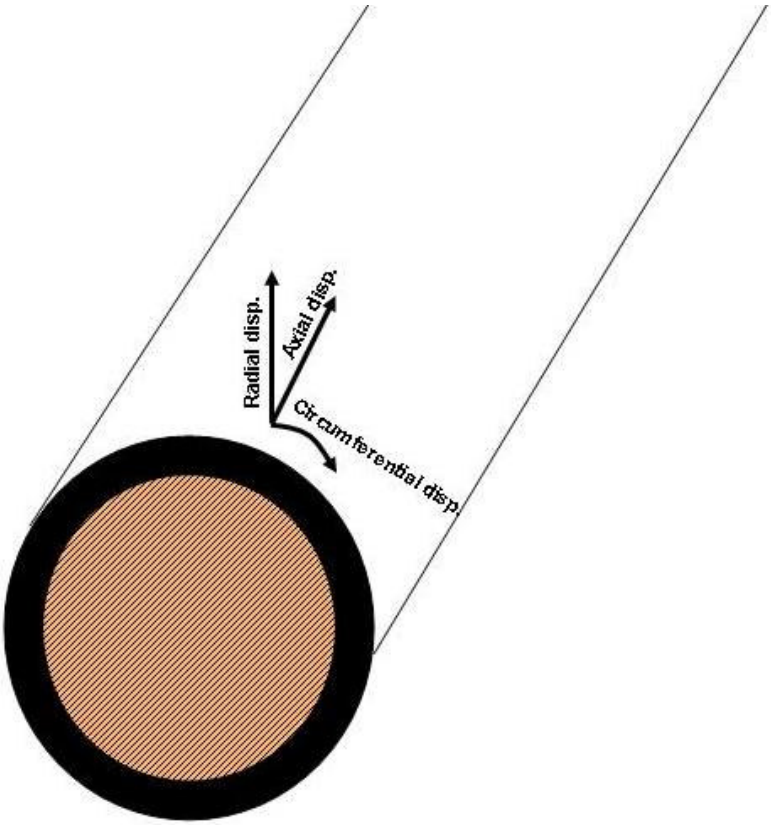

Figure 3-1 Possible displacements in a pipe

- SH (share-horizontal) waves are waves that propagate in plates; the direction of propagation is perpendicular to the direction of particle displacements.
- The longitudinal waves are waves whose displacements have the direction parallel to or along the direction of propagation.
- Torsional waves are share waves that propagate in pipes.
- Rayleigh waves are surface waves where particle displacements describe a circle or ellipse in the direction of propagation

- Lamb waves are waves whose particle motion lies in the plane defined by the plate normal and the direction of wave propagation
- The T-modes correspond to shear waves that propagate in the axial direction, while their displacements are in the circumferential direction and constant around the circumference of the pipe.
- In L-mode propagation in pipes, displacements can take places in both axial direction and the radial direction (along the radius of the pipe).
- The F-modes correspond to waves whose displacements vary around the circumference of the pipe. The F-modes have displacements in all three orthogonal directions—axial, radial, and circumferential.

Figure 3-2 shows simulated longitudinal, flexural and torsional wave modes respectively in A and B, C and D. In this case, the wave guide is a pipe with defect. A and B present displacements as deformation, while C and D contain a vectorial representation of the propagating torsional wave, transmitted as well as reflected by the defect.

The frequency range of these waves typically covers the lower segment of the ultrasonic frequencies (between a few kHz and 200 kHz) and can propagate over long distances (tens of meters) in any bounded structural parts, including rods, pipes, and plates [14].

Basic principles

In a linear, homogeneous and isotropic medium, in absence of body forces, the displacement field $\mathbf{u}(\mathbf{r},t)$ has to satisfy [15]:

$$\mu\nabla^2\mathbf{u} + (\lambda+\mu)\nabla\nabla\cdot\mathbf{u} = \rho\,\ddot{\mathbf{u}} \qquad (3\text{-}1)$$

being μ and λ Lamè's elasticity constants of the medium, while ρ is the density. This is the wave equation that describes the propagation of elastic waves in the considered body.

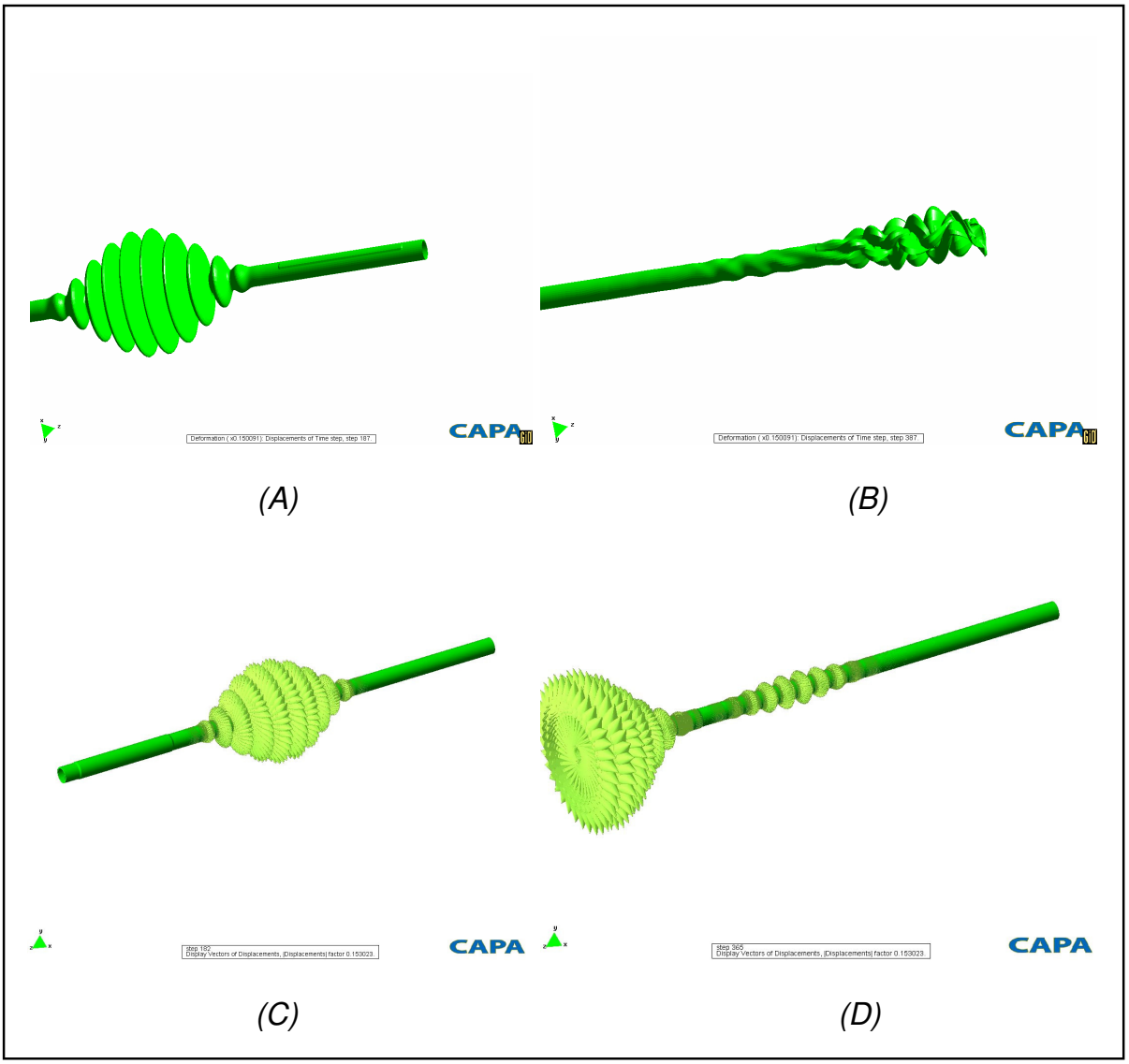

Figure 3-2 Propagation of UGW in pipes – A. L-mode (deformation); B.F-mode (deformation); C. T-mode transmitted wave (vectors); C. T-mode reflected and transmitted wave (vectors)

For as far as they are concerned, the cylindrical waves propagating in an unbounded medium are characterized by:

- Direction of radial propagation $\mathbf{i}_r$;
- Velocity of propagation c;
- Angular speed ω and frequency *f*: $\omega = 2\pi / f$;

- Wave number k and wave length λ: $k = 2\pi/\lambda$.

Considering the axial symmetry we have that:

$$\mathbf{u} = \mathbf{u}(r,t) = A(r)\cos(\omega t - kr)\mathbf{i}_u \qquad (3\text{-}2)$$

can solve the wave equation.

In the case of a cylindrical rod, the elastic waves propagate along the axial direction $\mathbf{i}_z$. Considering the free-surface boundary conditions and no traction:

$$\tau_{rr} = 0,\ \tau_{r\theta} = 0,\ \tau_{rz} = 0 \qquad (3\text{-}3)$$

the wave equation has the following solutions:

- **Torsional (T) waves**: $\mathbf{u} = u_\theta(r,z,t)\mathbf{i}_\theta$
- **Longitudinal (L) waves**: $\mathbf{u} = u_r(r,z,t)\mathbf{i}_r + u_z(r,z,t)\mathbf{i}_z$
- **Flexural (F) waves**: $\mathbf{u} = u_r(r,\theta,z,t)\mathbf{i}_r + u_\theta(r,\theta,z,t)\mathbf{i}_\theta + u_z(r,\theta,z,t)\mathbf{i}_z$

In the case of the hollow cylinder shown in Figure 3-3 the free-surface boundary conditions with no traction from (3-3) are imposed at the two surfaces in $r = a,\ r = b$ in order to find the possible motions in the wave guide. These motions (longitudinal or transversal) can be:

- independent of z;
- independent of θ.

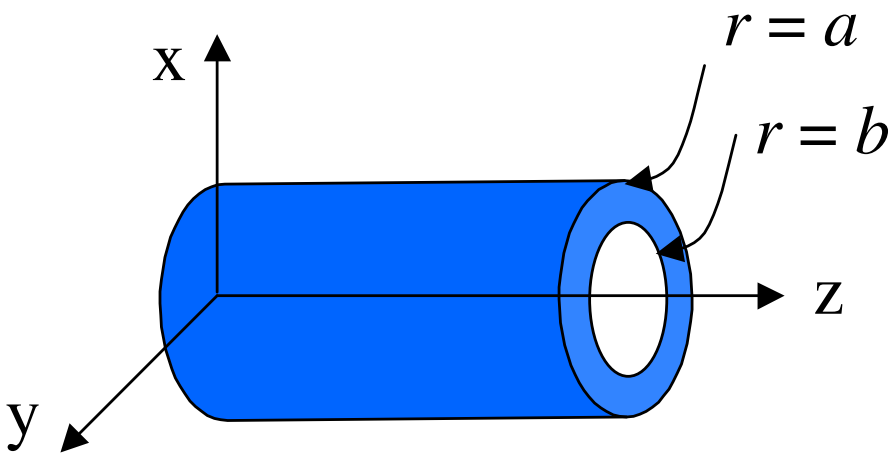

Figure 3-3 Parameters of a hollow cylinder

The velocity of propagation in an infinite medium of longitudinal (c_L) and transversal (torsional) (c_L) waves is given, respectively by:

$$c_L = \sqrt{\frac{\lambda + 2\mu}{\rho}} \qquad (3\text{-}4)$$

$$c_T = \sqrt{\frac{\mu}{\rho}} \qquad (3\text{-}5)$$

In this case, solutions u that satisfy equation (3-1) can be found by using Lamè potentials φ and H defined by[16]:

$$u = \nabla\varphi + \nabla x H \qquad (3\text{-}6)$$

with $\nabla \cdot H = f(r,t)$ *(3-7)*

In equation (3-7), f is a function of the coordinate vector r and the time. The displacement equations of motion (3-1) are satisfied if the potentials φ and H satisfy the wave equations:

$$c_L \nabla^2 \varphi = \ddot{\varphi}$$
$$c_T \nabla^2 H = \ddot{H} \qquad (3\text{-}8)$$

Considering the cylindrical coordinates r, θ, and z, the wave equations in (3-8), in the case of a hollow cylinder, can be written as functions of potentials f and g in the following form [16]:

$$\begin{aligned} \varphi &= f(r)\cos n\theta \cos(\omega t + \xi z) \\ H_r &= g_r(r)\sin n\theta \sin(\omega t + \xi z) \\ H_\theta &= g_\theta(r)\cos n\theta \sin(\omega t + \xi z) \\ H_z &= g_3(r)\sin n\theta \sin(\omega t + \xi z) \end{aligned} \qquad (3\text{-}9)$$

where n denotes the order of dependence of θ.

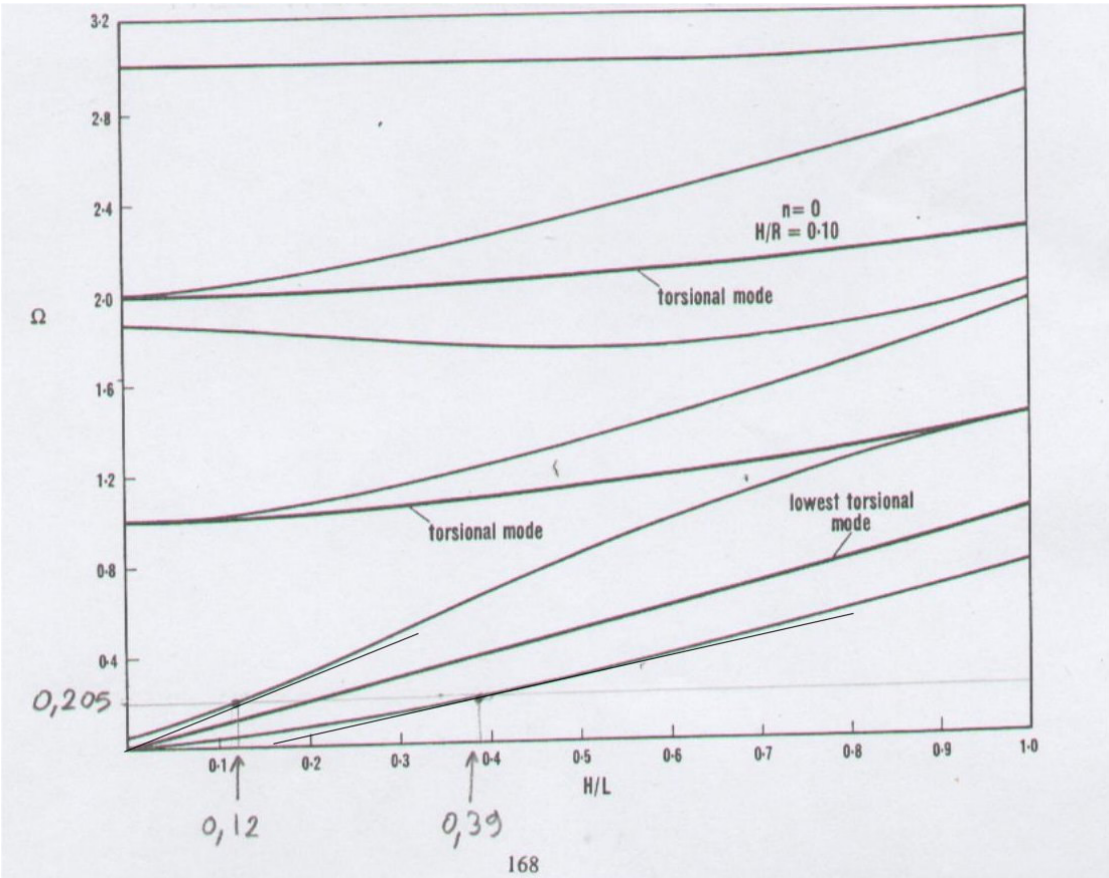

Figure 3-4 Frequency spectrum (L is the wave length) for a hollow with H/r=0.1 and n=0 (from [16] pp. 168)

Various modes of each kind (torsional, flexural etc) may exist, depending on the relation between frequency and wave length. Figure 3-4 shows the frequency spectrum for different torsional modes in a thin shell hollow cylinder approximation.

UGW modes are often identified by their type, circumferential order and consecutive order [35] as T(n, m), L(n, m), F(n, m) meaning torsional, longitudinal and flexural waves respectively. In this formulation n stands for the harmonic number of circumferential variation of amplitude, and m for the wave order, being a counter variable. For instance, with reference to Figure 3-4, the lowest torsional mode, in the case n=0 is identified as T (0, 1), the second torsional mode as T (0, 2) etc.

Figure 3-5 shows the dispersion curves of various guided waves in a 4.5-inch-OD, 0.337-inch-wall-thickness pipe [17]. In this case, the group velocities of the L-, F-, and T-modes change with frequency, except for the T(0,1) mode and L(0,2) mode in the frequency region between 40 and 100 kHz. The dispersion curves change significantly, depending on the pipe diameter and the wall thickness.

The guided-wave modes used for long-range inspection applications include the fundamental and the second-order longitudinal modes, L(0,1) and L(0,2), and the fundamental torsional mode, T(0,1), in piping-type structures and fundamental symmetric and antisymmetric Lamb modes, S0 and A0, and the fundamental shear horizontal mode, SH0, in plate-type structures. These modes are chosen in order to avoid changing in group velocities when varying the wave frequency.

During the research activity described in this thesis, fundamental torsional mode was used (T(0,1)) as it is the most stable in terms of group velocity variation over an important range of frequencies. Another reason why T(0,1) was preferred is it theoretical lack of interaction with internal and external pipe medium. This is explained by the fact that its displacements are oriented only in the circumferential direction.

UGW of different types can propagate in any bounded medium [11]. The use of guided waves in NDE has been discussed for over 40 years with great interest till present days.

UGW can be used in three different regimes as indicated in Table 3-1.

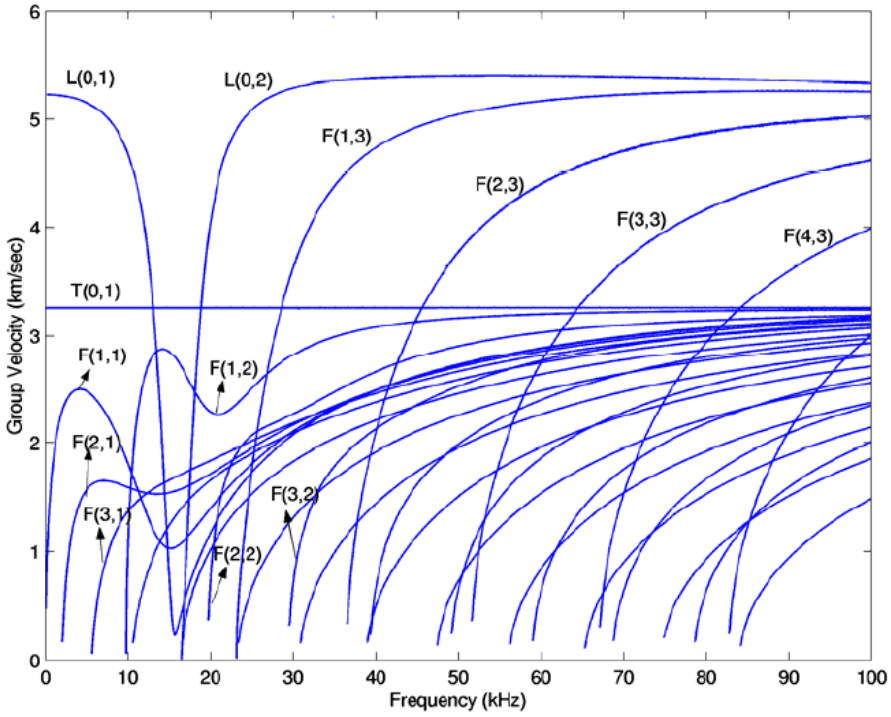

Figure 3-5 Dispersion curves of various UGW modes (the number in parenthesis indicates the order of the wave mode)

Table 3-1 Use of guided waves in different ranges and corresponding frequencies

	frequency	application
Short Range << 1 m	> 1 MHz	High frequency surface scanning: - detection of small surface defects (Rayleigh wave); - inspection of composite materials (leaky Lamb wave); - acoustic microscopy
Medium Range up to about 5 m	250 kHz ÷ 1 MHz	- plate, tube and pipe testing; - weld inspection; - aircraft lap joint and ice detection.

Long Range up to around 100 m	Up to 250 kHz	Inspection of large structures

In this thesis the interest is focused on the long range ultrasonic guided waves (LRUGW or UGW) used for the rapid survey of pipes, for detection of both internal and external corrosion.

3.2 UGW Inspection Systems

The main attraction of guided wave inspection is that [11] it allows a large area of structure to be tested from a single location, thus avoiding the time consuming scanning required by conventional ultrasonic or eddy current methods. The technique becomes even more attractive if part of the structure to be tested is inaccessible, for example a road-, river- or railway-crossing. The test is usually done in pulse-echo mode, the transducer transmitting the guided wave along the structure. Returning echoes indicate the presence of defects or other structural features.

As UGW have the ability to interrogate from a single probe position a structure over long distances for defects such as cracks and corrosion wastage, the technique can be a very effective means of surveying and monitoring large structures for their structural conditions. In many industries pipe corrosion is one of the major problems for plant maintenance. Thus, non-destructive detection and classification of pipe integrity using LRGW is of actual interest.

By UGW inspection it is possible to assess the integrity of entire pipelines requiring a limited number of accessible locations. Consequently, the time for the inspection procedure is reduced and the safety can be improved by choosing appropriate inspection locations. Furthermore, off-stream maintenance of continuous cycle industrial plants and excavation of a buried pipe for water or gas distribution can be avoided with considerable economic savings and public inconvenient reductions.

Figure 3-6 sketches the basic elements of the guided wave technology applied to the piping system inspection.

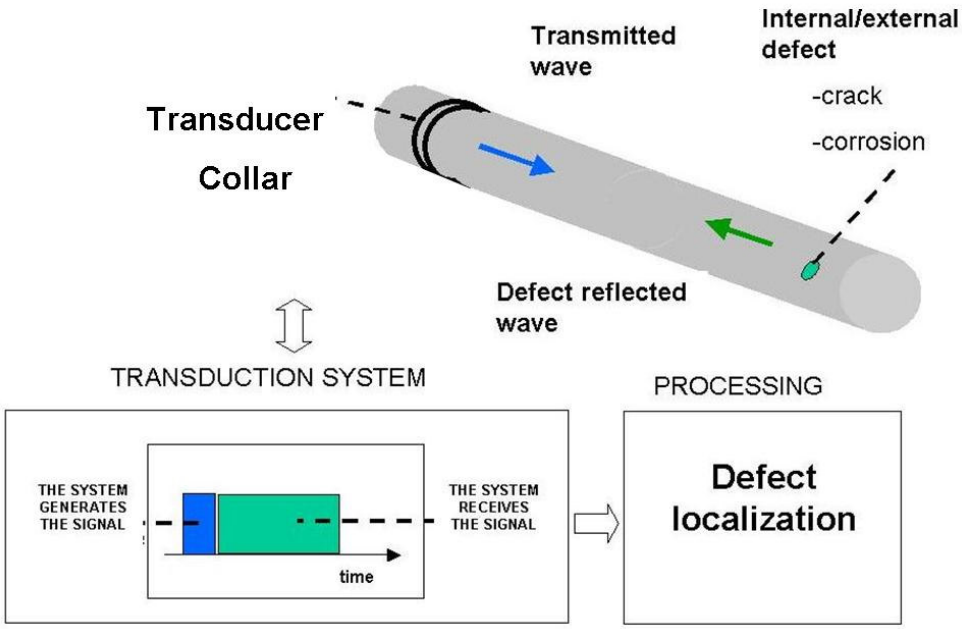

Figure 3-6 Basic elements for LRGW piping systems inspection

The UGW are generated in pipes via a transducing system, called “transmitter” that is driven by proper electrical signal. The transducing system can be made up of several elements (array) or a single element called transducer that transforms the electrical signal in mechanical vibration. The opposite effect must be possible. Most transducers are based on physical phenomena like piezoelectricity, magnetostriction or Lorenz force. The last is presently possible only for local detailed inspection, thus not for long range inspection.

Usually the same probe is used as a receiver as well (Pulse/Echo mode) or another one, called “receiver” is located at a proper distance from the transmitter to return an electric signal when detecting the elastic wave that travels in the pipe.

The transmitter/receiver probes are connected to the acquisition electronic system by a cable; the digital signal acquisition is controlled by a laptop computer.

The piezoelectric or magnetostrictive material expands and contracts under the action of an alternate electric or magnetic field. Their vibrations produce elastic waves having the same frequency as the exciting electric or magnetic field.

The wave propagates in the tested material with the same frequency of the generator and with a velocity that depends on the material itself [18]. When the wave impinges on an obstacle or a defect it is reflected and absorbed following the same laws of other wave propagation phenomena. The reflected wave has the same frequency as the incident one but may be shifted in phase or may present shape modifications due to interference. Generally, the reflected signal coming back to the transducer is very complex being the results of a combination of several echoes generated by the multitude of discontinuities found along the tested pipe. The information on the dimension, geometry and nature of defects should be extracted from this data set.

With an adequate power of the generated signal it is possible to detect very distant defects; in particular up to 30 meter lengths of pipes or more can be inspected in each direction [8]. The received signal is usually amplified and filtered, while the distance from the transducer is precisely detected if the velocity of propagation is known.

An estimation of dimensions of detected flaws may be obtained by comparing the intensity of the reflected signal with that of a signal reflected by standard artificial defects. In other words it is possible to say that the defect has a dimension and geometry that is able to generate an echo similar to the one given by a hole with a known diameter placed at the same position of the defect. This equivalent dimension is not actually related to the real dimension of a defect but is an approximate parameter presently used to classify the defects.

The possibility of the method to go beyond detection and localisation to classification and sizing, however, is still under investigation by researchers in the field. Moreover, research concerning the basic mechanisms of propagating modes of guided waves has to be intensified to obtain an efficient classification and identification of defect sizes.

A large variety of probes (transducers and receivers) has been produced to satisfy the characteristics of the different ultrasonic wave techniques. The propagating waves can be tangent to the pipe surface but also sidelong with respect to the probe axis (quite used are probes with propagating angles of 30, 45, 60 and 70°). The transmitters and the receivers can be included in the same probe or located separately to optimise inspection. Every probe has specific characteristic that can optimise the test results depending on the geometry and the position of the defect and on the pipe material (steel, aluminium, cast iron etc.). Every probe works or has a maximum operating frequency depending on the particular pipe under test. The choice of the probe and its operating condition is one of the crucial points to successfully using this technique.

3.2.1 Piezoelectric transducers

One of the commercial piezoelectric transducers for UGW inspection (Wavemaker™) has been developed by Imperial College of Science, Technology and Medicine in London. The instrument is a designated to generate relatively low-frequency guided waves for non long range destructive evaluation inspections of pipes in the petro-chemical industry [19]. However, the transducers may also be used for a variety of other applications in the frequency range 20 - 100 kHz.

Generally, a piezoelectric UGW system comprises one or more rings of dry-coupled piezoelectric transducers which apply a tangential force to the pipe surface, thus exciting the torsional mode [20]. Two or more rings of transducers positioned roughly a quarter wavelength apart along the pipe enable wave direction control. The transducer array is connected to the battery-operated testing instrument. This configuration offers considerable advantages to signal processing and in defect characterization.

When an axial symmetric mode is incident on an axially symmetric pipe feature such as a flange, square and/or uniform weld, only axial symmetric modes are reflected. However, if the feature is not axially symmetric (like a corrosion patch) some non-axially symmetric wave modes will be generated. These propagate back to the transducer ring and can be detected. If the T(0,1) mode is incident, the most

important mode conversion is to the flexural modes F(1,2), F(2,2). The amount of mode conversion obtained depends on the degree of asymmetry, and hence on the circumferential extent of the defect. The use of an array of transducers facilitates detection of the mode converted signal; if a monolithic transducer were to be used, the mode converted signals would not be detected since their displacements vary harmonically around the pipe. In this case the average displacement is zero. In order to measure the mode conversion it is therefore necessary to access the signals received by individual transducers (or group of adjacent transducers around the pipe) separately and to process them considering the appropriate phase shifts.

As declared by the producer and users, some of the advantages of using the Wavemaker ™ are:

- 100% of the in-service pipe can be inspected (within the diagnostic length of a test);
- Sophisticated signal analysis to interpret the results;
- Ability to detect internal and external metal loss and planar defects at long range;
- Sensitivity can be as good as 2% loss of cross-section in ideal conditions (typically set at 10%).

These capabilities are typical for most of the pipe configurations. However pipe systems can vary greatly in design and condition, and this affects inspectability. For example, bitumen wrapping greatly reduces the test range and sections of pipes with numerous features (e.g. several T's collected together) cannot be tested reliably. Well-trained operators are required for interpretation of the results.

The system has been designed to operate as a screening tool that can quickly identify problem areas. When the pipe is accessible, it is frequently recommended that a detailed inspection (using complementary techniques) is performed at any identified corrosion areas.

3.2.2 Magnetostrictive transducers

A commercially available UGW inspection instrument based on magnetostrictive transducers (MsS®) has been developed by The South West Research Institute, in San Antonio, TX, USA.

A magnetostrictive transducer is able to generate and detect UGW in ferromagnetic materials. The sensor is basically composed of two components:

- An electromagnetic component i.e. a coil that creates an alternate magnetic field oriented parallel to the direction of the wave propagation (wave generation) or inductively generates an electrical signal when excited by an alternate magnetic field (wave reception);
- A magneto-mechanical component i.e. a ferromagnetic strip attached to the structure to be inspected. After being properly magnetized with a static magnetic field, the strip vibrates under the influence of the alternate magnetic field (wave generation) or generates an alternate magnetic field corresponding to the received mechanical wave (wave reception).
- The whole magnetostrictive system is briefly sketched in Figure 3-7, where U is the voltage, B is the magnetic field and u is the displacement.

A more detailed description of the magnetostrictive sensors and the SwRi MsS® in particular will be given in 0.

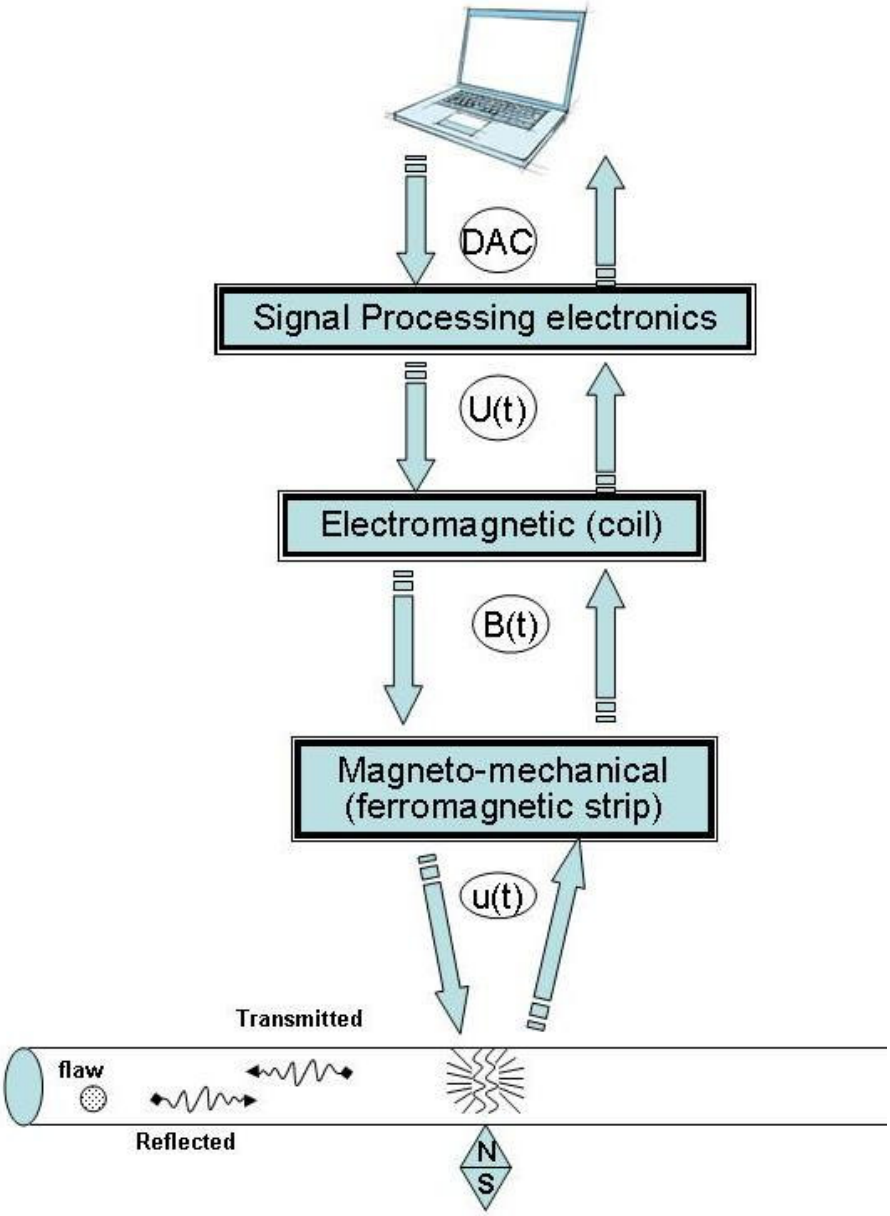

Figure 3-7 Components of a magnetostrictive inspection system

3.3 Benefits and limitations

3.3.1 Advantages of UGW inspection

The low frequency ultrasonic guided wave technique has been developed for the rapid survey of pipes, for the detection of both internal and external corrosion. The propagation of the UGW is affected by changes in thickness of the component, that

makes them sensitive to metal loss defects, notably corrosion [21]. The principal advantage is that long lengths, 30 m or more in each direction, may be examined from a single test point.

The capabilities of detecting corrosion are shown in Table 3-2 [20].

Table 3-2 UGW capabilities of detecting corrosion in pipes

Range	30 or more in each direction from singe test point
Wall thickness of the corrosion	< 30%
Circumferential width of the corrosion	< 25 %

Some of the benefits of long range inspection using UGW are:

- Reduction in the costs of gaining access to the pipes for inspection, avoidance of removal and reinstatement of insulation (where present), except for the area on which the transducers are mounted;
- The ability to inspect inaccessible areas, such as under clamps and sleeved or buried pipes;
- The whole pipe wall is tested, thereby achieving a 100% examination.

In order to better understand the importance of the rapid survey of long pipes by using UGW, the classical ultrasonic testing method or other local inspection methods have to be assessed from an economical point of view.

Ultrasonic thickness checks for metal loss due to corrosion or erosion are highly localised, in that they only measure the thickness of the area under the transducer itself. The survey of a large area requires many measurements and access to most of the surface of the component being examined. Where access is difficult or costly a detailed survey becomes unattractive economically, with the result that often limited sampling only is carried out. Similar restrictions also apply to other methods of measuring wall thickness, such as radiography, eddy currents etc. Partial inspection of this type is not likely to be effective in reducing the numbers of

significant defects which may cause leaks in un-inspected areas is zero. The benefits of using UGW for long range examination of 100% of the pipe wall along the pipe under test is therefore considerable.

Figure 3-8 shows the experimental probability of detection (PoD) obtained for guided wave tests in pipes by TWI, Cambridge, United Kingdom

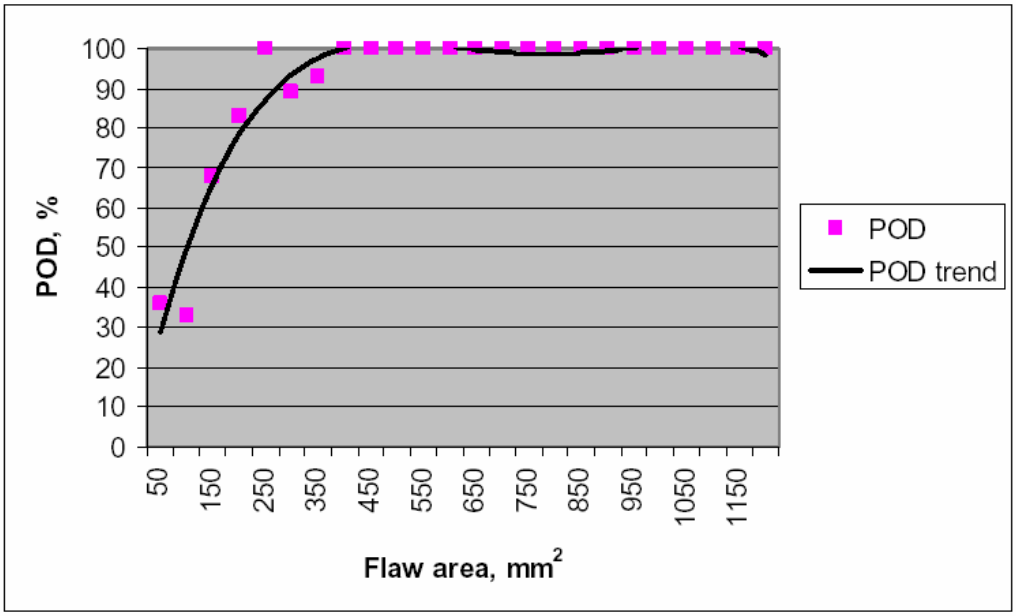

Figure 3-8 Experimental probability of detection (PoD) for guided wave tests

3.3.2 Limitations

It should be noted that all commercially available guided-wave test systems transmit axially symmetric annular waves which sweep along the pipe. The magnitude at which this wave interacts with an area of metal loss is determined by the depth and circumferential extent of the latter. The detection capability is therefore governed by the cross-sectional area of the defect. Therefore, it may be noticed that this technique do not return a direct measure of the remaining wall thickness, thus cannot currently be used to provide a replacement for conventional thickness gauging. Whilst there is a relationship between overall defect area and the amplitude of a reflection from it, this relationship is greatly affected by the shape and roughness of the defect itself and cannot be relied upon to predict severity. This limits the current technique to detection of suspect areas for follow up activity by other methods.

Another difficulty concerning long-range guided-wave inspection is the complexity of the wave mode system [21]. Under most conditions more than one ultrasonic wave mode exists (coherent noise) in the same pipe under test. These modes each travel at different velocities and may exhibit dispersive behaviour, i.e. the wave velocity varies with frequency, all of which makes interpretation of the resulting test signal difficult.

The coherent noise has two main sources [20]:

- excitation and reception of unwanted modes;
- transmission of waves in the opposite direction along the pipe and the reception of echoes from that direction.

The key to controlling coherent noise is therefore to excite and receive a single mode in one direction. The choice of the mode will be influenced by the ease of exciting it while minimising the excitation of other modes, and by sensitivity to defect type of interest.

Effect of pipeline features and other conditions on inspection capabilities is also an important issue concerning UGW inspection.

The effect of pipeline features and other conditions on inspection capabilities are summarized in Table 3-3.

Table 3-3 Effect of pipeline features and other conditions on inspection capabilities

Features/Condition	Effects
Flange/Valve	Prevents wave propagation; forms end point of inspection range
Tee	Causes a large disruption in wave propagation and limits inspection range up to that point
Elbow	Causes a large disruption in wave propagation and limits inspection range no farther than the elbow region
Bend	Has negligible effect if the bend radius is greater than 3

	times of OD; if the bend radius is less than the above, behaves like an elbow
Side branch	Causes a wave reflection and thus produces a signal; no significant effects on inspection capabilities
Clamp	Causes a wave reflection and thus produces a signal; no significant effects on inspection capabilities
Weld attachment	Causes a wave reflection and thus produces a signal; if the attachment is large (such as pipe shoes), can reduce inspection range
Paint	Has negligible effects
Insulation	Has no effects unless the insulation is bonded to the pipe surface, in which case the inspection range will be shortened due to higher wave attenuation
Coating	Has negligible effects if the coating is thin (e.g., fusion-bonded epoxy coating); thicker coating (e.g., bituminous coating, polyethylene coating) increase wave attenuation and shortens inspection range
Liquid in the pipe	No effect on T-wave; significant degradation on L-wave
General surface corrosion	Increase wave attenuation and shortens inspection range
Soil	If pipe is buried, the surrounding soil increases wave attenuation, and the inspection range is shortened

In [22] Heerings et al. provide a study of the capabilities of most of the existing NDE techniques, local and long-range, on-stream and off-stream. A detailed description and a parallel between all these techniques is listed in Table 3-34.

Table 3-4 ***Inspection performance***

	Visual	Radiography		UT, manual	UT mechanised		Magnetic	Liquid	Eddy current		Magnetic	Guided
		film	RTR	puls echo	puls echo	TOFD	Particle	penetrant	conventional	pulsed	Flux leakage	waves
Material	all	all	all	most	most	finegrain	magnetisable	non-porous	elec.cond.	elec.cond.	magnetisable	all
Wall Thickness Range (steel, mm)	arbitrary	0 - 100	0 - 30	2 - >500	2 - >500	6 - >500	arbitrary	arbitrary	0 - >2	Mar-45	2 - >20	0 – 35
Volume Inspection	no	especially	yes	yes	yes	yes	no	no	limited	no	yes	Yes
Weld Inspection	geometry	yes	yes	yes	yes	yes	yes, surface	yes, surface	yes	no	no	No
Surface Inspection	yes, only	yes	yes	yes	yes	limited	yes	yes	yes	no	yes	Yes
Degradation mechanism	**Definition of parameters: D = Detection capability S = Sizing capability Definition of values: 3 = Excellent / Good 2 = Fairly / Reasonable 1 = Moderate / Poor**											
Uniform corrosion / wall thinning	D: 1	D: 2	D: 2	D: 2	D: 3	D: 3	D: n.a.	D: n.a.	D: n.a.	D: 2	D: 1	D: 2
	S: 1	S: 1	S: 1	S: 3	S: 3	S: n.a.	S: n.a.	S: n.a.	S: n.a.	S: 2	S: 1	S: n.a.
Pitting corrosion	D: 2[1]	D: 3	D: 3	D: 1	D: 1	D: n.a.	D: n.a.	D: n.a.	D: 1	D: n.a.	D: 3[2]	D: n.a.
	S: 1[1]	S: 1	S: 1	S: 3	S: 1	S: n.a.	S: n.a.	S: n.a.	S: 1	S: n.a.	S: n.a.	S: n.a.
Branched type of cracking, e.g. due to corrosion	D: n.a.	D: 1	D: 1	D: 2	D: 2	D: 2	D: 3[3]	D:3[3]	D:2[4]	D: n.a.	D: n.a.	D: n.a.
	S: n.a.	S: n.a.	S: n.a.	S: n.a.	S: 1	S: 2	S: n.a.	S: n.a.	S: n.a.	S: n.a.	S: n.a.	S: n.a.
Non-branched type of cracking, e.g. due to fatigue	D: n.a.	D: 1[5]	D: 1[5]	D: 2	D: 3	D: 3	D: 3[3]	D: n.a.	D: 3[4]	D: n.a.	D: 1	D: n.a.
	S: n.a.	S: n.a.	S: n.a.	S: 1	S: 1[6]	S: 3	S: n.a.	S: n.a.	S: 1	S: n.a.	S: n.a.	S: n.a.
Delamination	D: n.a.	D: n.a.	D: n.a.	D: 3	D: 3	D: 3	D: n.a.	D: n.a.	D: n.a.	D: n.a.	D: n.a.	D: n.a.
	S: n.a.	S: n.a.	S: n.a.	S: 3	S: 3	S: 3	S: n.a.	S: n.a.	S: n.a.	S: n.a.	S: n.a.	S: n.a.
Corrosion Under Insulation	D: 3[7]	D: 2	D: 1	D: n.a.	D: n.a.	D: n.a.	D: n.a.	D: n.a.	D: n.a.	D: 2	D: n.a.	D: 3
	S: 1[7]	S: n.a.	S: n.a.	S: n.a.	S: n.a.	S: n.a.	S: n.a.	S: n.a.	S: n.a.	S: 1	S: n.a.	S: n.a.

(1): Provided that it is accessible and not coated (2): Dependent on the depth (3): Provided there is surface-breaking
(4): Only at greater wall thickness and provided there is surface breaking (5): Provided that wall thickness > 10 mm; if wall thickness < 10 mm then D = 2
(6): S = 2 provided that there is a sufficient number of transducers (7): After removal of insulation

CHAPTER 4 GUIDED WAVES AND MAGNETOSTRICTIVE SENSORS

4.1 Magnetostriction

Magnetostrictive materials were discovered in the 1840s by James Prescott Joule, when he noticed that iron changed length in response to changes in magnetism and named the phenomenon the **Joule Effect**. The effect is also called magnetostriction, and it is one of the magnetic properties which accompany ferromagnetism.

Internally, ferromagnetic materials have a structure that is divided into domains, each of which is a region of uniform magnetic polarization (magnetic domains). When a magnetic field is applied, the boundaries between the domains shift and the domains rotate, both these effects causing a change in the material's dimensions (Joule Effect).

Figure 4-1 lining up of magnetic domains by Joule Effect in a ferromagnetic material [23].

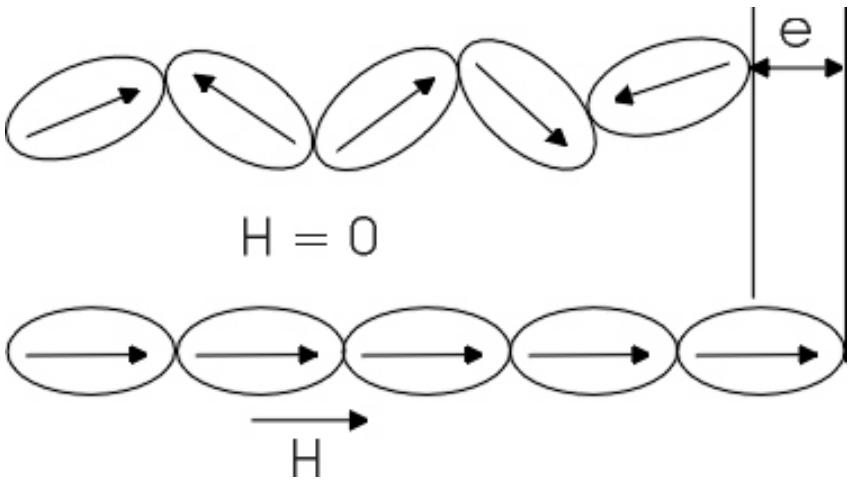

Figure 4-1 Lining up of the domains in a ferroelectric material by Joule Effect

It is also observed that applied mechanical strain produces some magnetic anisotropy. If an iron crystal is placed under tensile stress, then the direction of the stress becomes the preferred magnetic direction and the domains will tend to line up in that direction. This effect – i.e. the change of the susceptibility of a material when subjected to a mechanical stress, is called the **Villari effect**. Two other effects are related to magnetostriction: the **Matteucci effect** is the creation of a helical anisotropy of the susceptibility of a magnetostrictive material when subjected to a torque and the **Wiedemann effect** is the twisting of these materials when a helical magnetic field is applied to them. The **Villari Reversal** is the change in sign of the magnetostriction of iron from positive to negative when exposed to magnetic fields of approximately 40000 A/m (500 oersteds).

Some of the magnetostrictive materials are:

- cobalt
- iron
- nickel
- ferrite
- terbium Alloys (Terfenol-D)
- metglass

On magnetization a magnetic material under goes changes in volume which are relatively small - of the order 10^{-5}.

In formal treatments, a magnetostrictive coefficient Λ is defined as the fractional change in length as the magnetization increases from zero to its saturation value. The coefficient Λ may be positive or negative, and is usually on the order of 10^{-5}. Some examples of measurements of this phenomenon are included in Table 4-1[24].

Table 4-1 Saturation magnetostriction for various materials

Material	Crystal axis	Saturation magnetostriction Λ (x $10^{-5)}$
Fe	100	+(1.1-2.0)
Fe	111	-(1.3-2.0)
Fe	Polycrystal	-.8
Ni	100	-(5.0-5.2)
Ni	111	-2.7
Ni	Polycrystal	-(2.5-4.7)
Co	Polycrystal	-(5.0-6.0)

The highest room temperature magnetostriction of a pure element is that of Co which saturates at 60 microstrain. However, magnetostrictive materials can operate at higher temperatures than piezoelectric actuators. They can also undergo higher strains and lower input voltages that most piezoelectric materials can. On the other hand, magnetostrictive materials are not easily embedded in control structures.

4.2 Magnetostrictive Strip sensor – MsS®

The magnetostrictive transducer generates and detects guided waves in ferromagnetic materials electromagnetically. For a longitudinal or Lamb wave generation and detection, the transducer relies on the magnetostrictive (or Joule) effect and its inverse (or Villari) effect. For a torsional or SH wave generation and detection, the transducer relies on the Wiedemann effect (see Figure 4-2). The static bias magnetic field H_0 is supplied by using a permanent magnet or an electromagnet. Alternatively, it can be supplied by inducing a residual magnetization in the ferromagnetic material.

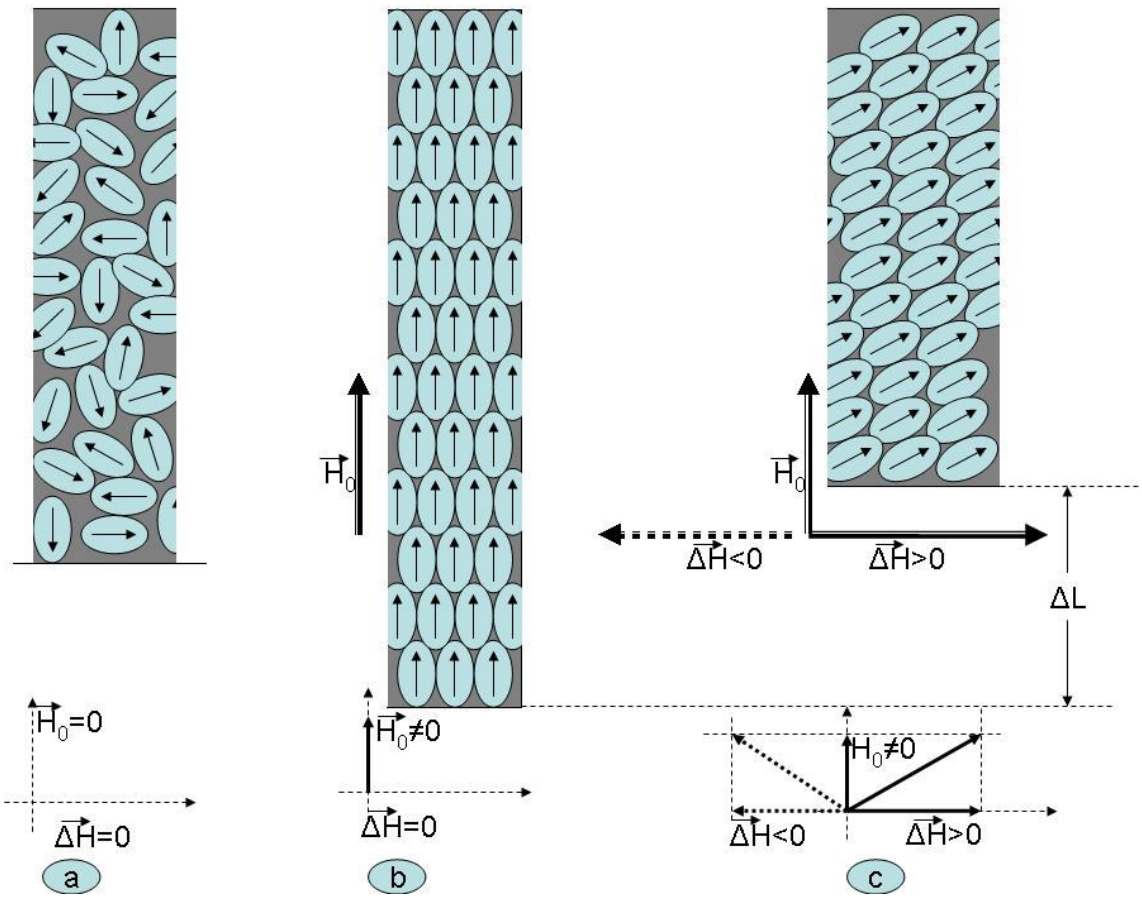

Figure 4-2 Applied magnetic fields orientation for torsion generation in a magnetostrictive strip by Wiedemann effect

Ferrous steel presents ferromagnetic and magnetostrictive properties. Therefore, on rods, pipes, and plates that are made of ferrous steel, UGW can be generated and detected directly in the structure by using the structure as a part of the transducer. For structures made of nonferrous materials such as aluminium or nonferrous stainless steel, a thin strip of ferromagnetic material that has good magnetostrictive properties, such as nickel or iron-cobalt alloy, is attached to the structure under test for transducing operation. This thin-strip approach is also used on ferrous structures when it is considered to be appropriate and advantageous, in order to increase the transducer efficiency. When a strip is used for transducer operation, the guided waves are generated in the strip and are coupled to the structure under test. For good coupling, the strip is typically attached to the

structure by using an adhesive. Other joining methods, such as plating, or inflatable air bladders can also be used for special applications.

The guided-wave modes are controlled using the relative orientation between the static bias magnetic field and the applied time-varying magnetic field ΔH. For a longitudinal mode in a pipe and Lamb modes in a plate, the two fields should be parallel to each other. For a torsional mode in a pipe and a SH mode in a plate, they should be perpendicular to each other.

Figure 4-3 shows the MsS® probe for T-mode piping inspection.

(a)

(b)

Figure 4-3 MsS probe for T-mode piping inspection: (a) magnetostrictive strip, (b) ribbon coils placed over the strip.

4.2.1 Hardware

MsS2020® instrument comes as a cheaper alternative to the classical PZT array sensors. Unlike these, MsS2020® takes advantage of the magnetostrictive property of ferromagnetic materials such as Iron, Nickel or Cobalt. The magnetostrictive

(Joule) effect assumes that ferromagnetic materials and their alloys change their shape when exposed to a variable magnetic field. The sensor uses thin strips of Ni or FeCo alloy mechanically attached to the structure (pipe) to generate mechanical waves (Guided Waves) that propagate through the entire volume of the pipe wall over long distances in the axial direction. Echoes caused by discontinuities present in the pipe wall (i.e. defects, joints, welds) are detected by the same transducer (pulse-echo modality) or by a separate receiver (pitch-catch modality). Wave detection is made possible by the inverse-magnetostrictive (Villary) effect - i.e. the change in the magnetic induction of ferromagnetic materials caused by stress (strain). This technology allows detection from a single location of both inner and outer defects (metal loss or corrosion) that are present along the pipe without the need to excavate or to remove the insulation over long distances.

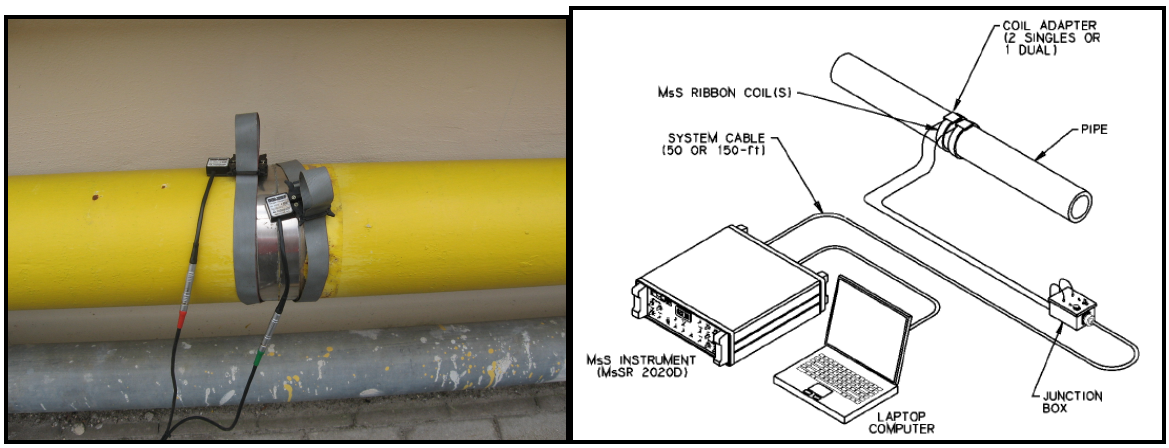

Figure 4-4 Experimental setup for the MsS® sensor.

Features [17], [25]:

- High sensitivity (can find defects that have up to 2~3% differences from the normal condition)
- Inspects carbon steel and alloy steel
- Inspects pipe and tube (up to 40 inch diameter)
- Inspects up to 1.5 inch thickness
- Works for high temperature applications (up to Curie temperature - 770 ℃ in steel, 354 ℃ in Nickel, up to 105 ℃ for ribbon coil in piping inspection)

- 2 inch sensor lift off from the surface of inspected materials

Applicable wave modes:

- Torsional, longitudinal and flexural wave for cylindrical structure
- Shear-horizontal, symmetric and anti symmetric Lamb wave for plate structure
- Some of the outlined features of the MsS® instrument were verified and confirmed by laboratory and field tests.

4.2.2 Signal processing features

MsS® sensor itself includes software that is capable of performing basic signal processing operations to estimate the main features detected along the inspected length of the pipeline [26].

First of all the acquired signal is being digitalized and displayed on the screen in the time and magnitude coordinates – the *so-called* RF signal (Figure 4-5- the lower visualization mode).

The second visualization mode is a user-friendly one, often called Video Signal (VS), which is actually a time representation of the spectral amplitudes corresponding to the operating frequency of the MsS® instrument (Figure 4-5- the central visualization mode). A detailed example of RF signal converted into video data is given in The procedures used in the software are as follows:

1. Segment the RF data to *N* number of data points, where

$$N = \frac{f_{sam} x(n+1)}{f_{op}} \qquad (4\text{-}1)$$

where f_{sam} is the sampling frequency of the RF data, f_{op} is the operating frequency of the MsS, and n is the number of cycles in the transmitted pulse.

2. Apply the Hanning Window to each segment;

3. Perform Fast Fourier Transform (FFT) to each segment;

4. Assign the spectral amplitude of FFT data at the operating frequency to the median distance of each segment;

5. Repeat steps (1) through (4) while moving the segment along the X-axis in small increments.

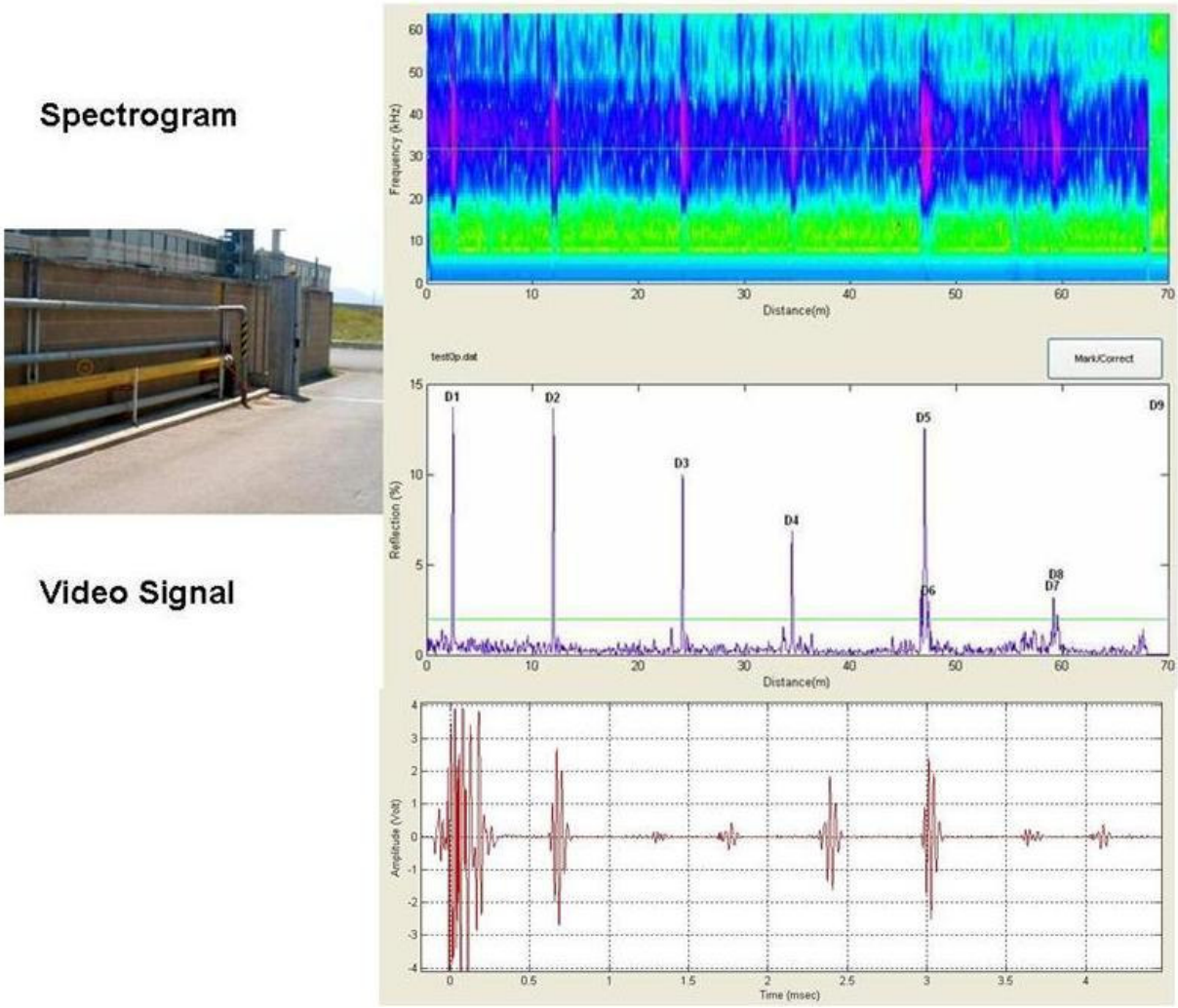

Figure 4-5 Results visualization for the MsS® software

In the next step, two thresholds are considered and applied on the video data representation:

- a 100% one that corresponds to the highest reflections that are usually due to the presence of welds or joints;

- a lower threshold that must be slightly above the noise level.

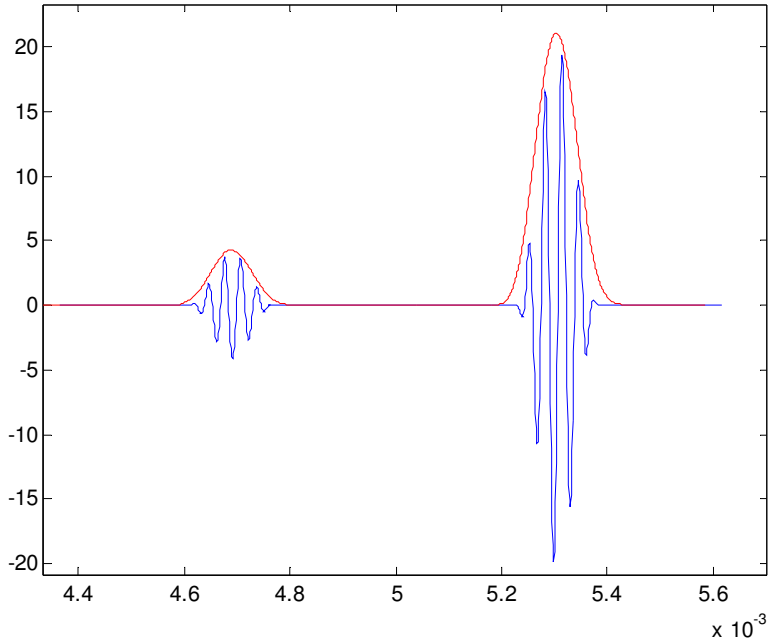

Figure 4-6 RF data converted into video data

The echoes whose amplitude ranges between the two thresholds and that are not known apriori, are deemed to be generated by defects. This procedure will be named “threshold criterion” as it helps to decide the presence of defects.

The last representation of the acquired data is the Spectrogram. The Spectrogram is a frequency time representation of RF data. It is obtained by performing FFT of the amplitude-time RF data within a window of predetermined length and plotting the spectral content of the RF data in that window while moving the window along the time axis at a predetermined interval.

The entire process from the RF signal acquisition to the defect identification is described in the flow chart sketched in Figure 4-7.

The main steps are:

- RF signal acquisition
- Signal calibration by performing normalization and attenuation correction

- Representation of the RF signal into a more comprehensible Video Signal (VS) based on the amplitude.
- Elaboration of the Spectrogram – a useful instrument for defect identification
- Application of the threshold criterion to the video signal: peaks exceeding the chosen threshold will be considered potential defects, unless already identified as pipeline usual features (For example, our inspected gas pipeline had welds approx. 10 m distant from each other, so they could be easily identified)

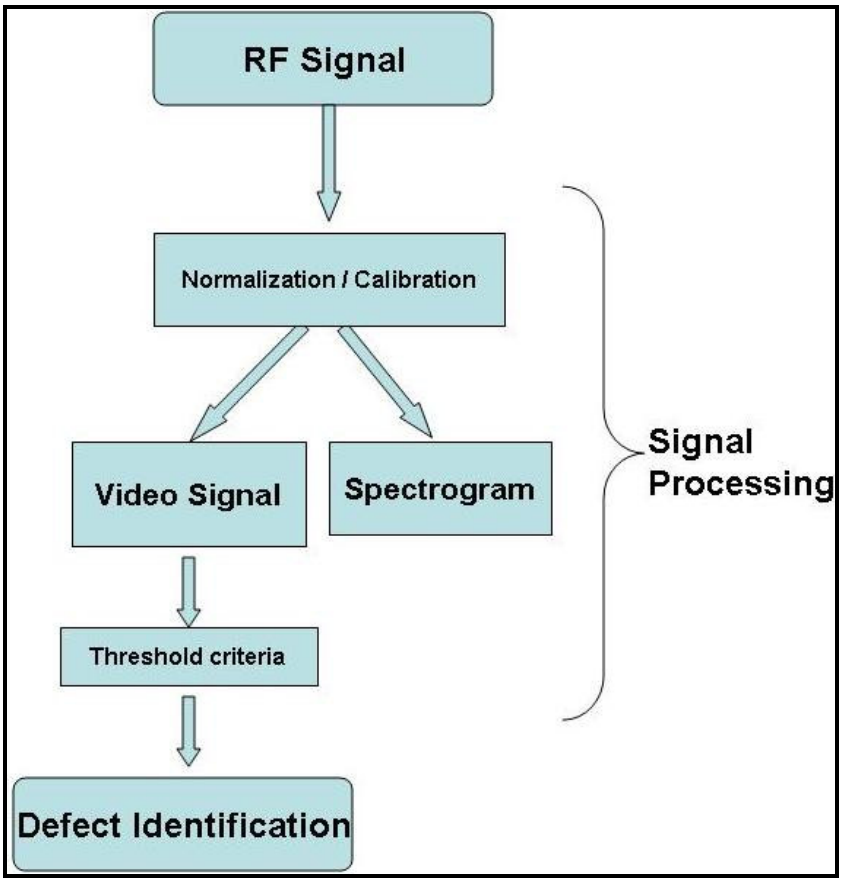

Figure 4-7 Flow chart of the inspection procedure using the MsS® software for data acquisition and signal analysis

CHAPTER 5 EXPERIMENTATION WITH U.G.W. USING AN MSS TYPE TRANSDUCER

5.1 Laboratory and field tests

The first phase of the research activity was the experimental evaluation of UGW inspection technique. For this purpose a commercial magnetostrictive system was used, namely MsS® 2020 produced by South-West Research Institute, Tx, USA.

This particular instrument was chosen because of its reduced costs, simplicity and flexibility regarding the diameters of the pipes that could be inspected. Another reason was the fact that in this case research was still needed to improve its diagnostic capabilities with defect characterization and classification. Moreover, the possibility to evaluate and eventually improve the instrument's monitoring capabilities was taken into account.

The test campaign included laboratory as well as field inspection with the following goals:

- to evaluate the sensitivity of the UGW instrument
- to estimate the inspection range in various pipeline conditions (suspended, buried, coated)
- to determine the monitoring potential of the MsS®
- to establish the advantages and limitations of the UGW inspection using a magnetostrictive sensor.

5.1.1 Artificial defects

For a better evaluation of the MsS® instrument and for a better understanding of the UGW scattering from defects, both simulations and experimental measurements were performed. However, a large number of artificial defects was needed and several issues had to be considered when creating them:

- *Safety*: artificial defects had to be placed also on in-service gas pipelines without jeopardizing the distribution activity.
- *Repeatability*: if an experiment was needed to be repeated, with the same settings, then one should have been able to recreate the defect's geometry.
- *Geometry quantification*: it had to be possible the precise measurement of defect's geometry.

The only defect type that could be artificially created and non-invasively placed on the pipelines was metal-gain type also called positive step-wise defects. Still, they effect on the incident UGW had to be studied with numerical simulations and confirmed by experiments.

Various artificial defects are shown in Figure 5-1. They are positive step-wise defects made by bonding to the pipe a certain number of metallic sheets with known geometry (axial extent, circumferential extent expressed in degrees, radial extent expressed in % of pipe wall thickness).

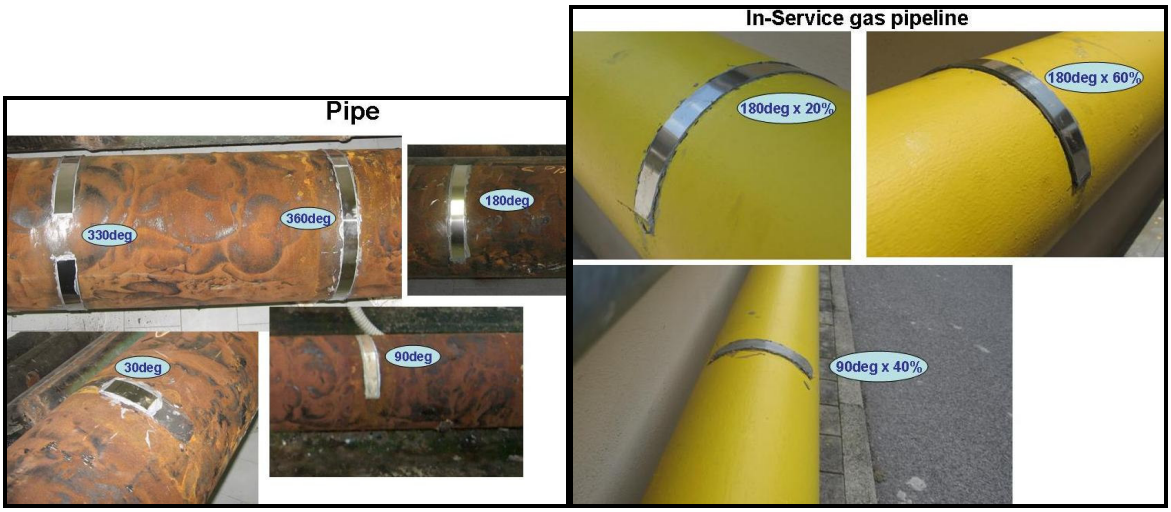

Figure 5-1 Artificial defects

The results for artificial positive step-wise defects were confirmed to be similar to those for negative step-wise defects by the results obtained from two different simulations. Figure 5-2 shows a set of experimental reflections obtained in correspondence of a 90 degree artificial defect whose radial extent was increased

up to 80% of the pipe-wall thickness (a). Furthermore, the normalized spectral amplitudes were represented as a function of defect's radial extent (b). The simulations available for evaluation corresponded to a 360 degree, negative step-wise defec The simulation results are illustrated in the Figure 5-2 (c) and (d). The reflection coefficient in the case of experimental defects becomes saturated for large defects that are close or larger than the pipe wall thickness. An important observation is that the reflected wave from the 90 deg defect has 1/4th of the amplitude corresponding to the 360 deg defect.

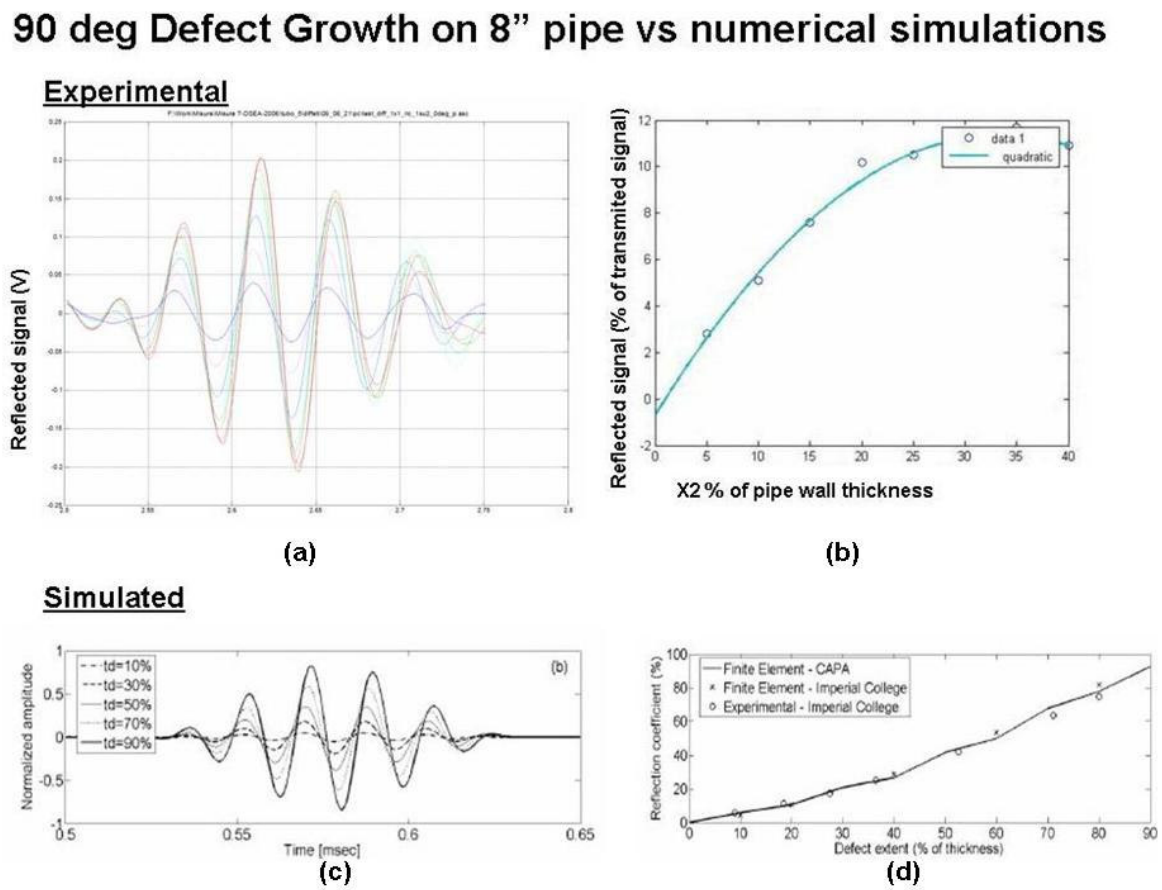

Figure 5-2 Experimental results for a 90 degree defect growth (positive stepwise) vs 360 deg simulated defect growth (negative stepwise).

It may be concluded that artificial positive step-wise defects have mainly the same response in terms of signal amplitude as the negative step-wise defects.

In this way, various tests have been performed even on in-service gas pipelines, in perfect safety conditions, being able to remove the defect, to precisely measure it or to repeat the tests considering other defect geometries.

5.1.2 Sensitivity analysis

In order to evaluate sensor's sensitivity, several experiments with artificial defects having various sizes have been performed. The defects considered were both metal-loss and "metal-gain" as it was noticed that positive as well as negative step-wise defects have roughly the same response.

For the sensitivity analysis a set of artificial defects and various pipes/pipelines were considered. The preferred parameters in terms of wave mode and frequency were:

- torsional wave mode was used. In theory torsional modes present displacements oriented along the circumference, thus no interaction with external medium (coating) or internal medium (fluid) is possible.
- the wave frequency was 32 kHz, the wavelength 10cm and wave velocity 3250 m/s. The 32 kHz frequency was chosen considering that the minimum axial extent of the artificial defects was 1.8 cm, thus less the ¼ wavelength.

See Table 5-1 for a detailed description of defect geometry and instrument's ability to detect them.

Table 5-1 Artificial defects and various tested pipes/pipelines

Test no.	Pipeline type and distance	Defect			Detection capability (Y/N)
		Type	Size (theta x thickness)	Total cross-section size (% metal loss)	
1.	2"	negative	10deg x 10%	0.83%	N

2.	dismounted pipe	stepwise (metal loss)	10deg x 20% and deeper	1.7%	Y
3.			20deg x 10% and deeper	1.7%	Y
4.	8” dismounted pipe	Positive stepwise	30deg x 20%	1.7%	N
5.			30deg x 40% and higher	3.4%	Y
6.			90deg x 20% and higher	5%	Y
7.			120deg x 4%	13.3%	Y
8.			160deg x 40%	17.8%	Y
9.			330deg x 20%	18.3%	Y
10.			360deg x 20%	20%	Y
11.	6” in-service pipeline Distance: 60m, 40m		90deg x 10%	2.5%	N
12.			90deg x 20% and higher	5%	Y

Results have shown that detection capability depends strongly on the pipe corrosion degree, coating type, pipe position (buried / suspended) and on the axial distance between the defect and the sensor. Some examples are illustrated in the sections below.

Short Range

Figure 5-3 shows tests made on a 2” pipe with up to 3 holes drilled into the pipe-wall. The defect becomes visible starting with the first hole.

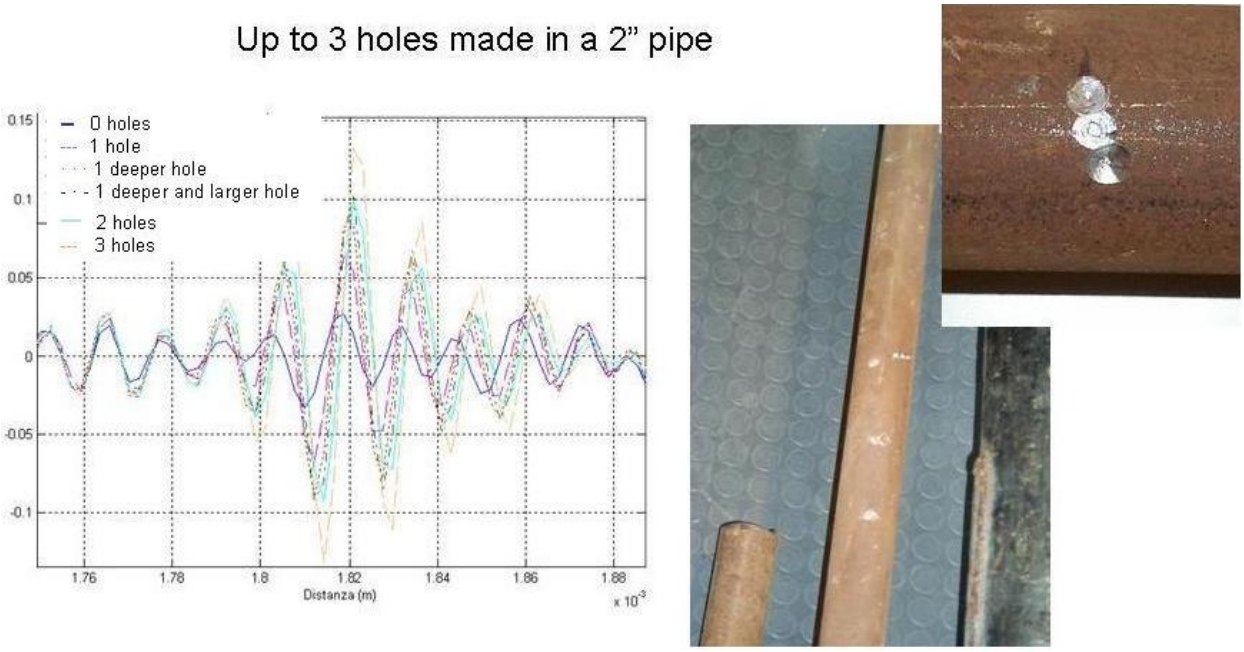

Figure 5-3 Defect growth (negative stepwise) in a 2" steel pipe

In the case of Figure 5-4 the tests were made on an 8" dismounted pipe, 5 m long with artificial features like a 360 deg (symmetrical) and a 30 degree defect bonded to the pipe. The symmetrical strip remains constant in dimensions during the measurements, the 30 deg defect being increased from 20% up to 80% pipe wall thickness. The increase in magnitude of the reflected signal is visible in both RF signal and visual signal. Considering a 5% (above noise level) threshold defects larger or nearly equal to 30 deg x 40% pipe wall thickness are detected. These dimensions are equivalent to a cross-sectional area of approx. 3.3% of the entire pipe wall cross-section.

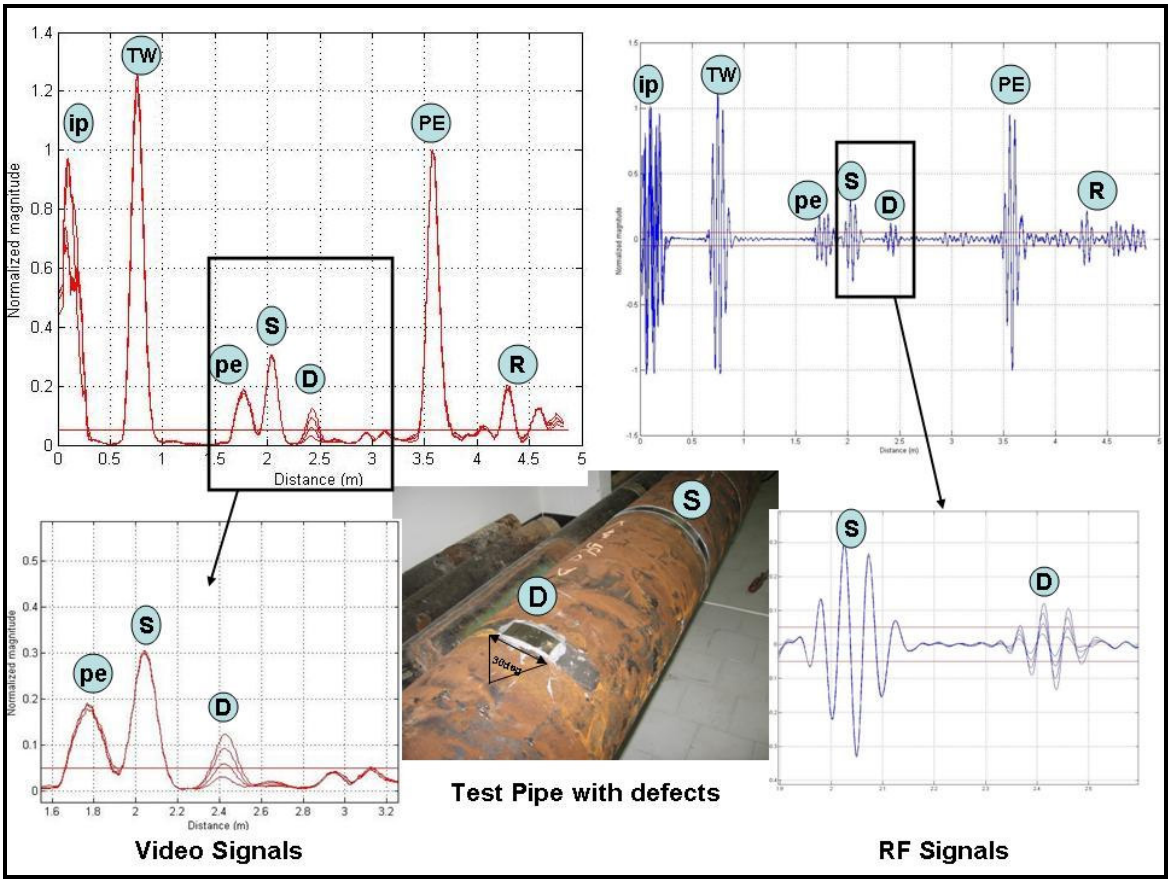

Legend: ip- initial pulse; TW – Transmitted Wave; pe – pipe end reflected from the undesired direction; S – Symmetrical feature (similar to a junction, weld etc); D – artificial Defect; PE – Pipe End; R – Reverberations.

Figure 5-4 Defect growth (positive stepwise) on an 8" steel pipe

Long range

A long range inspection case is provided in Figure 5-5. Two artificial defects were bonded on the pipe at about 40 m and 60 m from the transmitter respectively. The defects have a circumferential extent of 90 degrees and a thickness of about 60% pipe wall (that is 15% pipe wall cross-section). Both defects can be easily identified in the video as well as in the RF signal using a 25% threshold (i.e. above the noise

level). The other important reflections are generated by the symmetrical welds of the pipeline.

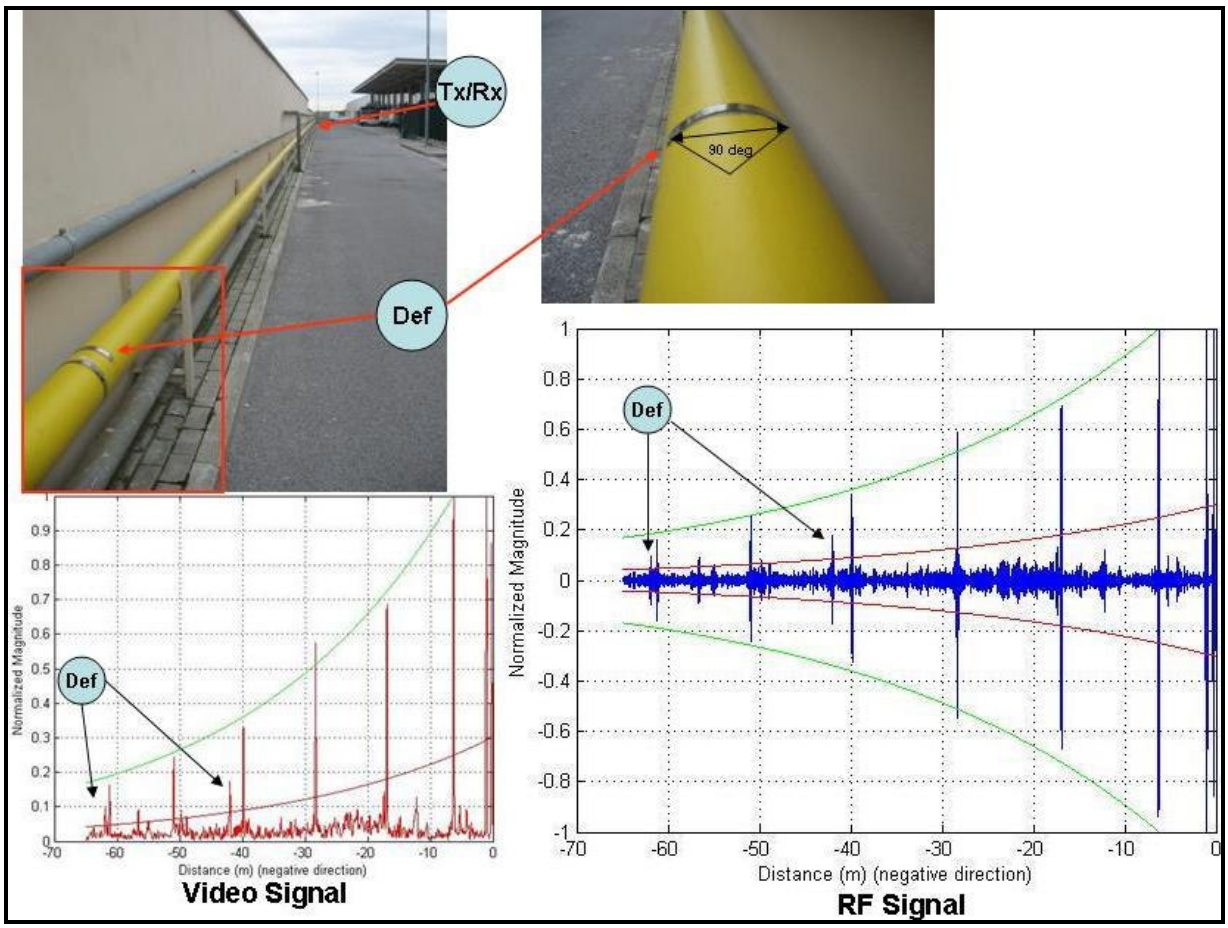

Figure 5-5 Long range inspection: in-service gas pipeline

5.1.3 Inspection Range

In this section various experimental tests are described. Inspections have been performed in multiple pipeline conditions: suspended, buried, coated with bitumen polyethylene, from water or gas distribution systems. The results allowed to evaluate the performances of the MsS instrument for issues regarding UGW inspection range.

On-stream inspection of a natural gas pipeline

The collaboration with the Regional Gas Distributor – Toscana Energia SpA allowed us to gain experience with on-stream piping inspection and to check the monitoring potential of the magnetostrictive guided wave transducer.

Some of the very first tests were conducted on a long 6'' in-sight pipeline, part of the gas distribution system. The pipeline was characterized by a visible state of generalized corrosion, while several features like welds joints and elbows could be noticed.

As shown in Figure 5-6, the sensor was placed on the pipeline and both positive and negative directions were inspected.

Figure 5-6 Experimental setup for the 6" gas pipeline

The inspection revealed all the known features present on the pipeline like welds, joints and elbows, as described in Figure 5-7. In addition, the relatively high level of

the coherent noise indicated an important level of generalized corrosion. The results were completely confirmed by classical visual inspection.

The pipe status of corrosion, and the presence of multiple welds an joints didn't affect the transmitted signal significantly, thus the inspection range. As can be noticed from Figure 5-7, pipe features can be distinguished without particular effort up to 60 m in both directions from the sensor's application point. No particular defect has been revealed.

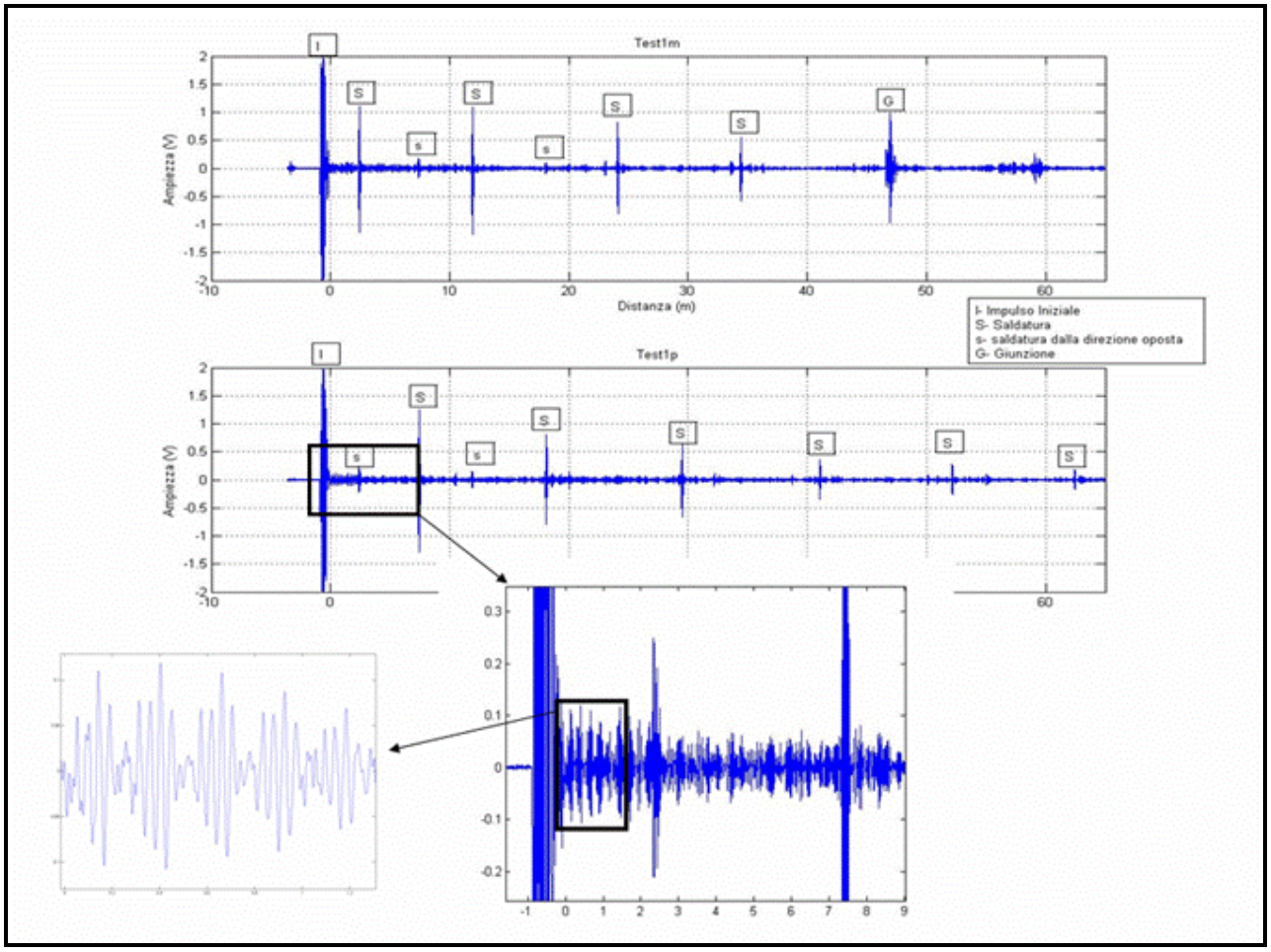

Figure 5-7 Features detected and noise level on the inspected gas pipeline

Water pipeline inspection

This test has brought to our attention the problem of the high complexity of some pipelines and outlined the need of discriminating between non symmetrical features – usual defects – and symmetrical features as joints, welds, and elbow joints –

features normally found on pipelines. The resulted RF signals as well as a schematic description of the inspected pipeline are given in Figure 5-8. The inspection range was situated around 20 m in each direction, being affected by the large number of discontinuities.

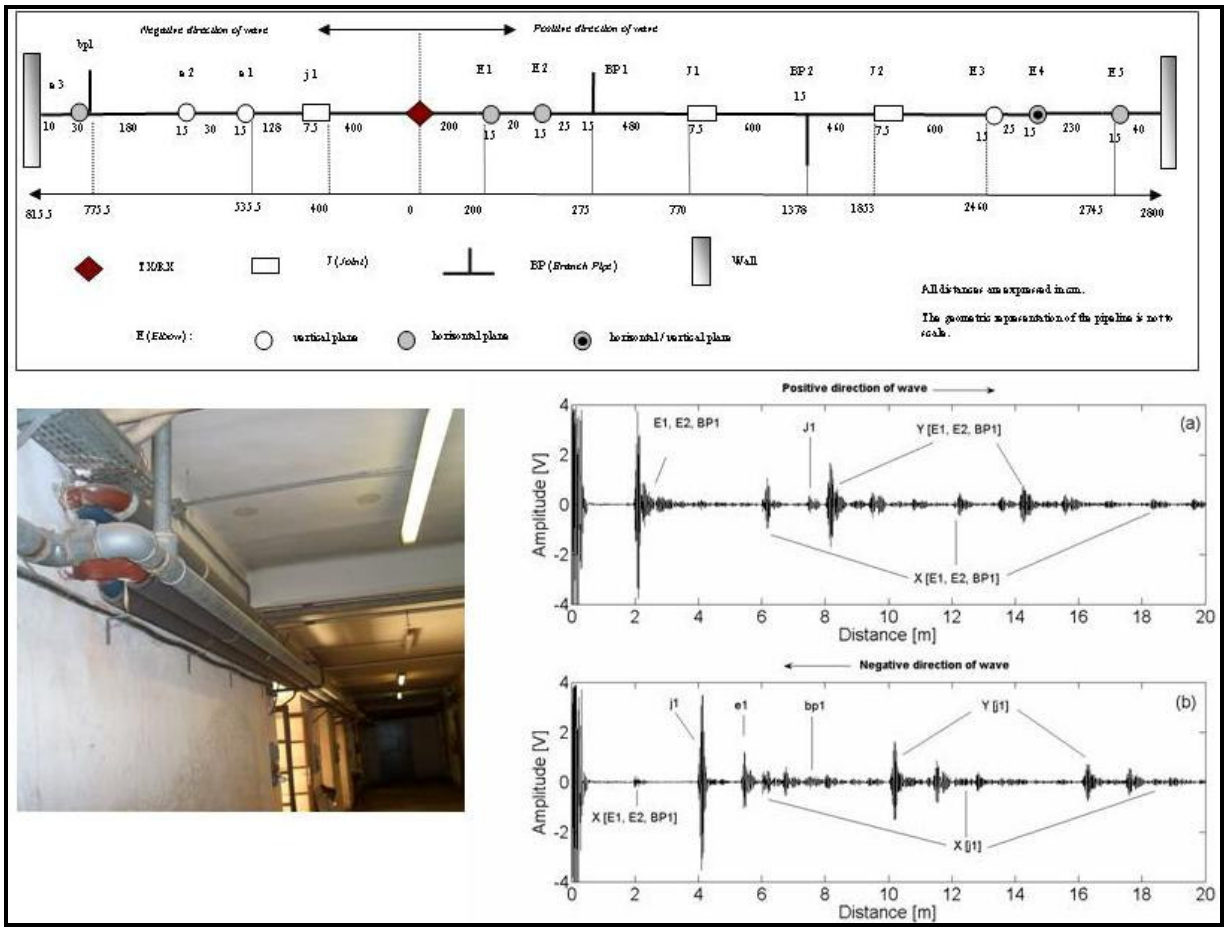

Figure 5-8 Inspection of water pipeline: complexity

The case of the pipes from the heating system was an important test for the magnetostrictive transducer. As it may be seen from Figure 5-9, the signal attenuation due to pipe condition allows inspecting only a few meters (the wave velocity was 3250m/s) from the transmitting transducer. Among the factors thought to be responsible for the high signal attenuation were the high degree of corrosion (visible), the coating type (polyurethane) and pipe position (partially underground). In addition the tests proved that the system could distinguish between two features (welds) distant a few centimetres (about 10 cm in our case) transmitting an

excitation pulse of 32 kHz. Another parameter that has been checked was the changing in the pipe temperature in the range 20-40-60°C. No significant variations in the acquired signal were detected in this case. Defects were not detected in this case as well.

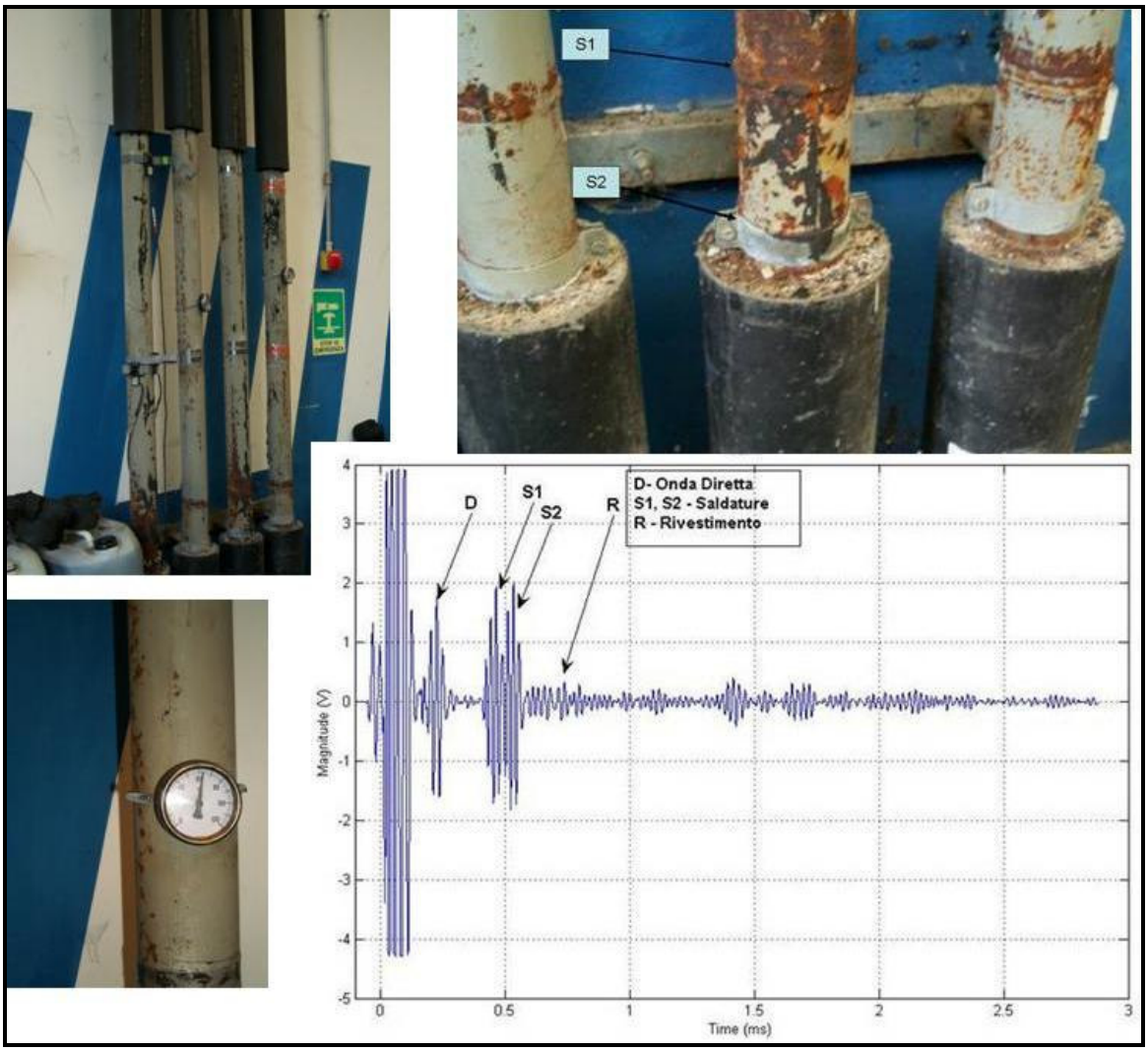

Figure 5-9 Pipelines from the heating system

Buried pipeline inspection

Figure 5-10 shows an example of a buried, bitumen coated section of a gas pipeline at a road crossing. It was inspected using the magnetostrictive sensor. As it may be noticed from the figure, there were some features that could be identified in the signal reflected from the underground section of the pipeline (the lower graphic). However, the features detected weren't confirmed visually, as excavation

of the pipeline couldn't be performed. The inspection range was drastically shortened by the underground pipe position and by the coating type.

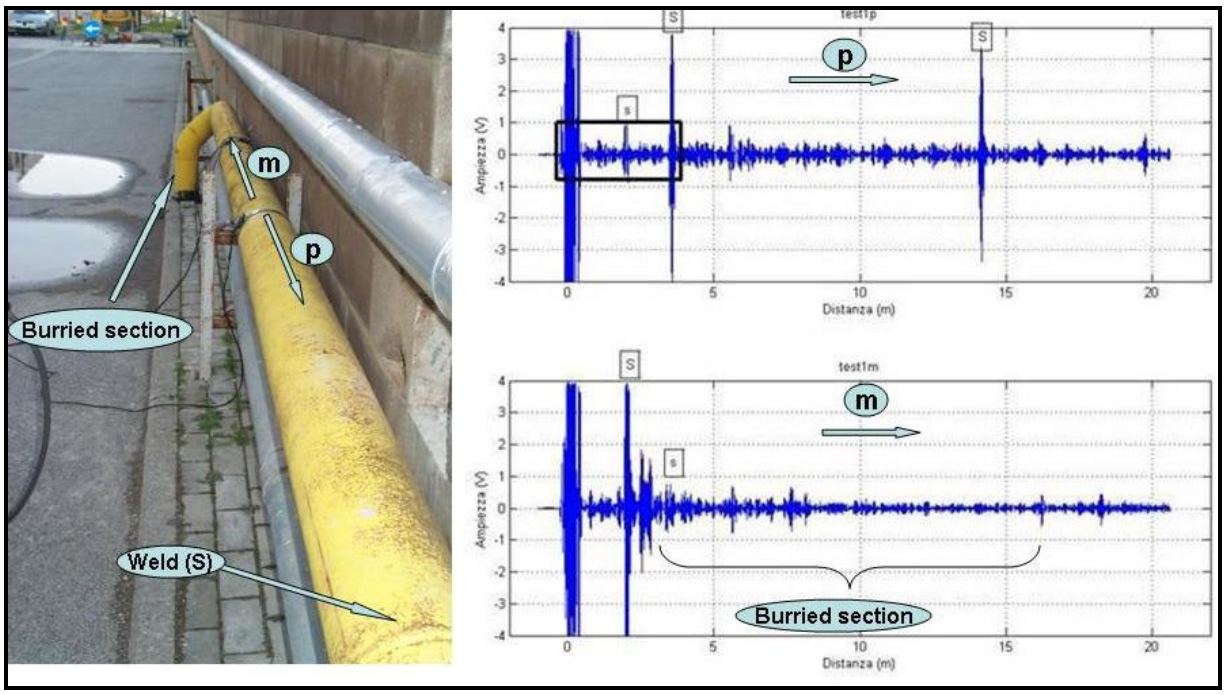

Figure 5-10 Buried pipeline section

Coated river-crossing pipeline

Another inspection was conducted on another in-service gas pipeline that was situated in correspondence of a river crossing, thus inaccessible for classical inspection methods. . The pipeline was coated in polyethylene for its entire length and presented elbows and welds at the two interfaces with the ground. The entire length of the suspended pipeline section was about 10 m.

The test used a 16 kHz impulse and was able to reveal the elbow weld from the opposite side of the pipe section with respect to the sensor's position. The instrument was able to inspect the entire suspended pipeline while only 10 cm of coating were removed in order to place the magnetostrictive transducer.

Figure 5-11 presents the test settings and the resulted RF signal.

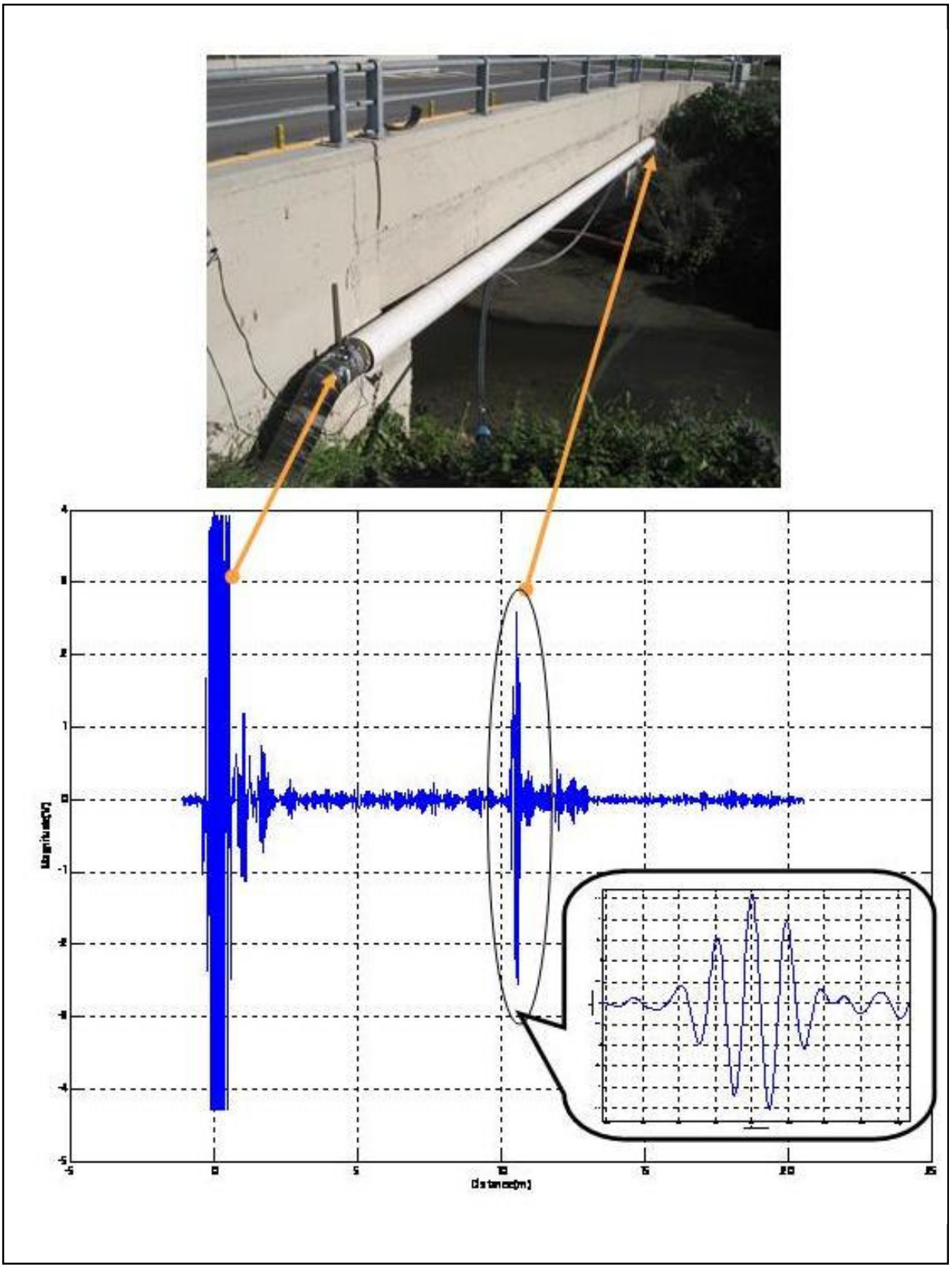

Figure 5-11 Inspection of coated gas pipeline at a river-crossing

5.1.4 Monitoring potential

Monitoring of piping systems is an important issue for the plant integrity management plan. Long-term survey of pipes can detect corrosion in early stages very cost-effectively.

When using the MsS® inspection system, monitoring can be performed by executing several consecutive tests using always the same inspection settings and comparing the results. In the following such a procedure will be detailed.

Figure 5-12 describes two tests performed for the monitoring of an in-line pipeline.

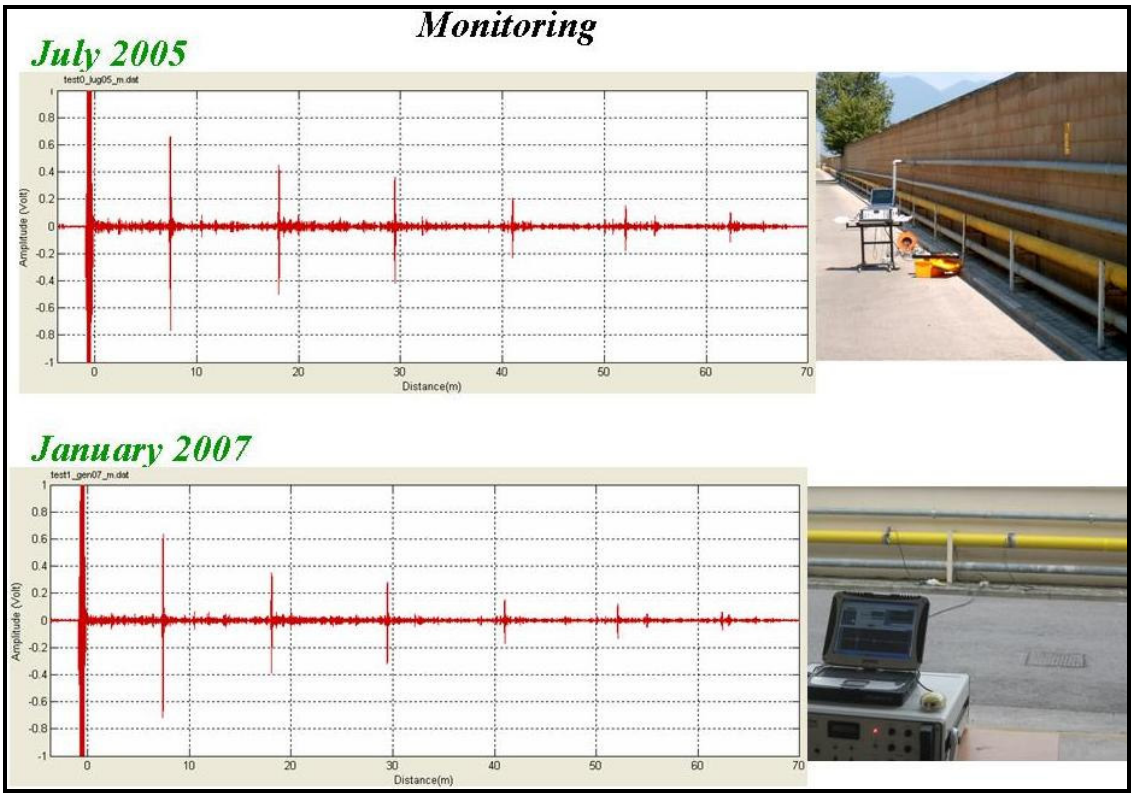

Figure 5-12 Monitoring of gas pipeline: sensor's stability

The very first tests on an in-line pipeline were performed in July 2005. The magnetostrictive strips were bonded to the pipeline, preconditioned and left in place for further tests. The first inspection revealed the main features of the pipeline like welds and joints over a range of about 120m from one location (60m in each direction).

In January 2007 the same magnetostrictive strips as in 2005 were used to inspect the gas pipeline. The acquired signal was found to be similar in shape to the one acquired 18 months before (see Figure 5-12). This result shows the stability of the magnetostrictive sensor over time and allows performing signal subtraction. This procedure involves the initial acquisition of a signal called reference signal. It is going to be used in future investigations when it will be subtracted from the acquired signal in order to reveal small changes in the inspected pipeline geometry (metal loss, cracks or corrosion).

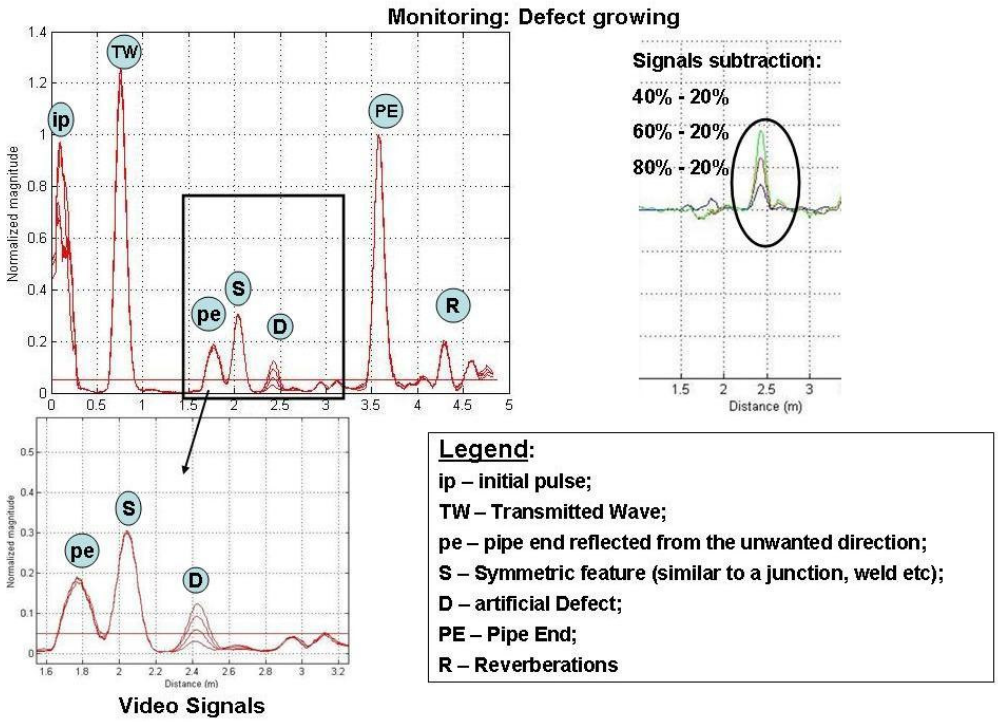

Figure 5-13 Monitoring procedure: signal subtraction to detect defect growth in an 8" steel pipe

An example of signal subtraction can be given for the 8" pipe with the artificial defect of 30 degrees ranging from 20% to 80% pipe wall thickness (Figure 5-13). The video signals corresponding to 4 defect types (20%, 40%, 60%, 80% thickness) are represented on the same graph on the left side of the figure. The reflections corresponding to features which remain constant in size roughly overlap – ex. pipe end (PE) or the symmetrical defect (S). On the right side are represented

the subtracted video signals, the one corresponding to the 20% defect being considered the baseline signal.

An important issue concerning the monitoring procedure is the need to remove the pipe insulation over a small axial section of the pipe (a few centimetres) to make possible the placement of the magnetostrictive component of the transducer. In order to accomplish the security requirements, the pipe to be monitored has to be fully protected by insulation and, as a consequence, the pipe section corresponding to the sensor's location has to be recoated.

Under these circumstances, the ability of the MsS® instrument to monitor the pipeline integrity while the magnetostrictive component (ferromagnetic strip) is completely covered by insulation has been tested.

Figure 5-14 shows the test settings and results for the case of a polyethylene coated pipe. The test steps were as it follows:

- the original pipe coating (the yellow material in the figure) was removed;
- the ferromagnetic strip was preconditioned and bonded on the pipeline;
- the pipe was recoated using an ordinary polyethylene tape (the dark material in the figure);
- the ribbon coils were placed over the coating and the signal was acquired.

In the resulted signal 5 multiple reflections of the pipe end were identified. It means that around 60 meters of coated pipeline in similar conditions can be inspected and monitored.

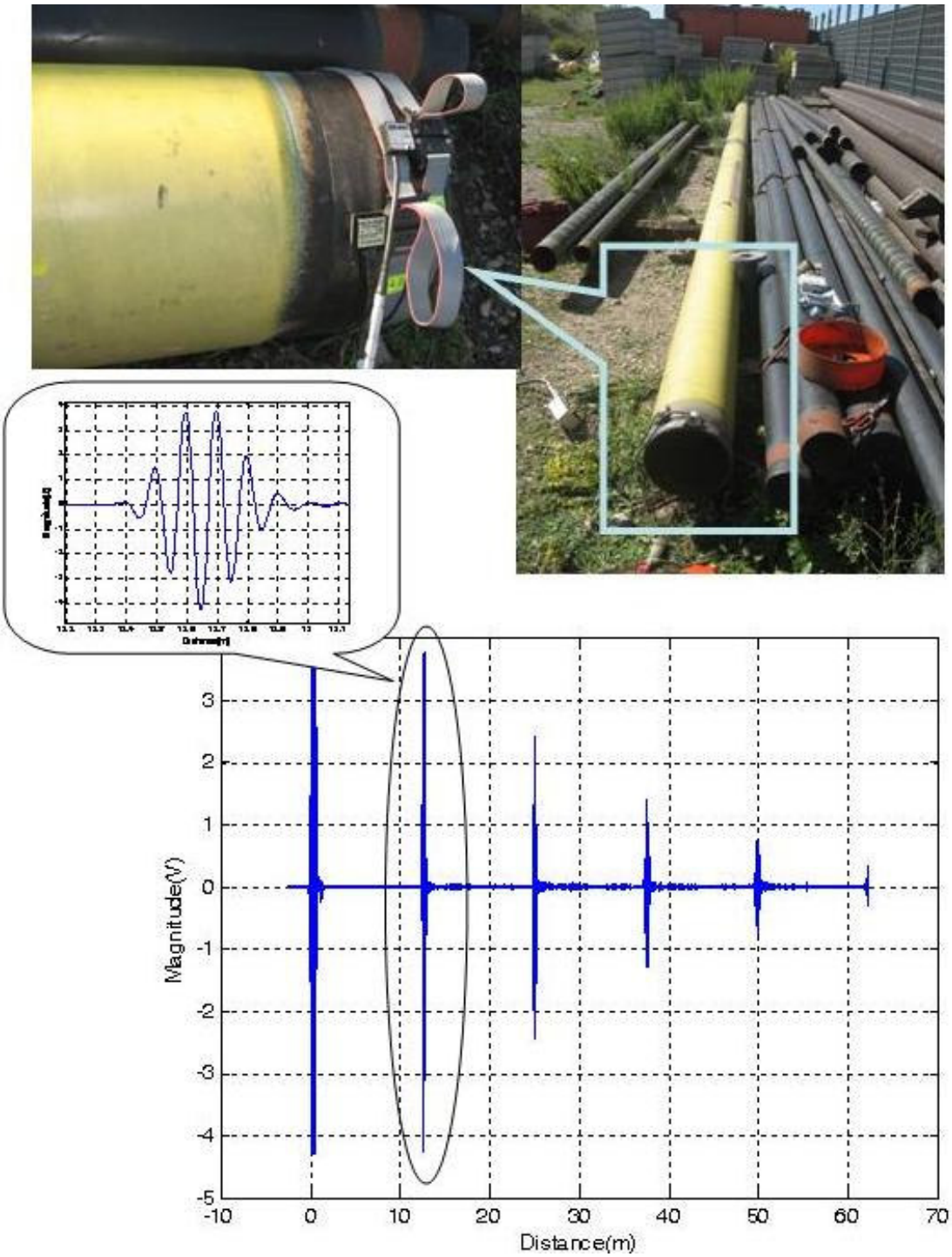

Figure 5-14 Monitoring of PE coated pipes

5.2 Conclusions

The tests that have been described in the sections above outlined some of the advantages of the MsS® inspection system as well as its main drawbacks and limitations. Some of them will be listed below and possible solutions will be suggested.

5.2.1 Advantages of the MsS® guided-wave technology

Good sensitivity

The tests outlined a good sensitivity for detecting small cross-section defects. A 3.3% artificial defect was detected in a laboratory test. Moreover, slight increases in the defect dimensions were detected.

Long Range

In optimal conditions 120 meters of pipeline were inspected. However, the inspection range can be affected by several factors, for instance general corrosion level, the large number of pipe features and coating material.

Monitoring

The sensor's stability has been confirmed by performing two identical tests at six months time difference. Long term condition monitoring of pipelines is therefore achievable with UGW using the magnetostrictive sensor.

Monitoring under PE coating

Tests demonstrated that the magnetostrictive technology is capable to generate UGW under the polyethylene insulation without affecting pipeline protection against corrosion over the sensor location area.

5.2.2 Limitations

Signal attenuation

As explained in the previous examples, signal attenuation can be a consequence of the high state of corrosion of the pipeline, of its coating type (bitumen, polyurethane or polyethylene) or its position – buried or above ground.

In order to overcome such problem, several solutions have been proposed. In the article “Effects of the orientation of magnetostrictive nickel strip on Torsional wave transduction efficiency of cylindrical waveguides” [27] the authors suggest an oblique orientation of the magnetostrictive strips with respect to the circumferential direction to increase transduction efficiency. The use of another magnetostrictive material – Co ferrites or the optimisation of the number of turns in the receiving coil would be also methods to increase sensor’s sensitivity [28]. In addition, more parallel strips can be used to increase the magnitude of transmitted signal.

Discrimination between joints, welds and defects

Defects are usually asymmetrical discontinuities like corrosion, notches or longitudinal or transversal cracks found on pipelines. On the other hand, features that are normally part of the pipeline, like welds, joints or elbow joints have mostly a symmetrical shape with respect to the longitudinal axis of the pipeline. Therefore it is mandatory for an inspection instrument to be able to distinguish among an asymmetrical and a symmetrical feature. In the present commercial version, MsS® 2020 inspection instrument cannot perform signal analysis that discriminates between symmetrical and asymmetrical features. That means that an echo or a reflection of the transmitted impulse is a representation of the entire circumference at a given axial distance. As a result it carries no information on defect’s axial

Defect identification and characterization

This issue is still a research subject for all guided-wave techniques and generally for all the NDE techniques.

Our solution involves special software to solve inverse problems, which is based on artificial neural networks. The software uses as inputs the signals acquired locally by the innovative magnetostrictive sensor.

CHAPTER 6 NUMERICAL SIMULATIONS OF UGW AND DEVELOPMENT OF SIGNAL PROCESSING ALGORITHMS

6.1 Simulations

Numerical simulations are necessary in order to better understand the phenomenon of UGW propagation in pipelines. Moreover, the scattering of incident UGW by discontinuities having various geometries need to be studied, thus a large number of simulated defects must be available.

6.1.1 Validation of the simulation software

Commercial FEM (Finite Element Model) simulation software was used. The software was validated by comparing simulation results with experimental data. Figure 6-1 and Figure 6-2 show the simulated test as well as experimentation on a 4" pipe with a welded patch [29]. Both experiment and simulation had the same settings (wave mode, frequency, number of cycles) and the comparison shown in Figure 6-1 reveals a good agreement between simulated and measured data.

This and other tests proved that the simulation software was reliable and the numerical results could be used for the research and further developments.

The simulated waves have a 2-cycle sine amplitude modulated with a Hanning window, similar to the impulse generated by the MsS instrument. The wave mode is torsional fundamental. Echoes generated by simulated defects were validated by further experiments.

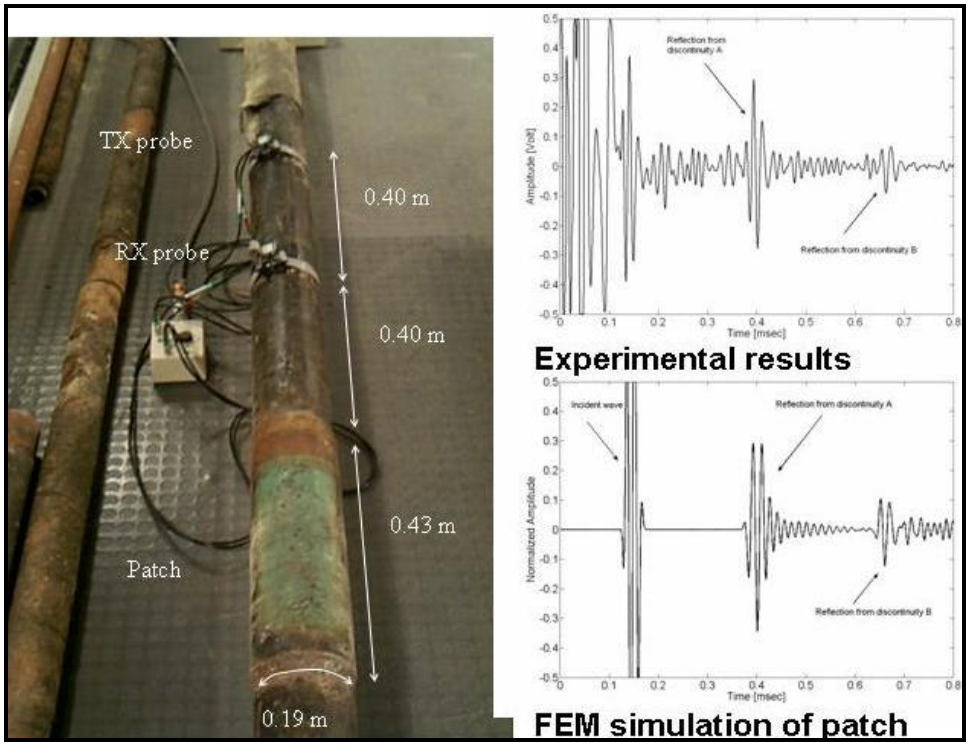

Figure 6-1 Experimental and simulated pipe with patch

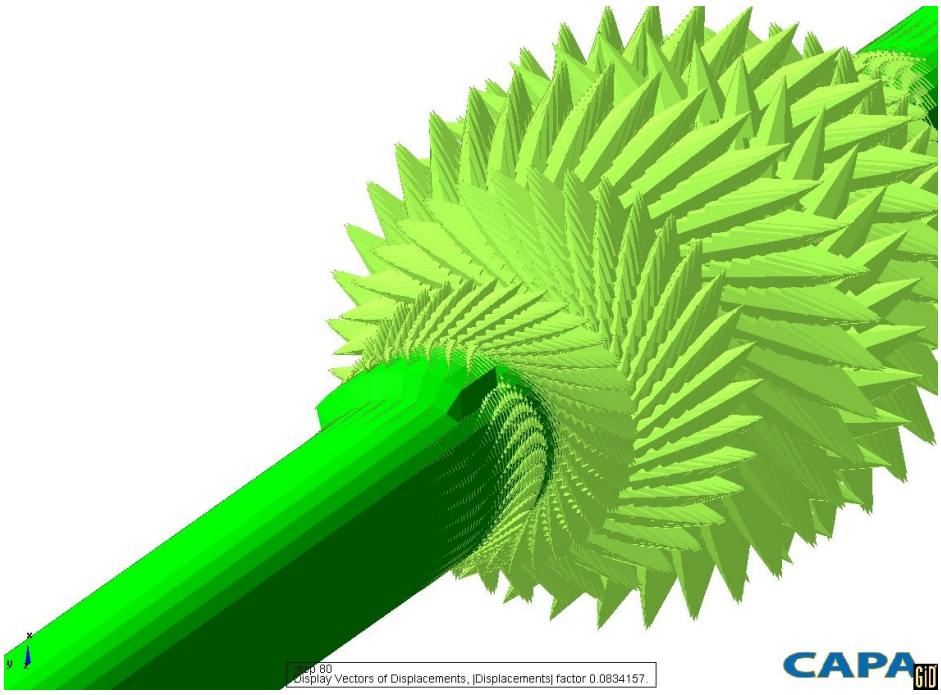

Figure 6-2 Simulated torsional wave (vectorial representation) interacting with patch

With the simulation software validated, further simulation campaigns were started to gain a deeper understanding of interactions between discontinuities and guided waves in pipelines.

6.1.2 Test settings

A first set of simulations has been carried out on the tube shown in Figure 6-3. Table 6-1 lists the geometrical characteristics of the simulated defects.

Table 6-1 Geometrical characteristics of simulated defects

Axial position (m)	Axial extent (x λ/8)	Radial extent (% of pipe wall thickness)	Circumferential extent (deg.)
0.4	0	+10% , -10%	10
0.8	5	+30%, -30%	20
1.2	1	+50%, -50%	30
1.6	1.5	+70%, -70%	40
-	…..	+90%, -90%	….
-	16	-	360

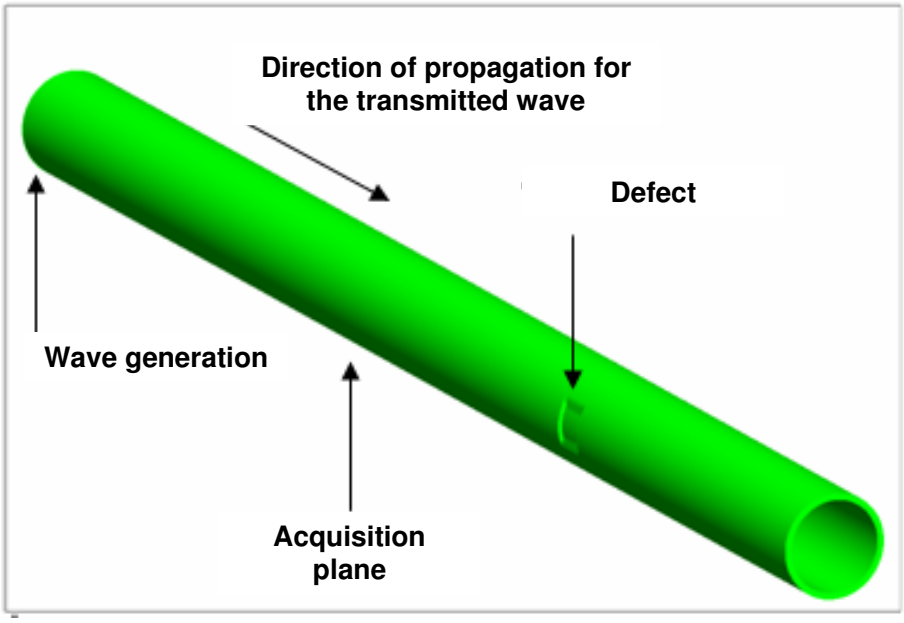

Figure 6-3 Simulated pipe with defect using CAPA® software

The other test settings are listed below:

- Pipe characteristics:

  Length: 2.4m;

  Diameter: 8''

  Internal radius: R_a=10.39 cm

  External radius: R_b=10.90 cm

  Wall thickness: 5.1 mm

- Transmitted wave:

  Wave generation plane: z=0

  Transmitted impulse: 5 sinusoidal oscillations amplitude modulated, having the frequency f=32 kHz

  Wave mode: torsional

  Velocity of propagation: c_T=3250 m/s

Wavelength: $\lambda = \frac{c_T}{f} = 10{,}16cm$

Figure 6-4 sketches the main test settings, while Figure 6-5 shows the simulation of the transmitted impulse. It was calculated to reproduce the actual measured signal from the MsS instrument as the average over the circumference in the acquisition plane.

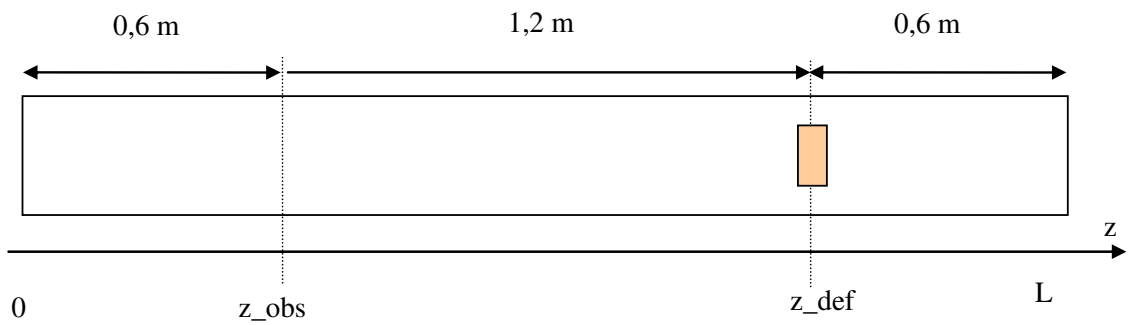

Figure 6-4 Test settings

- Defect geometry:

  Centrated in $P_d=(R_d, 0, z_{def})$, where: z_{def}=1.8 m, $R_d>R_a$, $R_d<R_b$(metal loss), $R_d>R_b$ (metal gain).

  Parameters that characterise the defect extent:

  Radial extent:

$$t_d\% = \pm\frac{|R_b - R_d|}{R_b - R_a}\cdot 100$$

  Axial extent: Δz_d ;

  Circumferential extent: $\Delta\theta_d$;

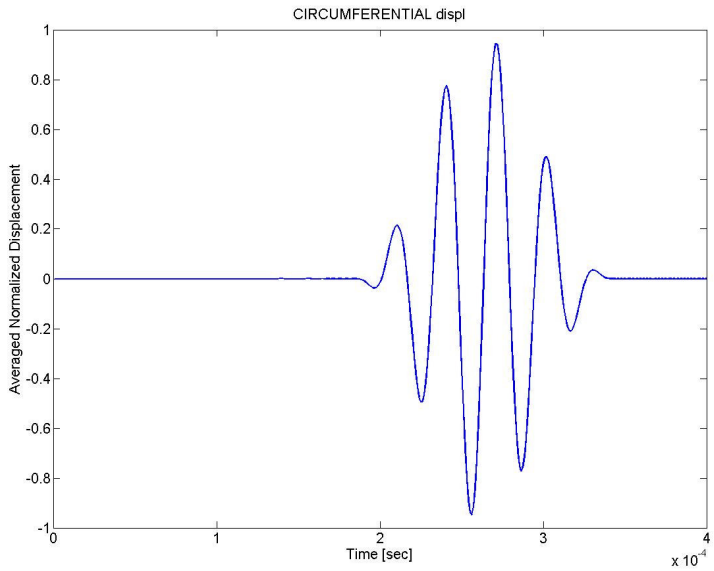

Figure 6-5 Transmitted wave detected in the plane z = z_obs = 0,6 m

- Acquisition:

  72 points for signal acquisition uniformly distributed (every 5°) over the external pipe circumference (Figure 6-6) in the plane $z_{obs} = 0{,}6m$.

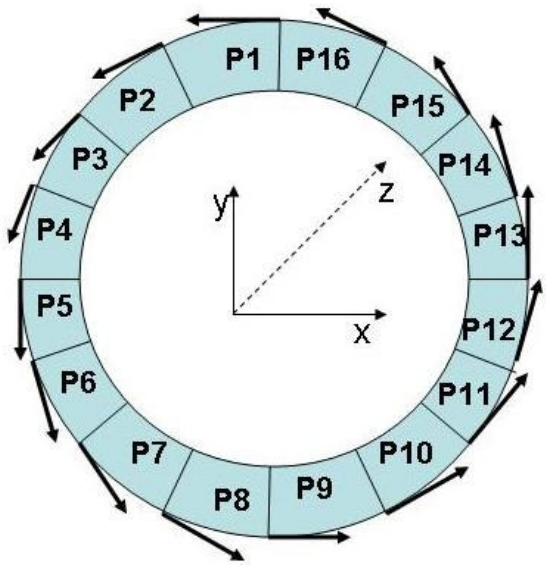

Figure 6-6 72 circumferential points for local displacements in the pipe-wall cross-section for a torsional wave

6.1.3 Results

The results of the simulations performed by varying the defect parameters listed in Table 6-1are shown in the figures below. The transmitted and acquired waveforms correspond to the average circumferential displacement of the reflected wave. The average is performed over the 72 circumferential acquisition points present in the acquisition plane.

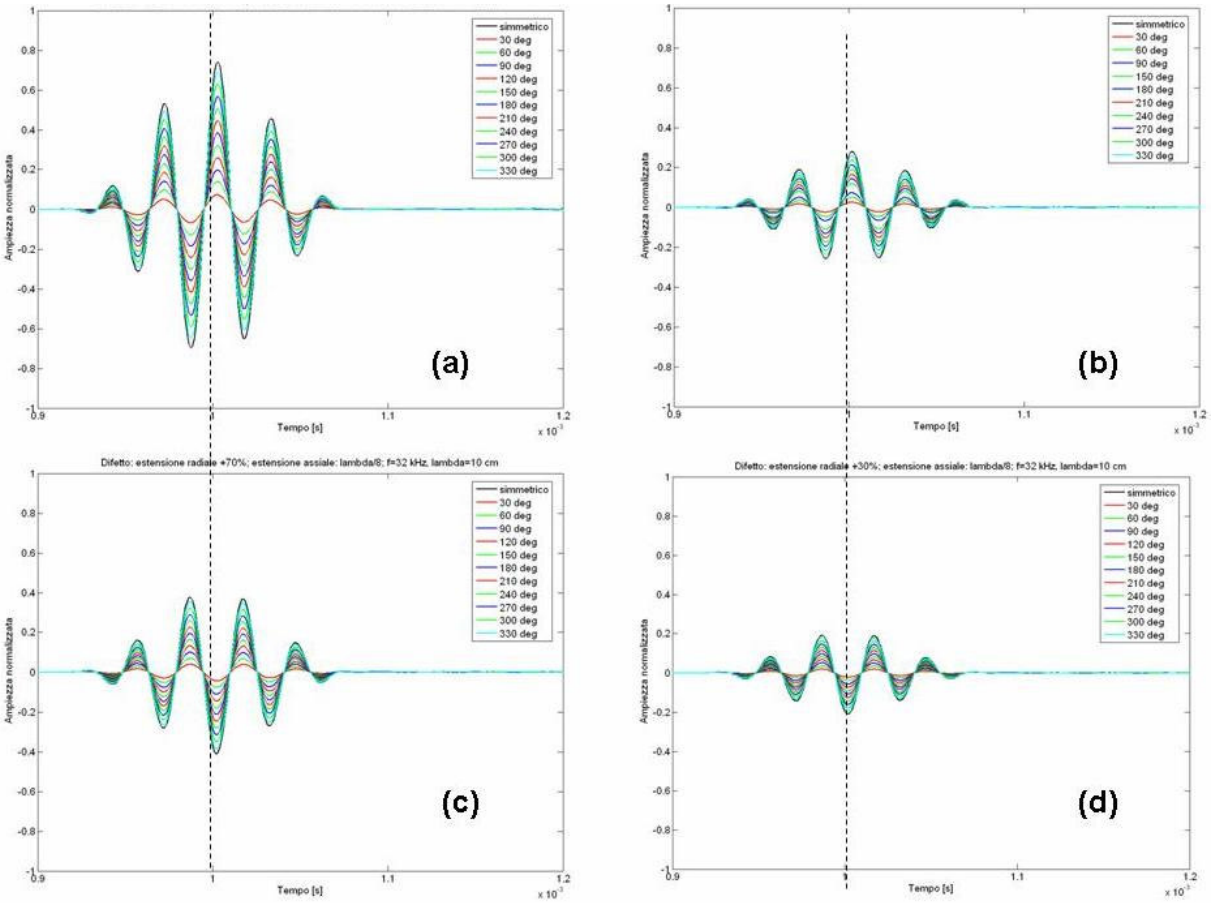

Figure 6-7 Simulation results: $\Delta z_d = \lambda/8$, $\Delta\theta_d$ = 30, 60, ….,330, 360 deg, t_d = -70% (a), t_d = -30% (b) t_d = +70% (c) t_d = +30% (d)

Figure 6-7 shows time-amplitude representations of simulated reflected waves. The defects considered had various geometries as specified in the figure. Figures (a) and (b) correspond to -70% and -30% radial extent respectively, while figures (c) and (d) correspond to +70% and +30% radial extent respectively. The main parameter to be varied was the circumferential extent. To be noticed that the

difference between the metal-loss defects and metal-gain defects is the change in sign of the reflected wave.

Another observation to be made is that –in the case of averaged acquisition- changes in defect's circumferential extent have no effect over the shape or frequency of the reflected wave, but only variations in amplitude.

Figure 6-8 shows reflected waves from defects whose axial extent was varied from λ/2 to λ, being λ the wavelength. In this case, due to the increased distance between the two edges of the defect two distinct reflections are generated.

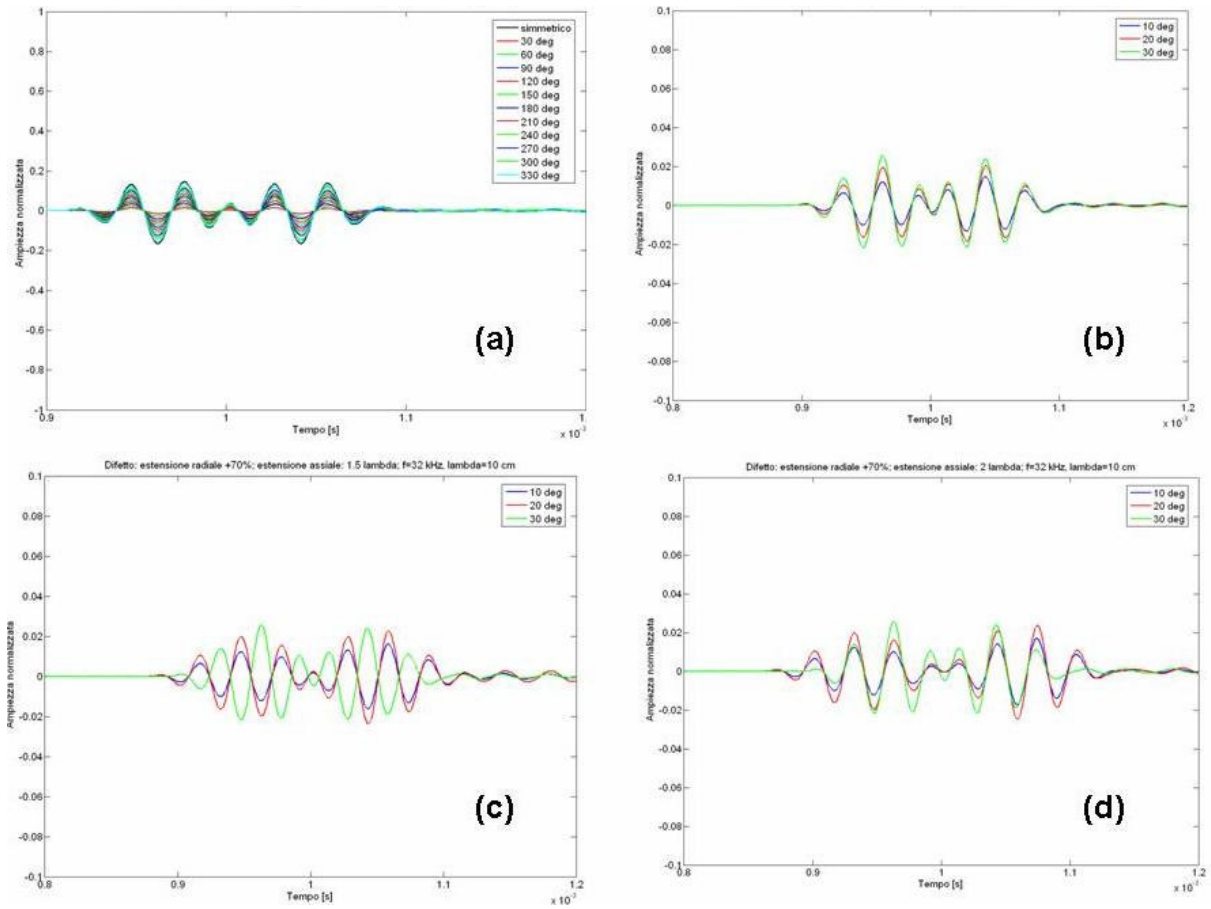

Figure 6-8 Simulation results: t_d = +70%, $\Delta z_d = \lambda/2$, $\Delta\theta_d$ = 30, 60, ….,330, 360 deg (a), t_d = +70%, $\Delta z_d = \lambda$, $\Delta\theta_d$ = 10, 20, 30 deg (b), t_d = +70%, Δz_d = 1.5 λ, $\Delta\theta_d$ = 10, 20, 30 deg (c), t_d = +70%, Δz_d = 2 λ, $\Delta\theta_d$ = 10, 20, 30 deg (d)

6.1.4 Conclusions

The analysis of the simulation results outlined how reflected wave averaged over all the circumferential acquisition points depends on the defect's geometrical characteristics: axial, radial and circumferential extent. Considering the other parameters unchanged, these dependences can be listed as it follows:

- the amplitude of the reflected wave increases when increasing the radial or circumferential extent of the defect;
- the impulse shape and frequency don't exhibit any changing when interacting with defects having low axial extent;
- impulse duration depends on the distance between the two defect edges, while impulse separation can be observed when the axial extent of the defect is larger then λ/2.

The signals resulted from the simulations described have been used in the signal processing methods that will be explained in the further sections.

6.2 Signal processing algorithms for the UGW signal averaged over the circumference in the same pipe-wall cross-section

Signal analysis was conducted in time, frequency and wavelet domain to determine criteria for the identification of the geometrical characteristics (axial, radial and circumferential extensions) of discontinuities detected in the pipe wall.

6.2.1 Time domain analysis: axial extent estimation

A first criterion to estimate a defect's axial extent is based on the interference of the reflected waves from the axial edges of defects.

The example shown below is for several defects having two different circumferential extents (30 and 240 degrees) and axial extent ranging from λ/8 to λ.

In Figure 6-9, the ratio T'/T is represented as a function of defect length, where T is the time duration of the transmitted impulse, while T' is the duration between two

major peaks of the reflected impulse. The trend is the same for both circumferential extents. For defects whose axial extent ranges from λ/8 to λ/2 the trend is exponential (interference without impulse separation), and linear for other extents (separation of echoes).

Another method was the evaluation of the width of the peak in the visual signal representation. The measurement was done at half peak amplitude, in correspondence of an echo (Figure 6-10) and related to the wavelength.

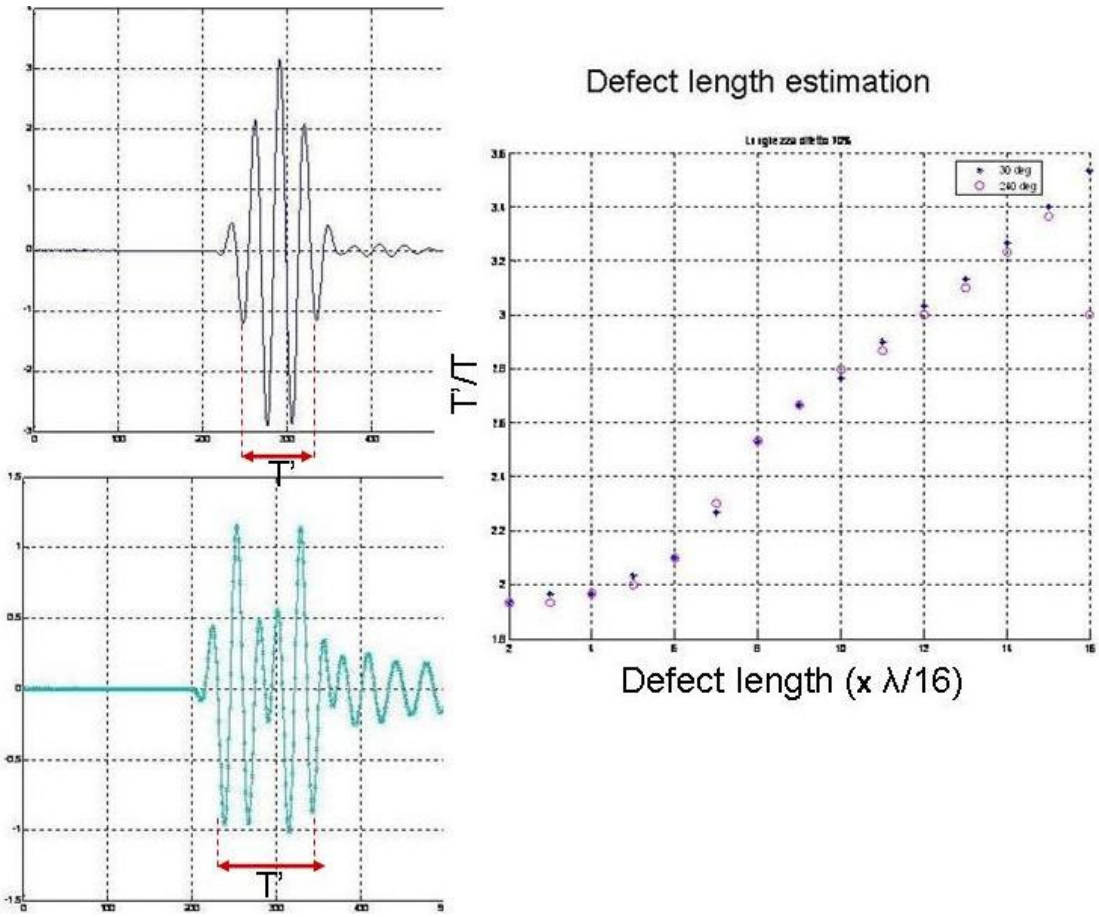

Figure 6-9 Simulated reflections for two defect lengths and length estimation

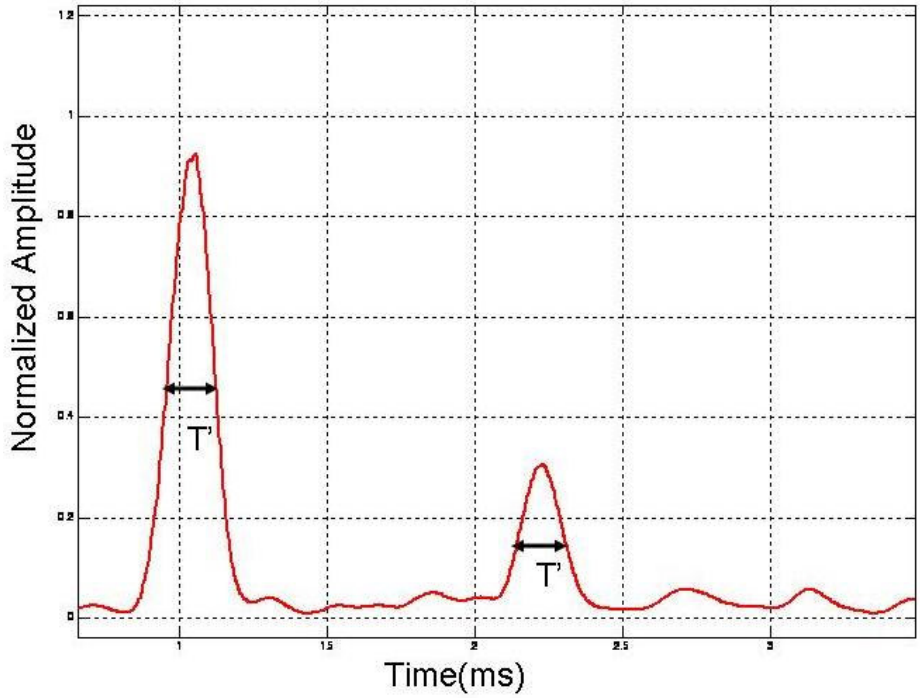

Figure 6-10 Estimation of the axial extent using the video signal

6.2.2 Fourier domain analysis

A frequency domain analysis has been performed to asses the effect that flaw's cross-sectional area has upon the magnitude response of the reflected wave.

In [18], a two-port representation has been determined considering the frequency spectrum of the input and output signals. The transfer function (frequency response) of the two port equivalent has been computed and evaluated. To size the defects gain-band product (GBP) was used, being defined as product among a useful frequency band between 40 and 70 kHz and the average gain for this band (Figure 6-11 (a)). Figure 6-11 (c) shows that GBP cannot be related to defect volume. The poor information that GBP brings on the defect volume is due to the axial dimension of defects that is not proportional to the amplitude of the reflected signal for a torsional guided wave. This is confirmed by the trend of gain-band product shown in Figure 6-11 (b). The scatter plot shows that the cross-sectional area is more tightly related to GBP, and its sizing can be detected within an error

range of 40%. The errors are likely due to the uncertainty on the axial length of the defect.

Results have shown that various defects having different geometries, but with the same cross-sectional area have similar magnitude responses, though similar gain-band product. This technique provided a good estimation of the defect's cross-sectional area. On the other hand, axial dimension and consequently volume of defect could not be sized by using this technique.

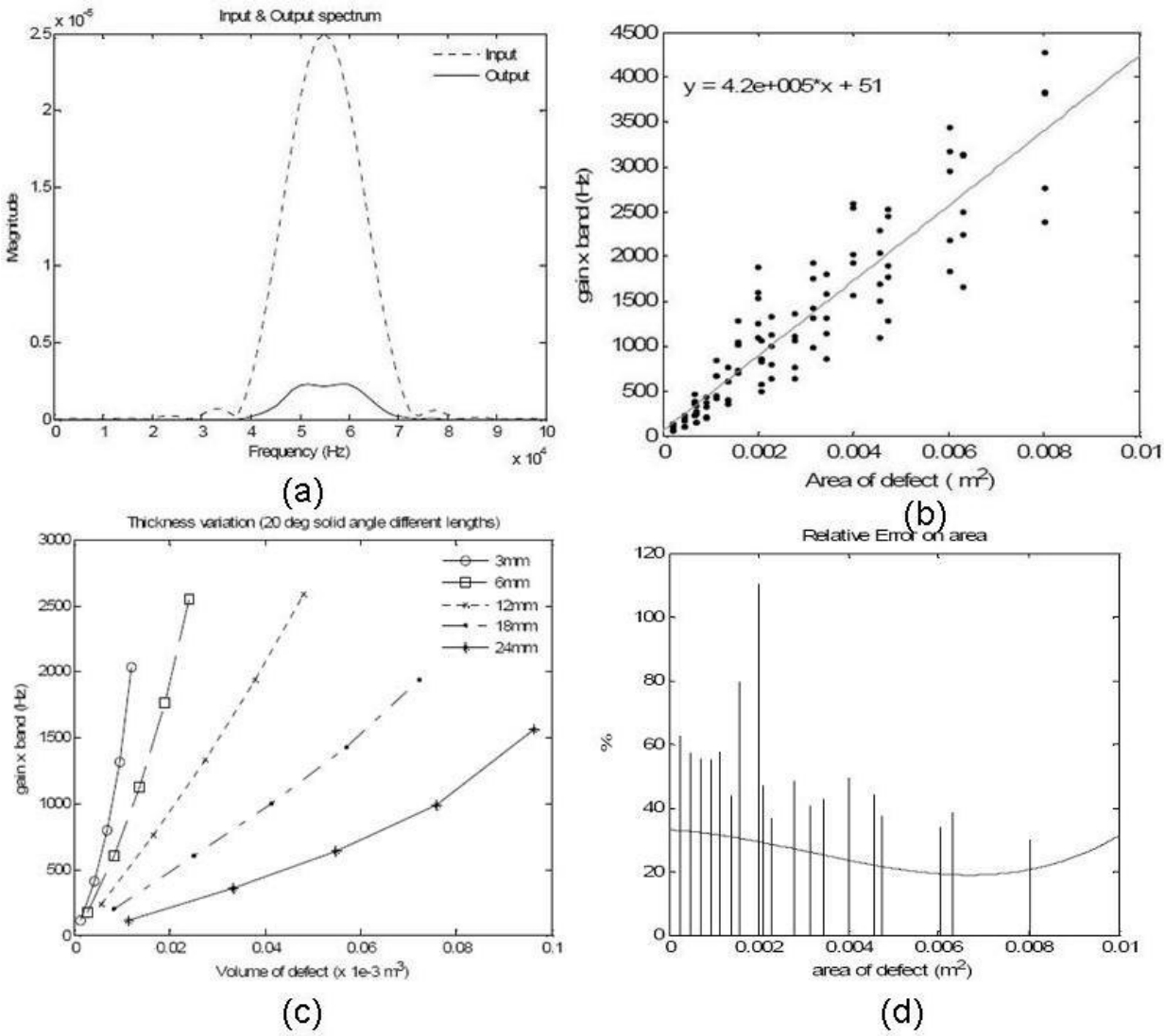

Figure 6-11 Input and output spectrum (a), PGB vs. dimension of cross-sectional area of the Defect (b), PGB vs. volume of the Defect (c) and error range for the cross-sectional area estimation

6.2.3 Wavelet analysis

In [18] Wavelet Expansion (WE) was used as a tool for defect characterization. Through WE a transfer function represented by a matrix of constant coefficients (W) was constructed. The identification of this matrix could be obtained from data in the time or frequency domain. Furthermore a two-port equivalent was considered, with the matrix W relating the WE of input and output quantities. The norm of this matrix was plotted against various defect dimensions. Figure 6-12 shows the representation of the norm of W as a function of solid angle (circumferential extent) and as a function of flaw thickness (radial extent).

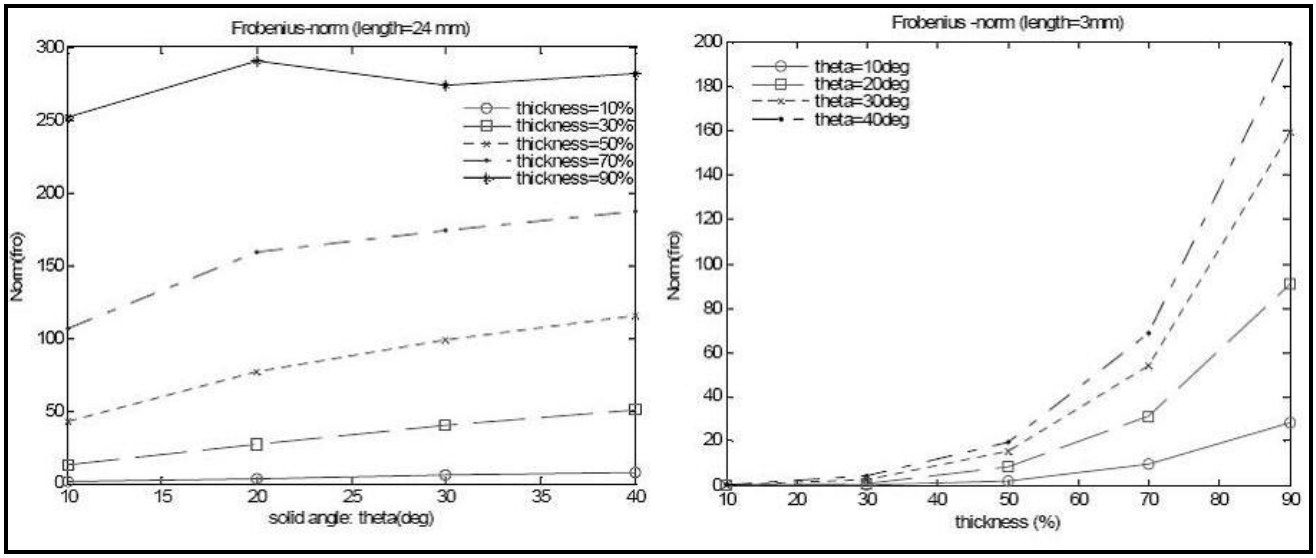

Figure 6-12 Norm of Matrix W for various defects

The results proved that the W matrix was more sensitive to the radial extent of the defect than to its angular or axial extent and therefore could be a useful instrument for the evaluation of at least one dimension of the flaw.

6.2.4 Conclusions

The analysis of the signal processing methods described in the previous sections have proved that the signal obtained as an average over the entire circumference of local displacements can provide some information on the defect geometry.

However, in order to increase the precision of classification algorithms, more detailed information is needed. The possibility to extract this information from “local” circumferential data (as in the case of the PZT collar transducer) has been investigated.

6.3 Signal processing algorithms for sets of local UGW signals corresponding to the same pipe-wall cross-section

The development of algorithms for UGW signal processing proceeded with the evaluation of multiple signals acquired in the various points of the circumference, all in the same circumferential plane.

6.3.1 Simulations

The pipe circumference was divided in 72 points similar to those in Figure 6-6. In each of these points the returning signal was analysed. The simulated defects were the same as listed in Table 5-1.

An example of local UGW acquisition is given in Figure 6-13. Both graphics present reflected signals that correspond to each circumferential point located in the same acquisition plane. While the first reflection from the signal is due to a non-axis-symmetric defect, the second one is reflected by a defect that is symmetrical with respect to the pipe axis. In this last case, all the 72 circumferential waves are overlapped while in the first reflection, differences in amplitude and phase shifts around the average wave (represented by the thick red line) are clearly noted.

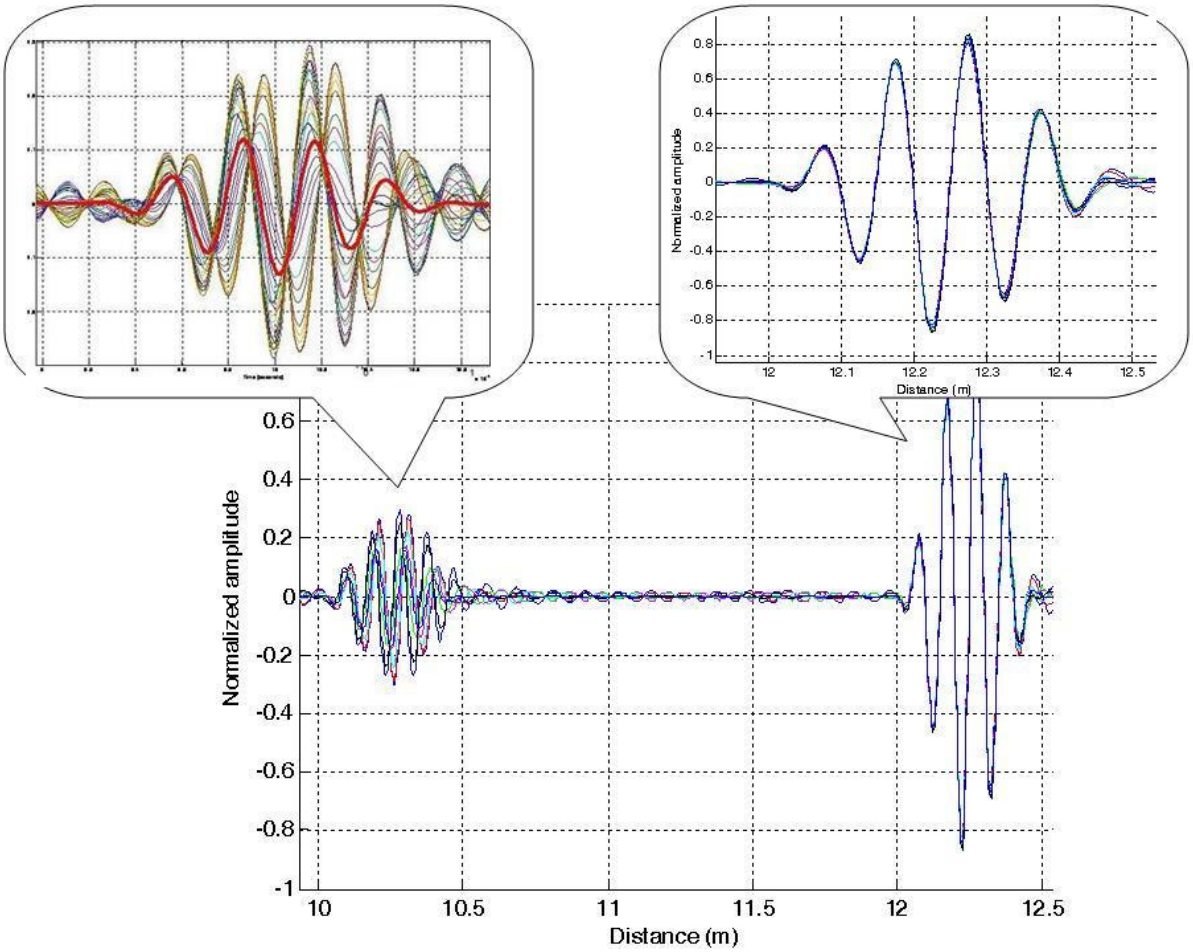

Figure 6-13 Acquisition in 72 circumferential points for: a non-axial-symmetric defect (t_d = +70%, $\Delta z_d = \lambda/4$, $\Delta\theta_d = 90^o$)- left; reflection from the pipe-end – right.

These results confirm the fact that local circumferential signals carry the information on the geometry of the discontinuity that generated them. However advanced methods are needed to classify detected discontinuities and to characterize defects.

6.3.2 Neural network approach for defect characterisation

One way to classify and characterize defects is the neural network approach. The first method [31] consisted in performing the extraction of time and frequency features from simulated ultrasonic guided waves and the proper reduction of the number of these features. Then a neural network classification evaluates the

dimension of the flaws in the pipe under test. The results showed low error rates for all classes considered (Figure 6-14).

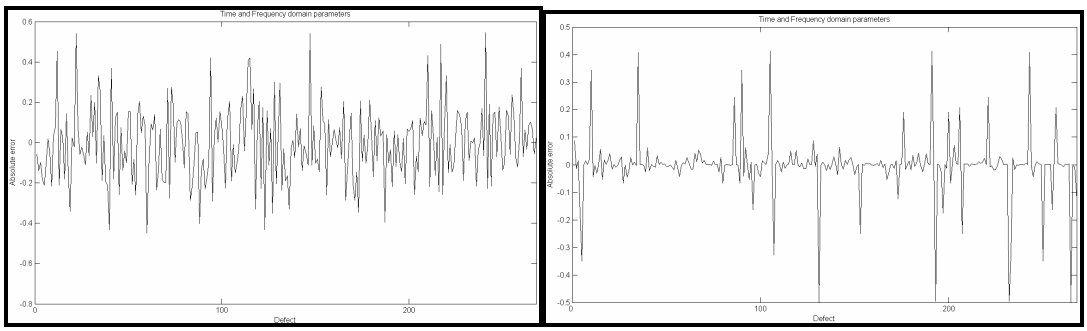

Figure 6-14 Classification error: left- for the angular size of the defects, right - for the axial size of the defects

The second method [32] considered a signal database for the training and, validation. This test set that has been obtained by using the finite element method as well. For this set of data, FFT and Principal Component Analysis (PCA) have been sequentially applied to the time signals without performing feature extraction. The time signals have been firstly processed by FFT. Then PCA has been used to reduce the number of the inputs. It has been demonstrated that the defect depth influences the FFT amplitude, while the defect width influences the shape of the waves, and, consequently, the FFT phase. Thus, PCA has been applied to the FFT amplitude components obtaining 8 inputs to be used to predict defect depths, with a loss of information of 1%. The PCA has been applied to the FFT phase components obtaining 4 inputs to be used to predict defect width, with a loss of information of 1%.

Depth [mm]	Width [mm]
0.55	63
0.55	123
0.55	210
1.65	60
1.65	120
1.65	180
2.75	45
2.75	105
2.75	165
3.85	30
3.85	90
3.85	150
4.95	15
4.95	75
4.95	135

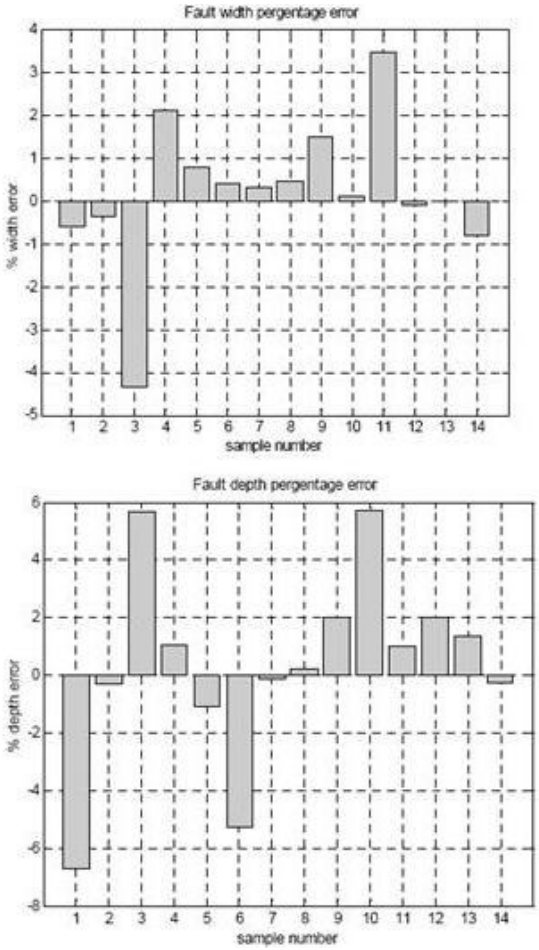

Figure 6-15 Simulated Defects and Neural Network performance

The network performances have been tested on the test set in table shown in Figure 6-15. In particular, the percentage errors of the neural network trained for the depth fault classification are less than 6.1%, with an average error of 5.4%. The percentage errors of the neural network trained for the width fault classification are less than 5.9%, with an average error of 1.5% (Figure 6-15). Also for torsional mode excitation, the performance of the neural network models for the fault classification was very encouraging, offering good classification accuracy.

6.3.3 Phase diagram and Magnitude profile

Another method used for the classification of UGW echoes was the evaluation of the angular profiles in terms of magnitude and phase of signals acquired in the circumferential points.

The use of the angular profiles as an instrument for defect identification with UGW has been proved previously. In [30], Rose at all, have studied the possibility of tuning of UGW angular profiles for the L(M,2) UGW mode. An angular profile is composed of magnitude and phase information. The first one is a representation of circumferential amplitude distributions of displacements, while the second one sketches circumferential phase distributions of displacements.

Phase diagram

In our case the angular profiles of phase are a representation of the phase shift values of each circumferential echo with respect to the average echo.

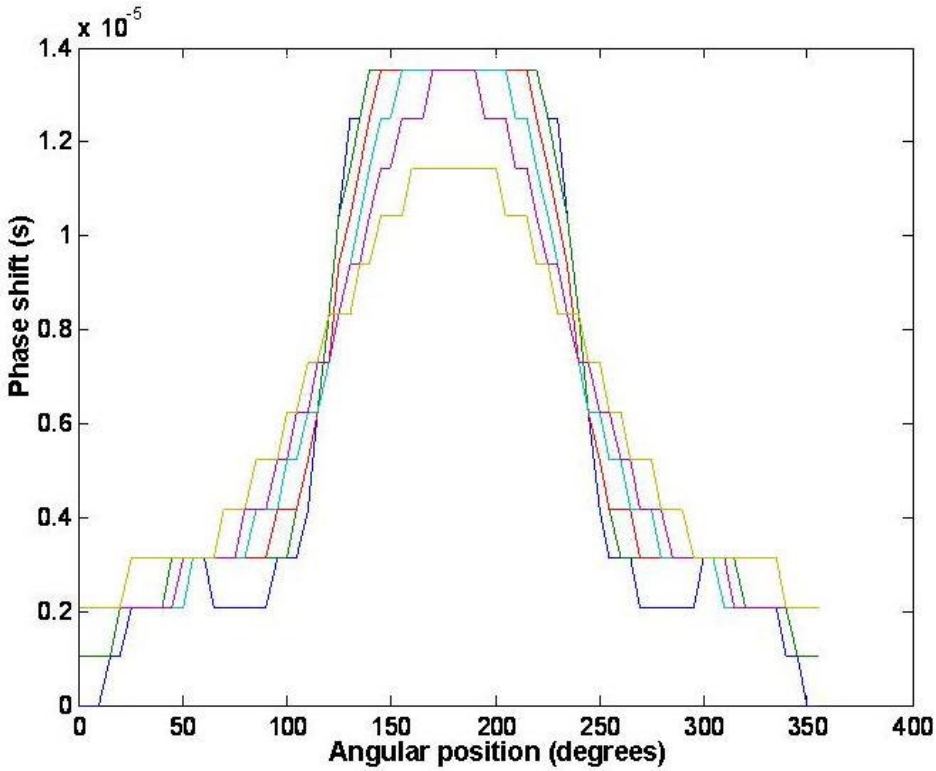

Figure 6-16 Angular profiles: Phase shifting with respect to the average acquisition

Figure 6-16 presents the delay between signals shown in Figure 6-13 and the average signal. The delays (phase shifts) are represented versus angular position of the acquisition. In the same figure, cases of defects having an increasing circumferential extent are shown. The phase shift decreases when the

circumferential extent tends to 0° or 360°, thus a symmetric discontinuity. In the case of symmetric discontinuity, the phase shifts are all nulls.

Magnitude profile

The angular profiles of amplitude were computed from the normalized spectral amplitudes in correspondence of the defect echo. The procedure can be described as it follows:

1st step: Convert the RF data corresponding to the ith circumferential acquisition into "video data" by computing spectral amplitudes over the entire length of the signal; this operation is done for each circumferential point (θ_i) acquisition.

2nd step: Take the maximum amplitude (m_i) in the time window (Δt) in the correspondence of the defect echo. The time window has the same duration as the transmitted impulse. This operation must be performed for each circumferential point acquisition.

3rd step: Represent the angular profile in Cartesian coordinates or polar coordinates. Every angular point in the representation is the normalised amplitude found at step2: $P=f(m, \theta)$.

The first two steps in computing an angular profile of amplitude for a given echo are briefly explained in Figure 6-17. The final results, i.e. Cartesian and polar representations of angular profiles of amplitude are described in Figure 6-18 (a) and (b) respectively. In the case of the Cartesian graph, angular profiles of amplitude are represented for defects having circumferential extent ranging from 30 to 360 degrees that were simulated on an 8'' pipe. The polar representation is corresponding to an 8'' pipe with a defect having a circumferential extent of 40 deg. The other geometrical characteristics for both cases were $\lambda/8$ axial extent and 70% radial extent. The circumferential position of the simulated defect was in correspondence of the 0° acquisition point.

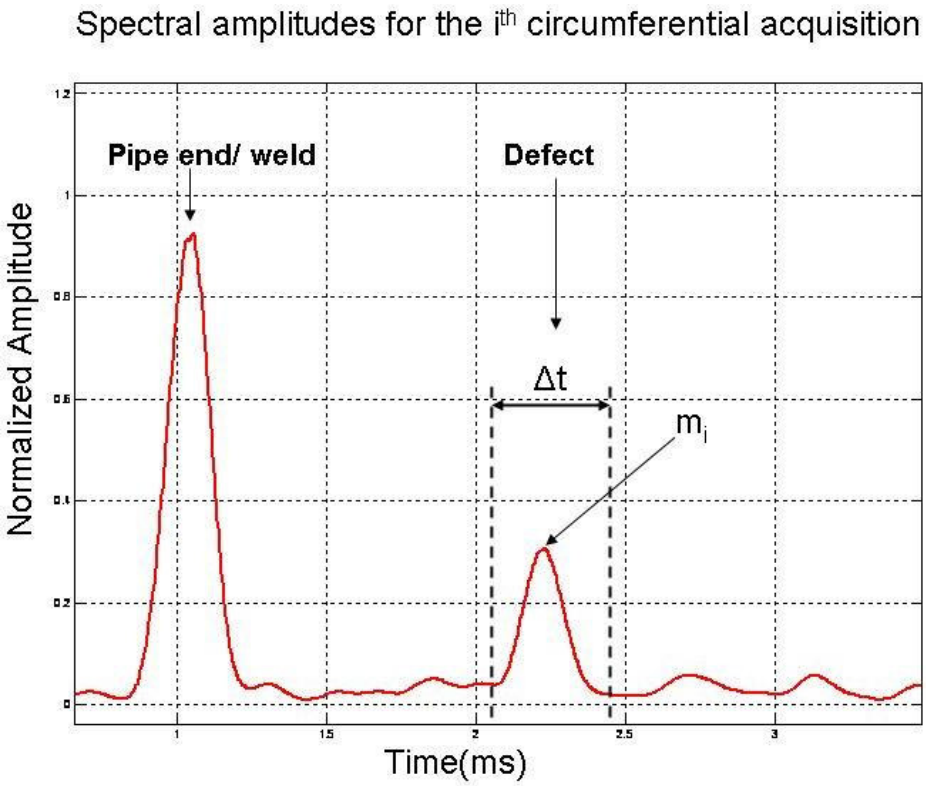

Figure 6-17 Spectral amplitudes representation of the ith circumferential acquisition

The polar representation was chosen for further research, because it was thought to be the most comprehensible representation of an angular profile of the propagating wave.

Further simulation results have been analyzed to check for the influence that various defect parameters and pipe geometry have on the amplitude profile of the reflected torsional wave. Among them, axial, radial and circumferential extent, axial and circumferential position of defects and pipe diameter are the most significant.

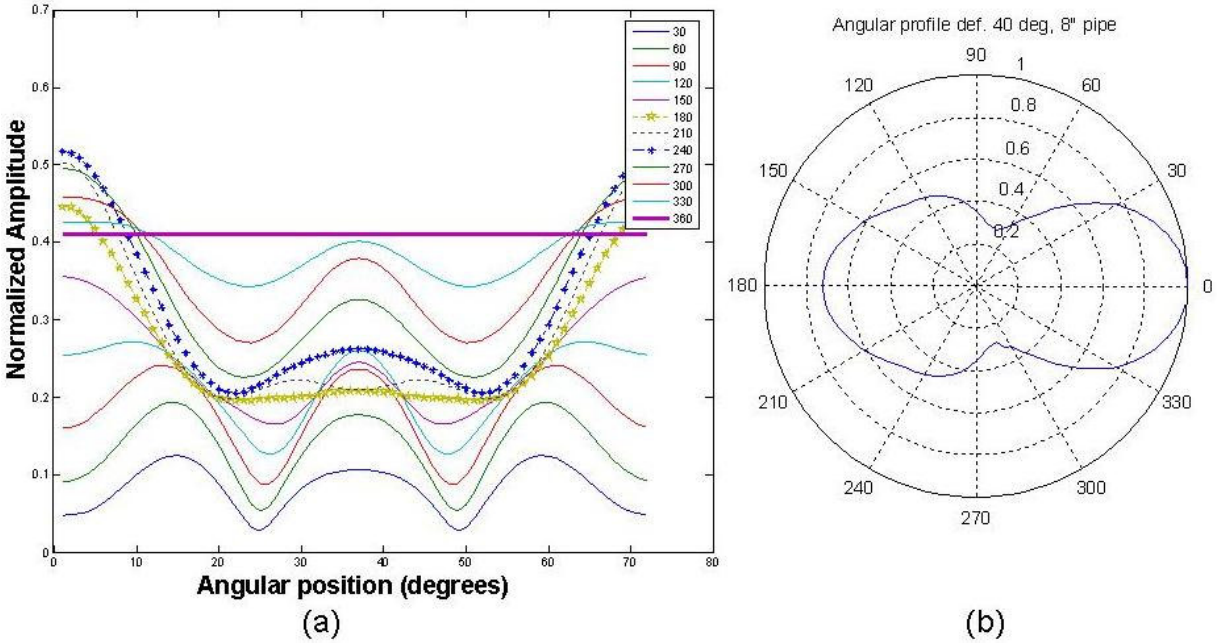

Figure 6-18 Angular profiles: amplitude distribution over circumference for several defects in Cartesian coordinates (a); polar coordinates for a 40 deg defect in an 8'' pipe

Figure 6-19 lists angular profiles of amplitudes for pipes having different diameters with defects of various circumferential extents. Pipe diameters range from 6 to 16 inches, while axial extents of defects range from 30° to 360°. The smaller circumferential extent simulates an asymmetric discontinuity (defect), while the 360° extent simulates a symmetrical discontinuity.

These results clearly denote a dependence on the pipe diameter. When increasing the pipe diameter, wave's energy tends to focus on the circumferential position of the discontinuity.

Another observation is that the distribution of amplitudes of the reflected wave depends also on the circumferential extent of the defect. Figure 6-19 (a) shows how reflections from discontinuities that tend to 360° tend to have the amplitudes uniformly distributed around the circumference.

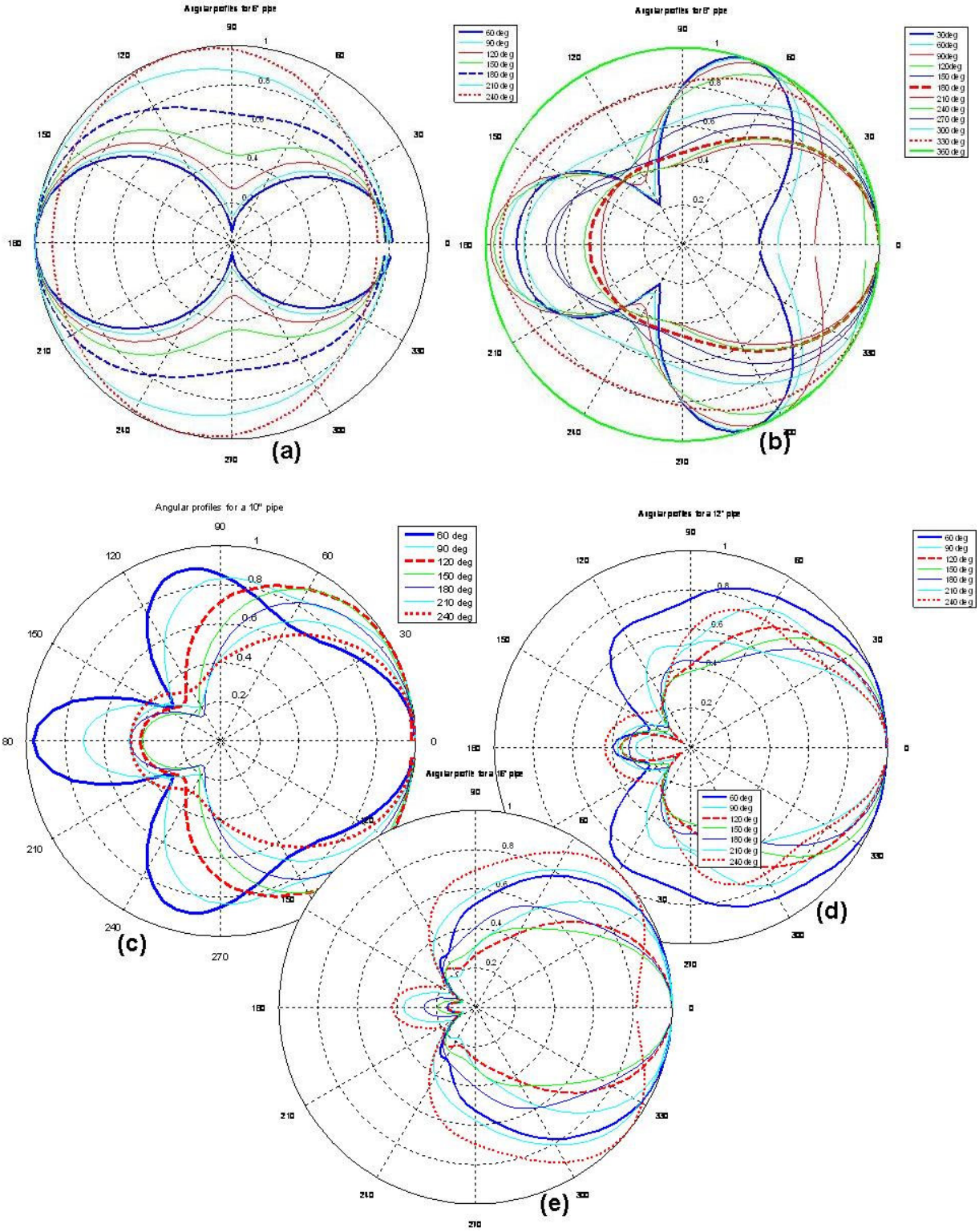

Figure 6-19 Angular profiles of amplitude for various pipes and defect circumferential extent

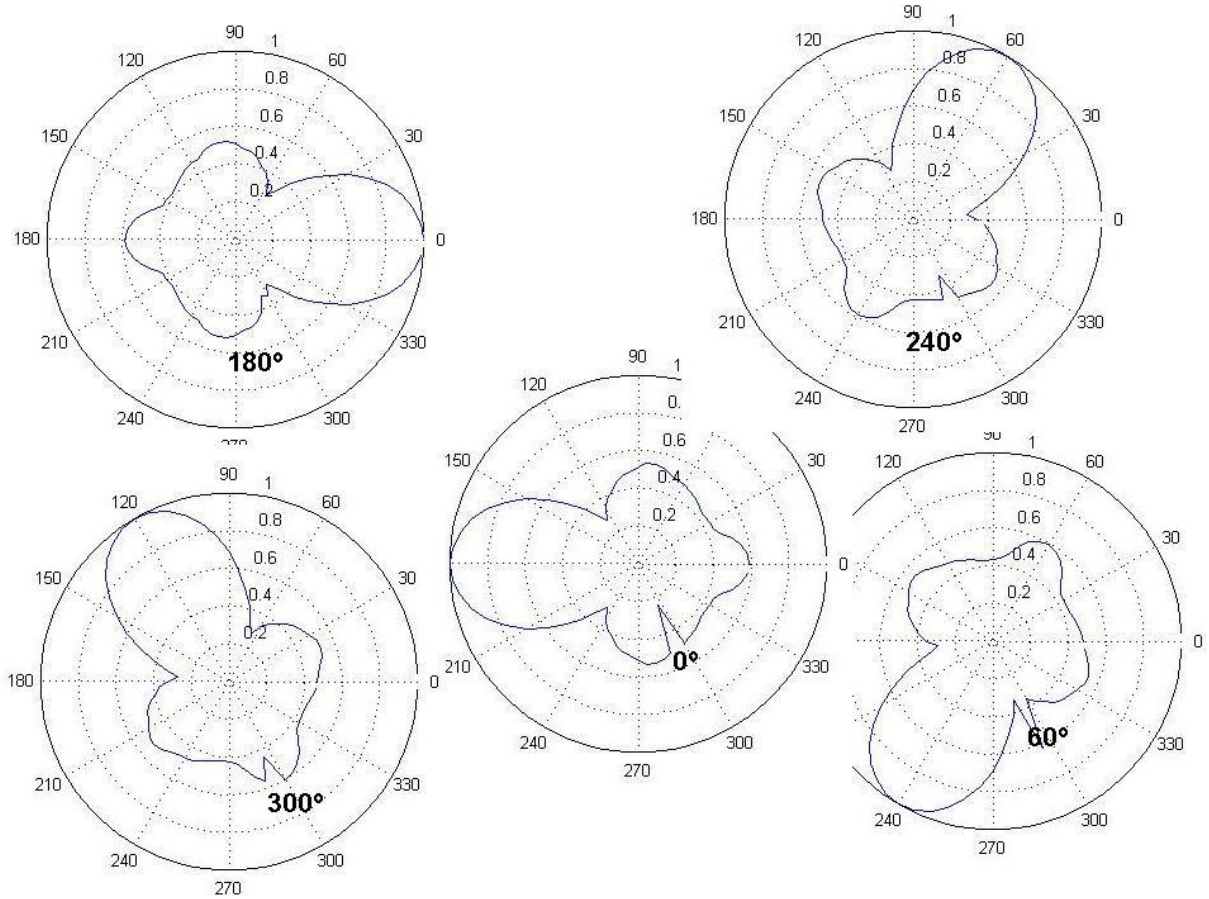

Figure 6-20 Angular profiles of amplitude of the same defect situated at different circumferential positions

Figure 6-20 shows the dependence of the angular profile of magnitude on the angular position of the defect, while Figure 6-21 illustrates the angular profile for a defect situated far from the acquisition plane (11m in this case on a 6'' pipe). By increasing the aforesaid distance, the profile tends to get a more regular shape with two equal maximum lobes.

6.3.4 Asymmetry coefficient

The study of angular profiles of amplitude of an echo has outlined two important facts:

1. If an echo is generated by an asymmetric discontinuity located far enough from the receiver, the profile tends to have a specific shape with 2 maximum lobes and 2 points of minimum (Figure 6-21).
2. If an echo is generated by a symmetric discontinuity located far enough from the receiver, the profile loses the 2-lobe shape tending to a complete circular shape, thus a constant value.

These facts have led to the development of an asymmetry coefficient (AC) able to differentiate a symmetrical discontinuity from an asymmetrical one.

The algorithm for the computation of the AC searches for the points m_1, m_2, M_1, M_2, that mostly satisfy the configuration in Figure 6-21 and then calculates:

$$AC = 1 - \frac{m_1 * m_2}{M_1 * M_2} \qquad (6\text{-}1)$$

The value of the AC ranges between 0 and 1, where the 0-value indicates a symmetrical discontinuity, while an AC of 1 indicates a symmetrical one.

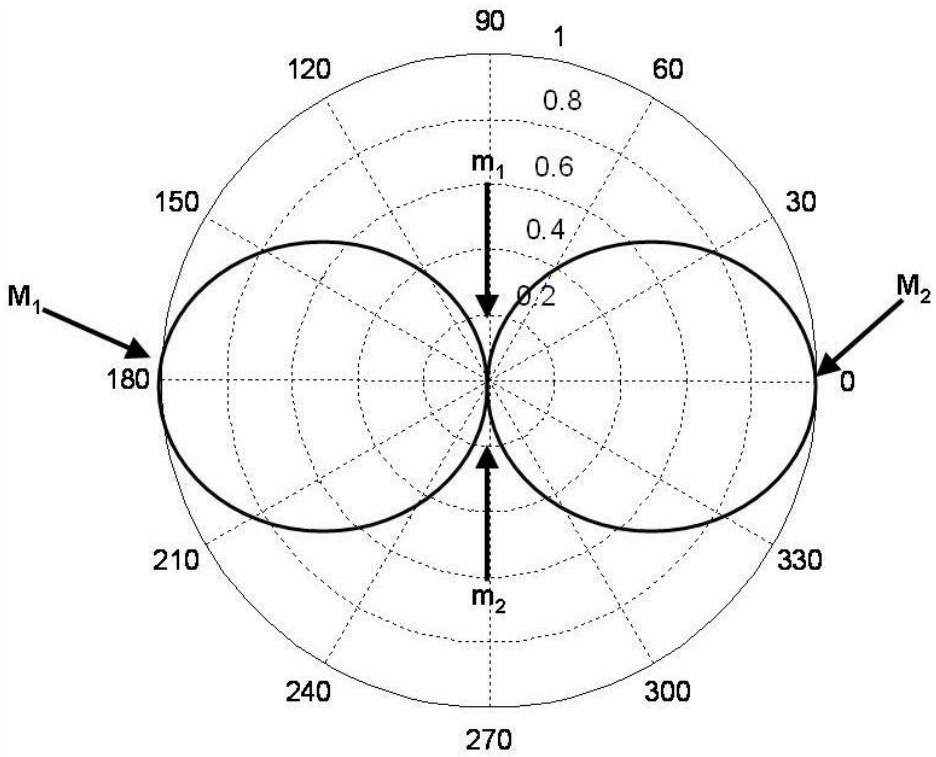

Figure 6-21 Computation of the Asymmetry Coefficient (AC)

6.3.5 Conclusions

The analysis of the simulated data has demonstrated that valuable information can be extracted from the reflected UGW, that is useful for the characterization and classification of defects. In addition, the large quantity of information provided by the local circumferential acquisition of signals, have made possible implementation of advanced techniques for pattern recognition like the neural networks.

Moreover, the reconstruction of the angular profiles from the spectral amplitudes and the computation of the asymmetry coefficient can be very useful for the classification of echoes when these are detected with a local magnetostrictive transducer.

CHAPTER 7 DEVELOPMENT OF NEW MAGNETOSTRICTIVE SENSORS FOR UGW ACQUISITION

7.1 Background

A long-range inspection system for pipelines has an important advantage over the local NDE techniques: the rapid, cost-effective, 100% inspection of long sections of pipelines.

Unlike the PZT based methods that use a matrix of transducer elements, a magnetostrictive transducer makes use of a standard single continuous element that completely surrounds the pipe circumference. As already mentioned in the previous chapters, signal processing consists in transforming the RF signal into a more user-friendly one, called visual signal and choosing a threshold above which reflections are considered to be generated by defects.

This hardware configuration allows the acquisition of the average signal over the full pipe circumference losing precious information about the non axial symmetric features which is provided by each individual circumferential point. The effect of this drawback is the limitation of the capacity to characterize the detected features or to distinguish between flaws and symmetrical features normally located in pipes or pipelines – i.e. flanges, welds etc. Consequently, further investigations are needed to identify and classify the detected discontinuities, as the threshold criteria applied on a magnitude-based visual signal cannot provide valuable information on the defect's geometry.

Figure 7-1 and Figure 7-2 show an example of signals acquired with the commercial MT system. A threshold criterion has been applied for the identification of defects, i.e. reflections with amplitudes between the 25% threshold (the lower curve) and the 100% threshold (the upper curve) were considered as potential defects. Further visual inspection denied this result. As a conclusion, the threshold criteria applied on an average data signal cannot characterize echoes or

distinguish among symmetrical discontinuities (joints) and non-symmetrical ones (potential defects).

To overcome this issue, intensive research has been carried out in the field of signal processing as well as hardware development.

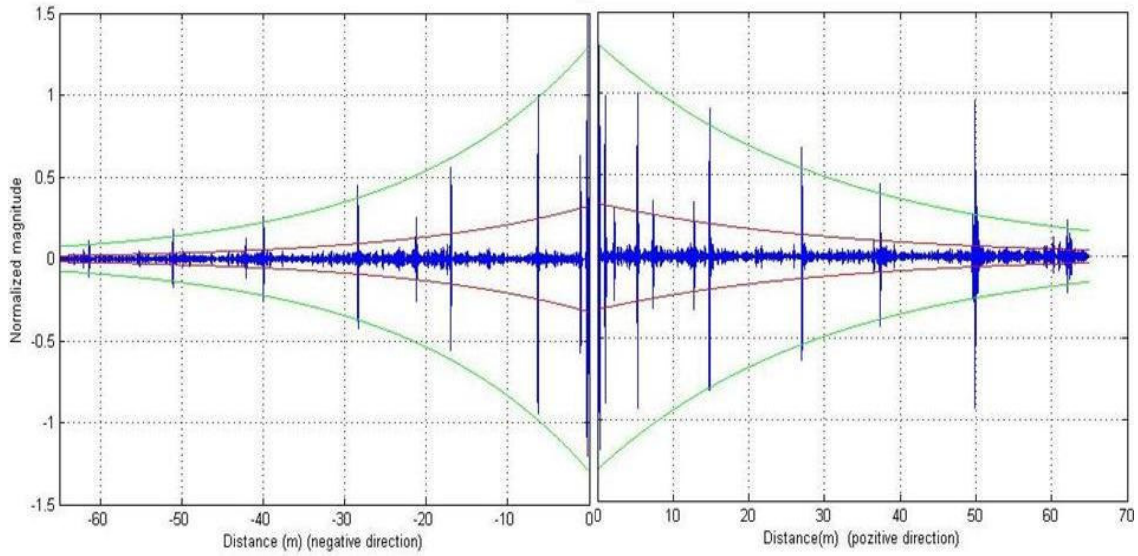

Figure 7-1 RF signal of a long-range inspection using the MsS Instrument.

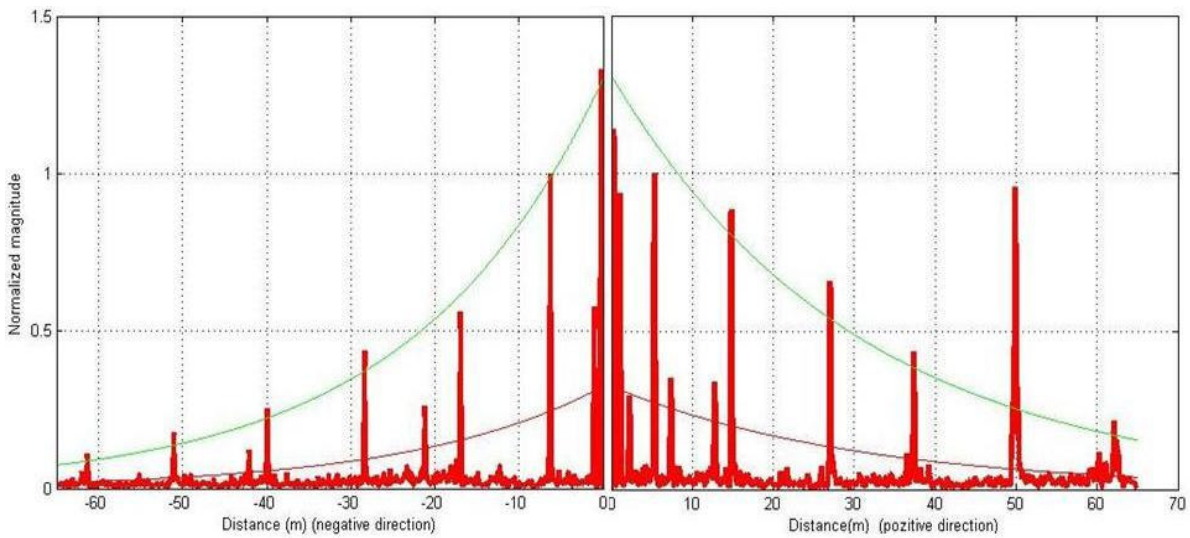

Figure 7-2 Video signal of a long-range inspection using the MsS instrument.

The simulations described in 0 have shown that data acquired locally in various circumferential points can provide enough information for the classification of

echoes. Moreover, advanced algorithms for pattern recognition as well as direct methods for defect characterization can be applied.

Consequently a new magnetostrictive transducer (MT) is needed which is able to acquire data locally on the pipe circumference.

7.2 Guided Ultrasonics Local Acquisition System

We outlined in the previous paragraph the reasons that brought to the need of a new type of magnetostrictive transducer (MT). The most representative is the lack of information on the defect geometry that the classical MT carries within. The new MT covers a circular sector along the circumference and records signals locally on the pipe circumference, instead of the classical acquisition of the average signal over the total circumference.

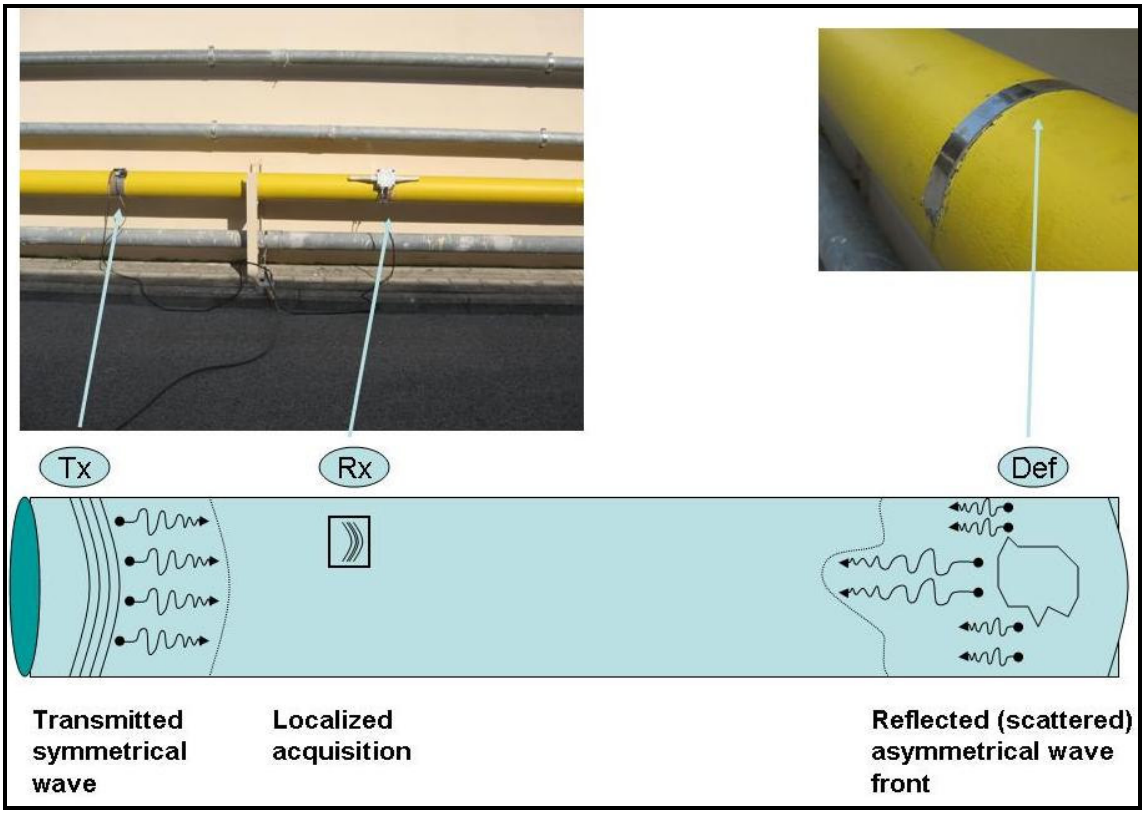

Figure 7-3 Experimental setup: transmitter (Tx), receiver (Rx) and defect (Def)

The design and development of the new sensor was based on both simulated and experimental data. Furthermore other experimental results validated the new

methods of data acquisition and processing. The commercial MT was used to generate the transmitted signals. A step-by-step data acquisition around the pipe circumference by using the new sensor provided signals containing information related to the defect geometry in a specific circumferential point. A complete scan over the pipe circumference would provide enough data to reconstruct the entire geometry of the detected features along the inspected pipeline.

Figure 7-4 Local Acquisition Sensor for UGW: 1st and 2nd version

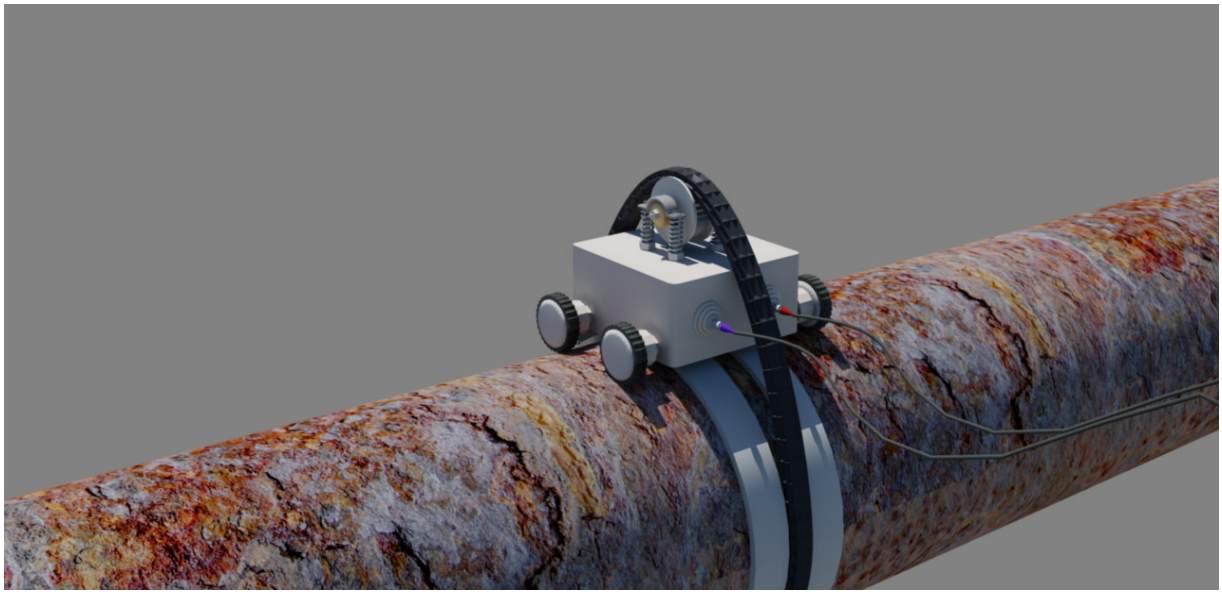

Figure 7-5 Local Acquisition System: 3rd version

Figure 7-4 and Figure 7-5 show three versions of the transducer for local circumferential acquisition of UGW. Version 1 and version 2 were manually rotated around the pipe, while the last version is semi-automatic.

In order to validate the new system and the signal acquisition procedure, two acquisitions were made for the same experimental settings: an 8'' pipe with a defect having $\Delta\theta=90^{o}$, $r_d=70\%$, and an axial extent << $\lambda/2$. The transmitted wave was in both cases a torsional symmetrical wave.

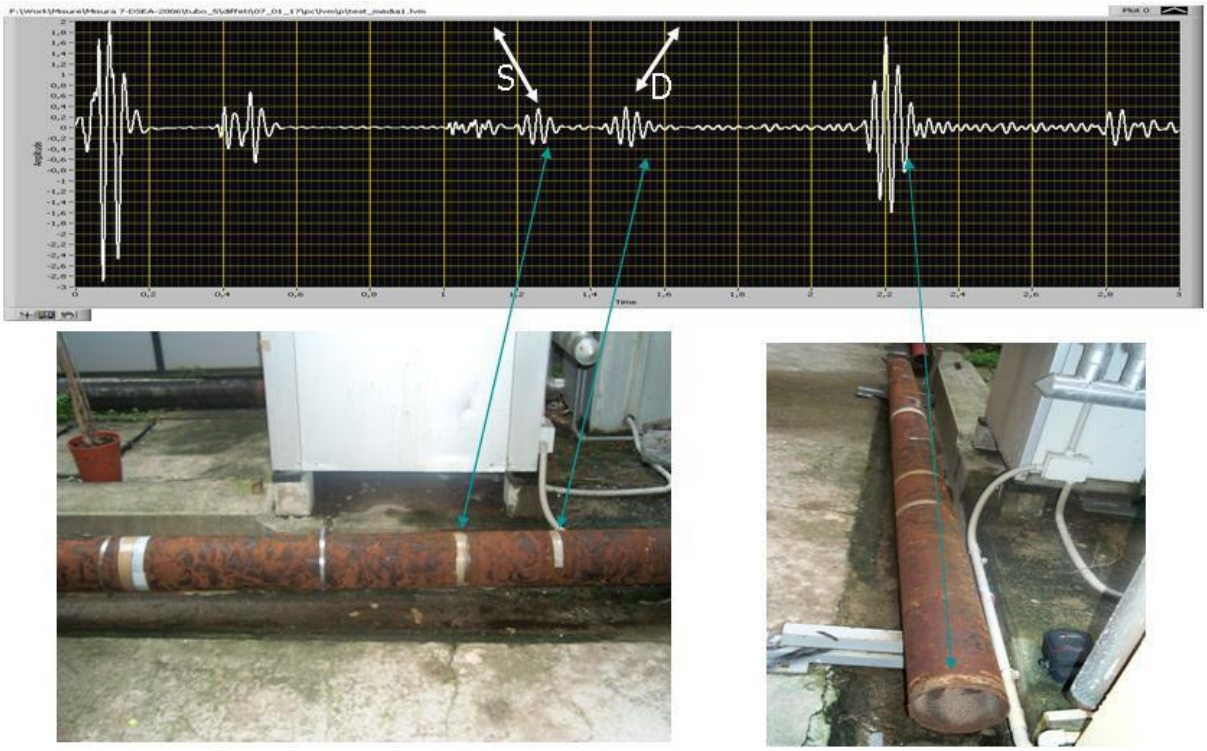

Figure 7-6 Test settings

Figure 7-6 illustrates the test settings: an 8'' pipe with 2 artificial discontinuities (a symmetrical and an asymmetrical one – the defect). On the top of the figure the average signal is represented, where S and D denote the symmetrical discontinuity and the artificial defect respectively. To be noted that both reflections are indistinguishable.

In the first experiment the classical MT system was used to acquire the average signal over the circumference. In the second experiment the same acquisition plane was divided in 4 circumferential sectors and 4 signal acquisitions were performed using the local MT system. The average of the 4 signals was compared to the one from the single acquisition. The results are illustrated in Figure 7-7. The

average acquisition and the calculated average from the 4 sectorial acquisitions are represented with a thick blue and red line respectively. The other waves in the figure are corresponding to the sectorial acquisitions in the positions 0, 90, 180 and 270 degrees respectively.

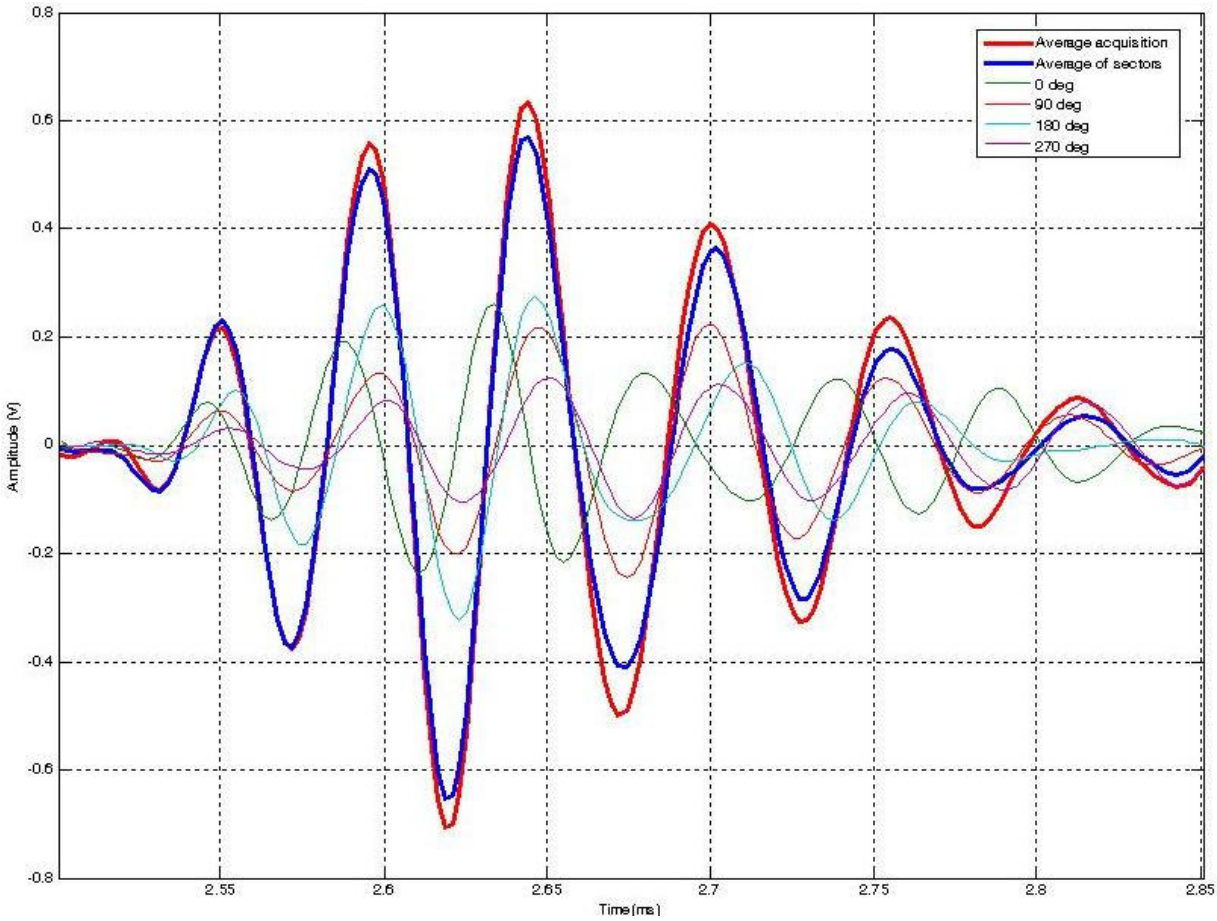

Figure 7-7 Experimental validation of the local acquisition system

7.3 Development of dedicated software for signal acquisition and processing

New software with a graphical user interface was needed to perform operations like:

- Signal acquisition
- Results representations
- Signal processing

7.3.1 Representation of results

The new sensor performs several signal acquisitions for each inspection; in this case several signals must be visualized contemporarily. Figure 7-8 shows circumferential data corresponding to a 32 kHz torsional wave reflected by a defect with the following characteristics: radial extent, t_d = +70%, axial extent, $\Delta z_d = \lambda/4$ and circumferential extent, $\Delta\theta_d = 90^o$. The red line is the average data. It is notable the variation of amplitudes and phase shifts around the average wave.

However, for a better understanding of the acquired data, a new meaningful and easily interpretable way of representing it, was needed.

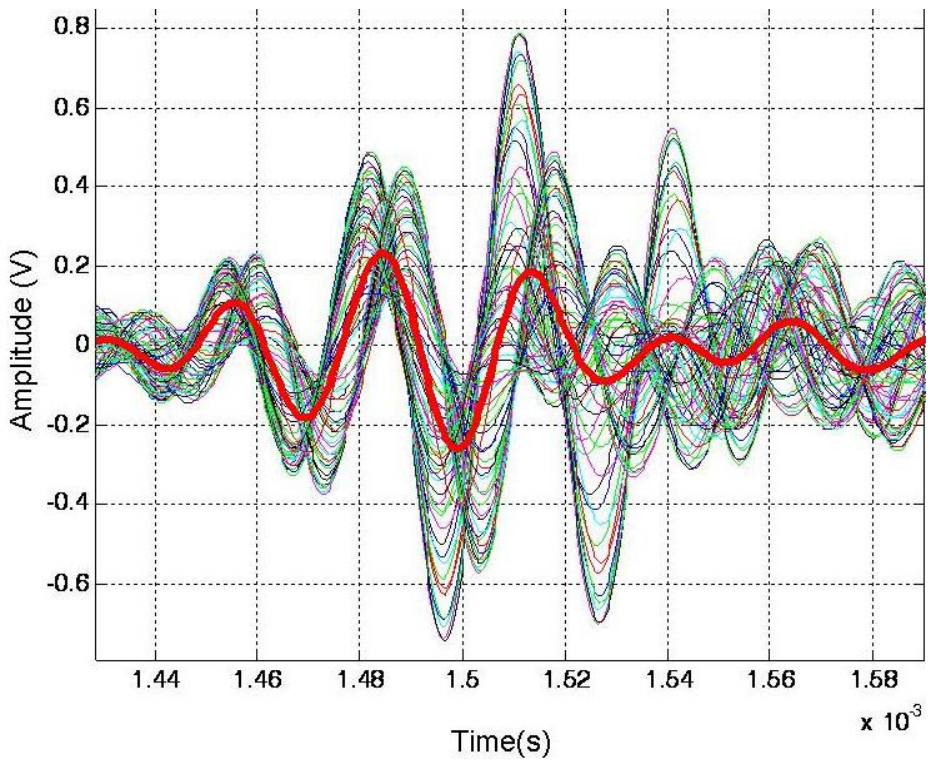

Figure 7-8 72 circumferential acquisitions for an 8'' pipe with an artificial defect (t_d = +70%, $\Delta z_d = \lambda/4$, $\Delta\theta_d = 90^o$)

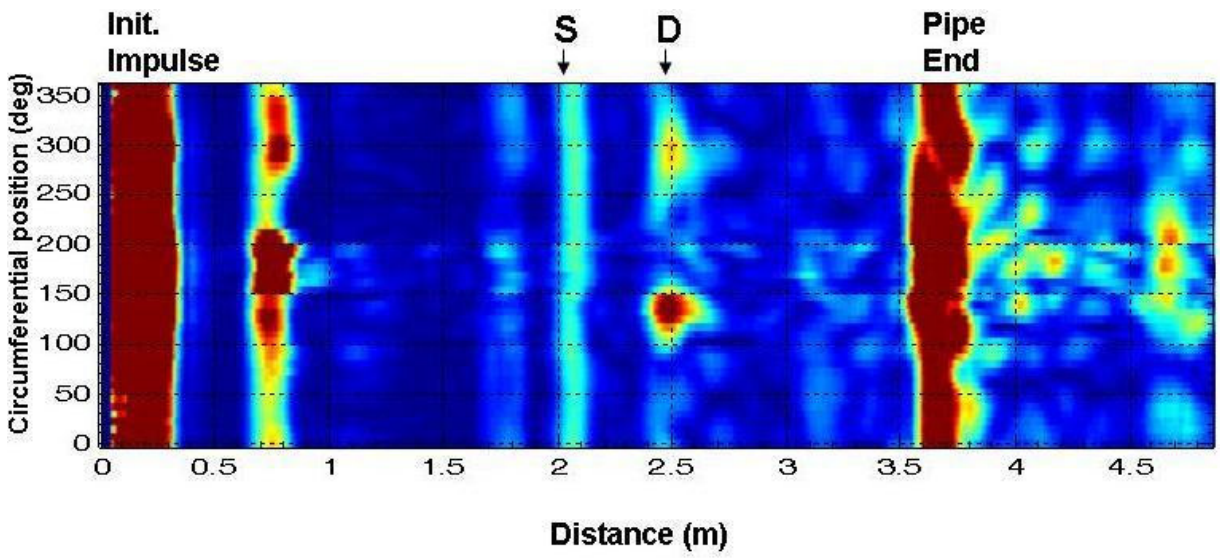

Figure 7-9 Colour map representation of data from pipe inspection

Figure 7-9 illustrates a colour map representation of the acquired signals. These results correspond to the test described in Figure 7-6. In this case the normalised spectral amplitudes were plotted against distance on the axial direction and circumferential position. In this way a detailed map of the pipe surface and its integrity can be given. The colour scale ranges from blue too red, that is from the lowest amplitude values to the highest ones. In this case the highest peaks correspond, in this order, to the initial impulse, the left pipe end, the two artificial discontinuities and the right pipe end. An important aspect in this representation is the fact that the two discontinuities (S and D) can be easily distinguished.

7.3.2 Denoising

Wavelets are considered powerful instruments for signal processing. Some of their applications include edge detection, feature recognition, data compression, or signal or image denoising [33].

In our case, wavelet analysis was used for signal denoising as well as a tool for defect characterization. Denoising was successfully performed on the signal resulted from the gas pipeline inspection.

Wavelets are functions used to divide a time signal into different frequency components [34]. A wavelet transform is the representation of a function by wavelets. The wavelets are scaled and translated versions of finite waveform called mother wavelet. Figure 7-10 shows an example of a mother wavelet – the Morlet wavelet. By scaling and translating the wavelet over the analyzed signal, the latter can be decomposed in various frequency components. Using such decomposition, high frequency components can be eliminated.

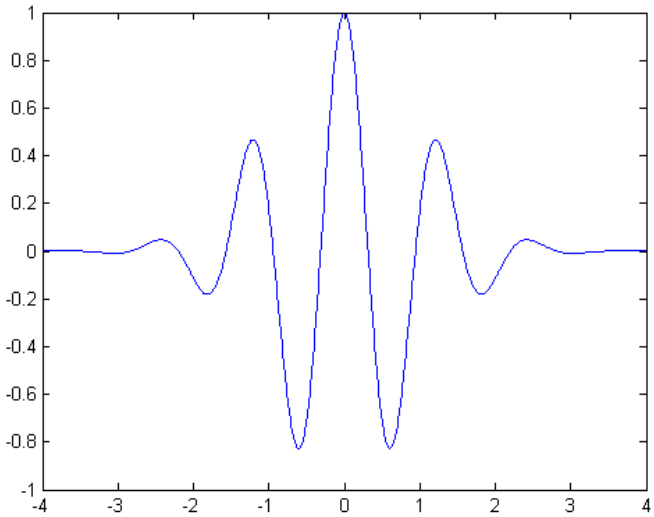

Figure 7-10 Morlet wavelet

In this case, a Matlab® implemented Stationary Wavelet Transform was used to create the software in Figure 7-11 to perform denoising of signals acquired during UGW inspection of pipelines.

The algorithm was able to remove high frequency noise and to reveal potential regions of accentuated corrosion along the pipeline under test (Figure 7-12).

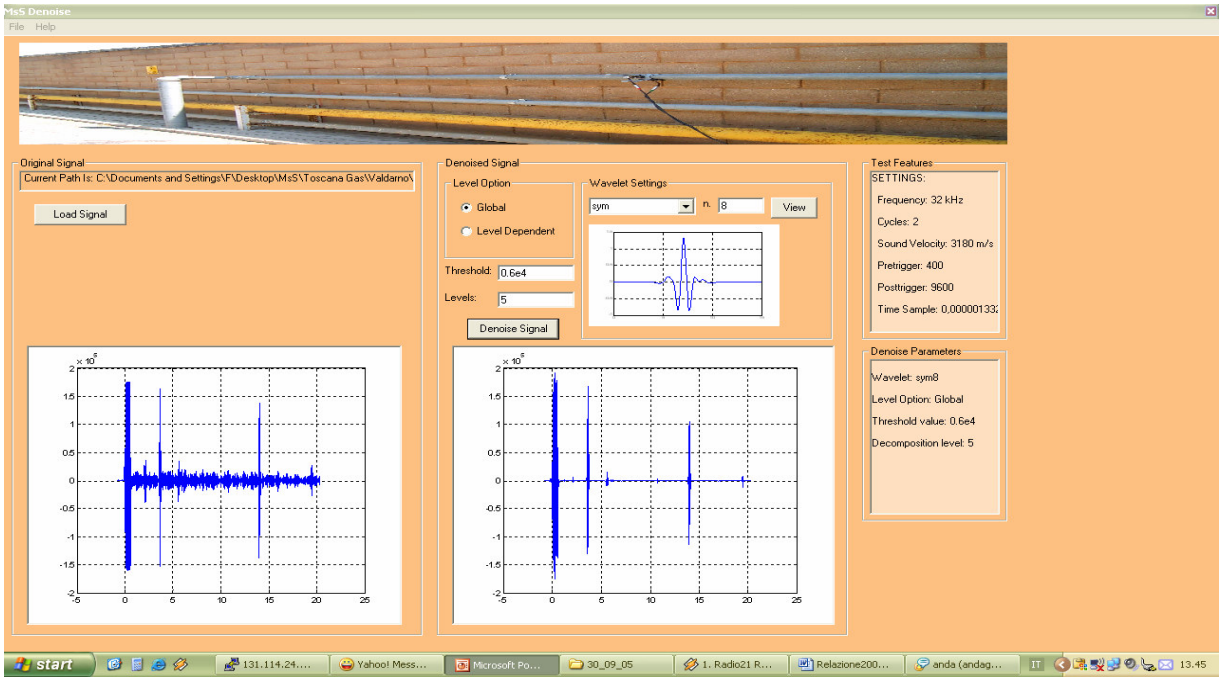

Figure 7-11 Signal denoising software

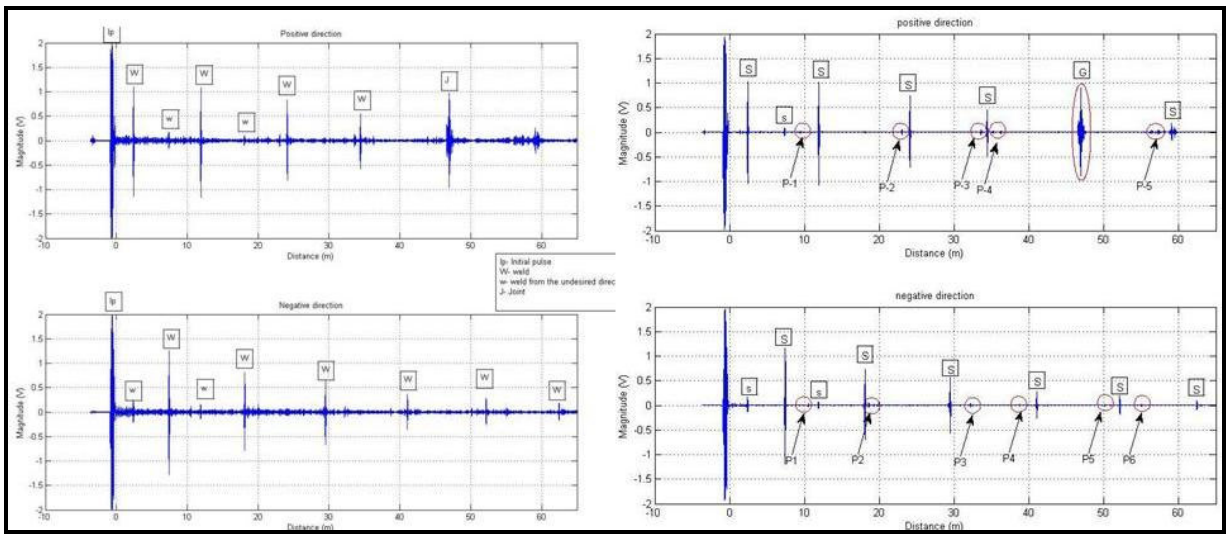

Figure 7-12 Signal denoising: case of 6" gas pipeline.

7.3.3 Discrimination between symmetrical and asymmetrical features

It is well-known that most pipeline defects (corrosion, notches, cracks) have an asymmetrical shape and on the other hand most of the normal pipeline features (welds, joints, branch joints, and elbow joints) have a symmetrical shape with

respect to the pipe axis. Therefore, an important step in the estimation of the defect's geometry is to classify it as a symmetrical or asymmetrical feature. To do that several procedures have been implemented: *phase diagram* and *angular profile* evaluation and *asymmetry coefficient* computation. All these procedures involve local signal acquisition around the pipe circumference using the innovative sensor described in the previous chapter.

Phase diagram

The phase diagram is a representation of the angular profile of phase, as described in the previous chapter. As specified in 0, the phase diagram of an individual echo is a representation of the phase shift of each locally acquired signal with respect to the average signal.

A first test was conducted on the dismounted pipe describe in the previous section, in Figure 7-6. It may be noticed that echoes due to asymmetrical features present an accentuated phase shift between -90 and 90 degrees compared to roughly no phase shift for the case of the symmetrical feature -Figure 7-13.

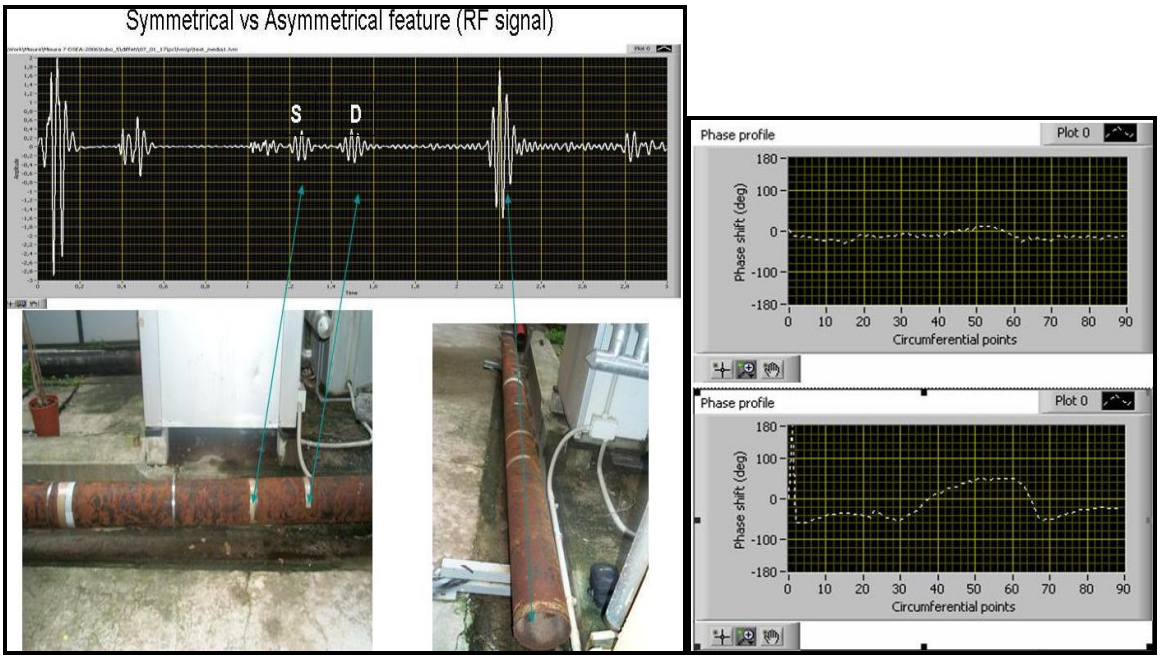

Figure 7-13 Left: symmetrical (S) and asymmetrical features (D) on an 8" pipe; right: phase diagram - symmetrical (top) and asymmetrical (bottom)

This test confirms the simulations results and the fact that the phase diagram can indicate an asymmetry, thus the presence of a defect.

Further experiments have been conducted on the 6'' gas pipeline described in Figure 5-6. Two artificial defects were bonded having 70% radial extent and λ/4 axial extent. The first was a symmetrical discontinuity, while the second had a 90 deg circumferential extent. The phase diagrams were computed to outline the differences between the two defects (Figure 7-14).

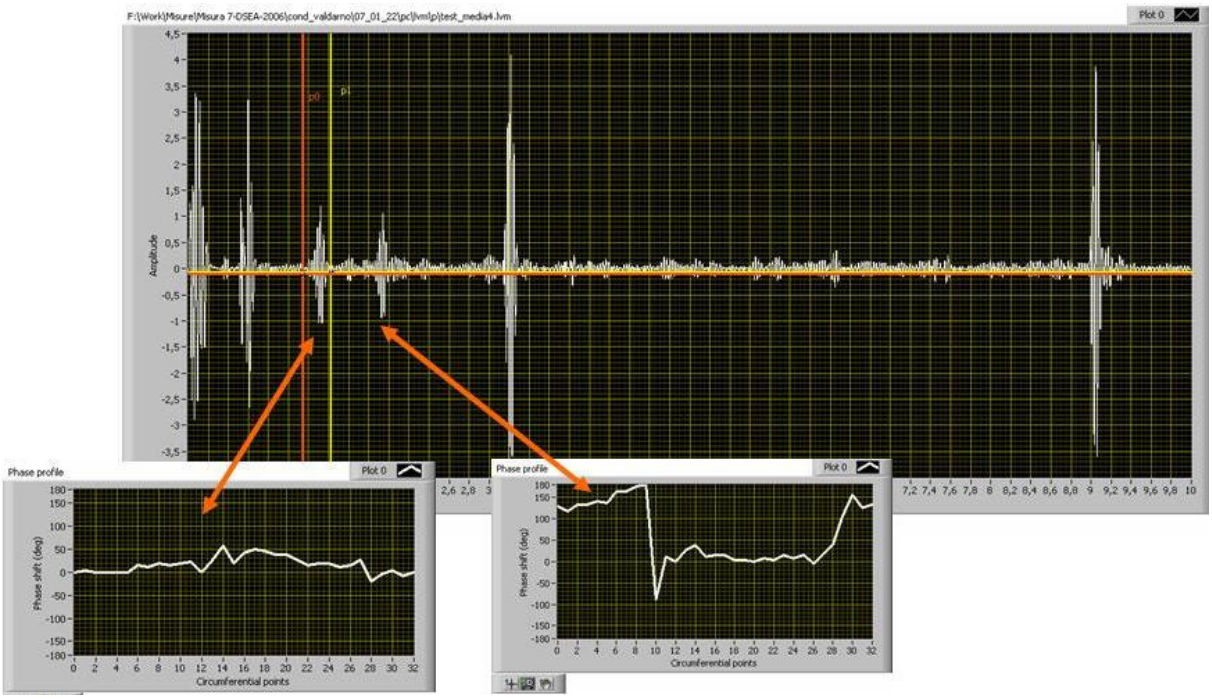

Figure 7-14 Phase diagrams for two artificial discontinuities on an in-service gas pipeline

Amplitude profile

The amplitude profile for an echo is a representation of the magnitude response of the defect, along the pipe circumference. The simulations showed that the shape with two maximum and two minimum points are characteristics of the asymmetrical features only.

Figure 7-15 shows results for a simulated defect and an artificial defect on the dismounted 8'' pipe described in Figure 7-6. Differences between the two results – simulated and experimental- are due to simplifying hypothesis in the simulations.

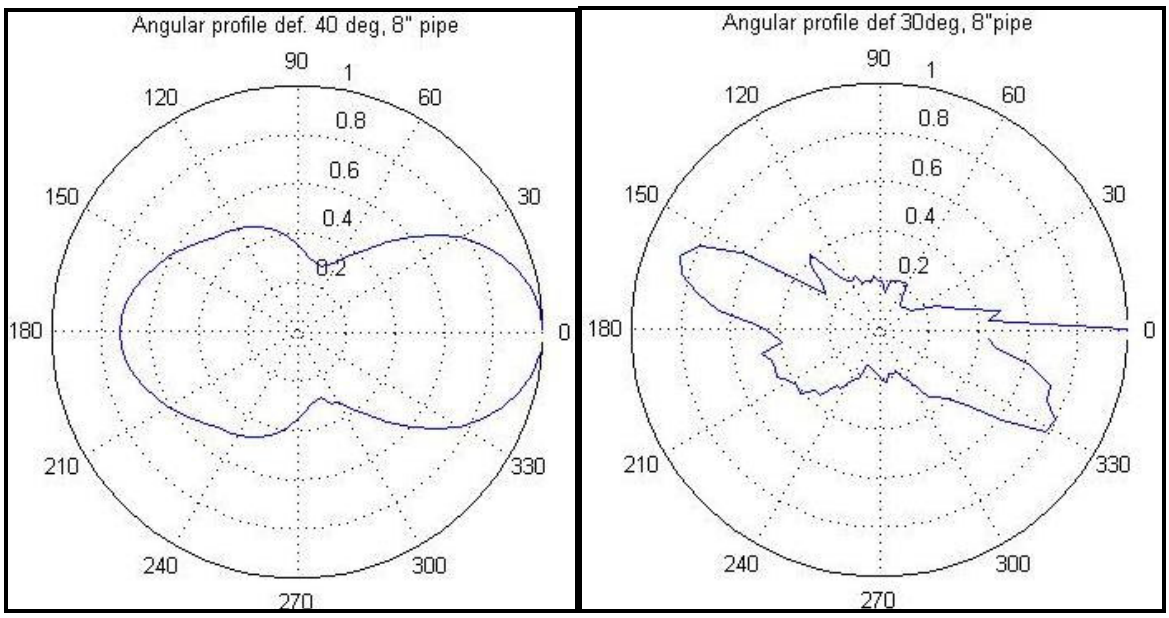

Figure 7-15 Left: Amplitude profile for a 40 deg simulated defect; Right: experimental local acquisition for a 30 deg defect.

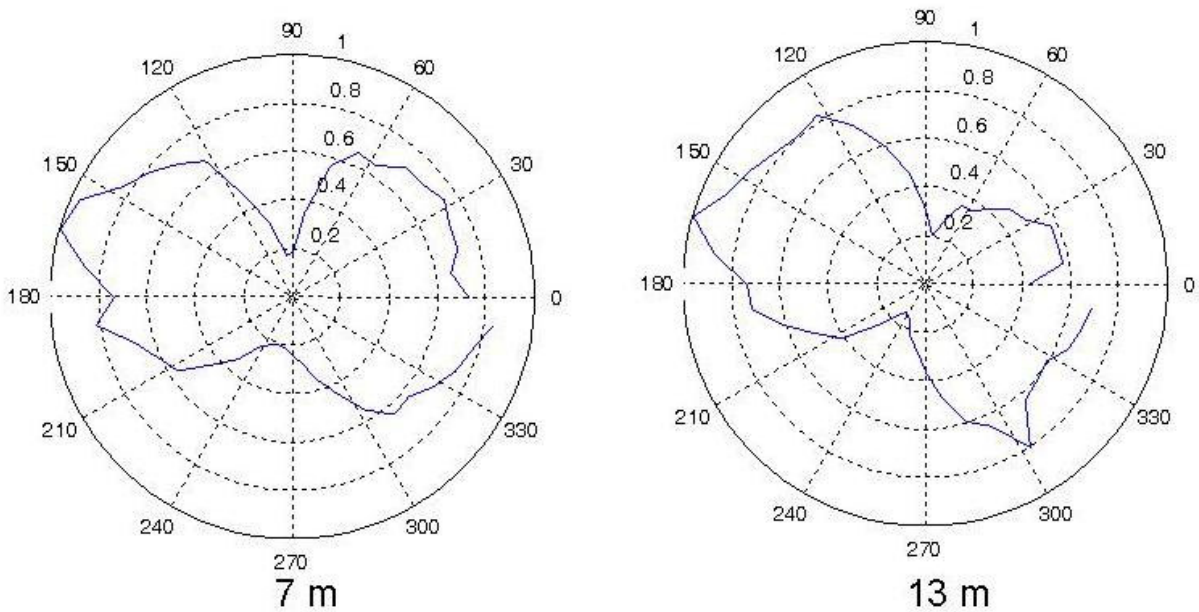

Figure 7-16 Amplitude profiles of two defects situated at different axial distances

Figure 7-16 shows two amplitude profiles corresponding to artificial defects on the in-service gas pipeline described in Figure 5-5.

7.4 Graphical user interface

Most of the signal processing methods that were described above were integrated into a complete software provided with a Lab View® based user-interface (Figure 7-17).

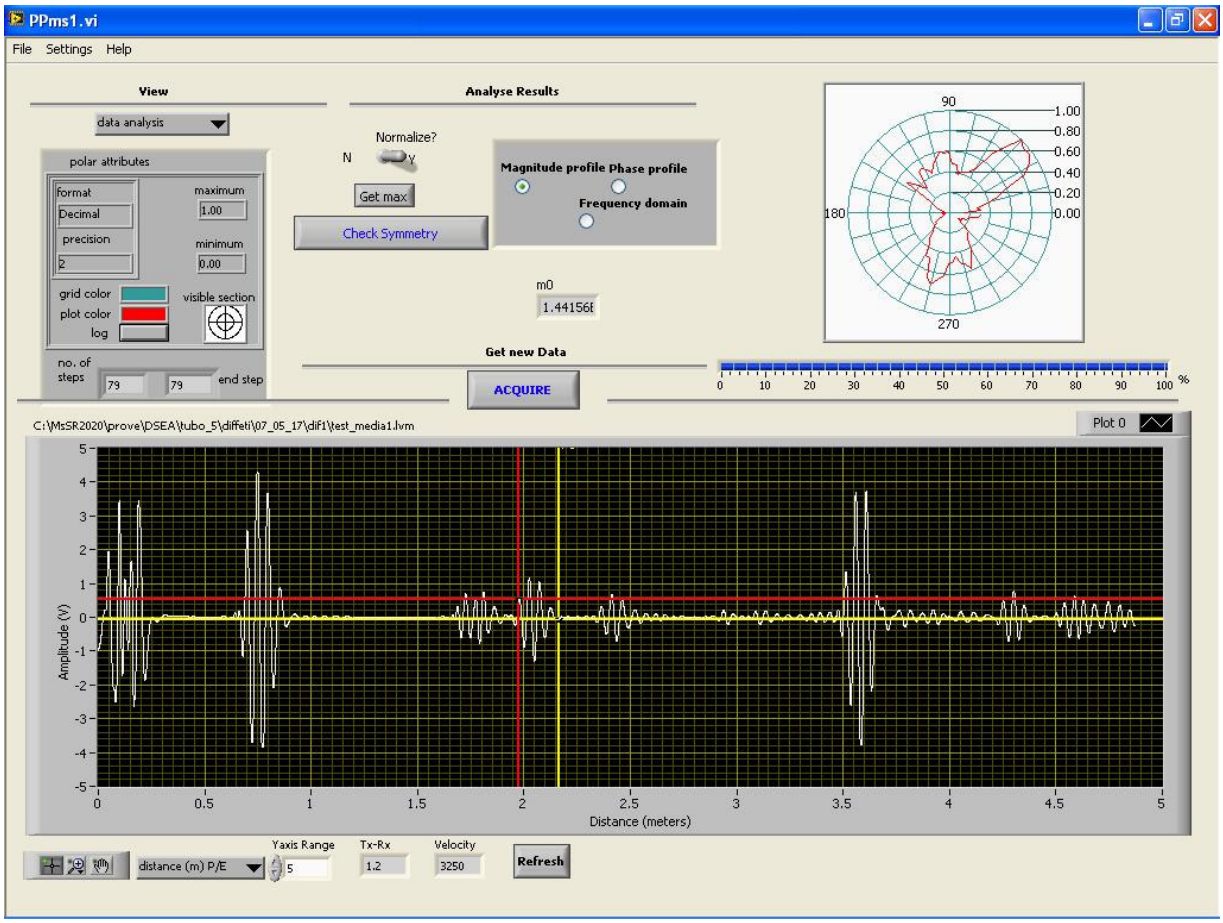

Figure 7-17 User-interface of the new software packet

The software allows operations like:

- signal acquisition and visualization
- data saving in text format

- signal processing (frequency domain analysis, phase diagram and magnitude profile elaboration)
- report elaboration

7.5 Inspection procedure

Along with the hardware design, a new software packet has been developed and a new procedure that brings to defect identification has been prepared. The individual steps from signal acquisition to defect identification are described below.

- local acquisition of signals until the complete scan of the circumference
- apply a denoising algorithm for each RF signal (wavelet analysis or frequency domain filtering)
- take a reference wave reflection (generated by a known feature as a junction or a weld) and normalize the signal with respect to its maximum magnitude value
- create Video signal from the RF signal
- apply the NN classification algorithm to all the detected features and identify possible defects OR
- build the magnitude profile from all the signals for each detected feature
- compute asymmetry coefficient
- identify possible defects

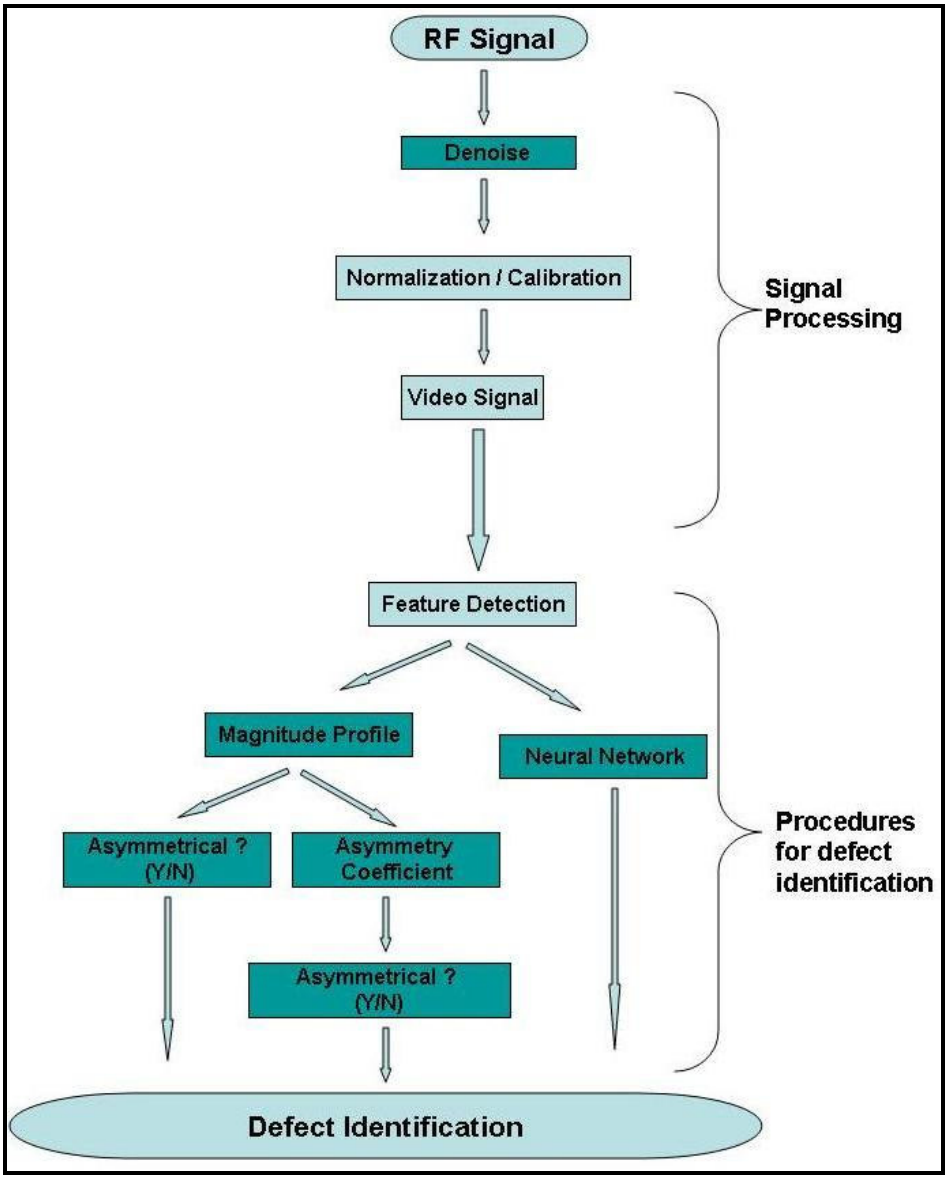

Figure 7-18 Flow chart for the new acquisition system – dark elements represents new signal processing procedures

The software that is being developed for the local magnetostrictive sensor includes various signal processing procedures in order to recognize and classify all the features detected in the measured signal. The techniques involved in defect recognition include *Wavelet analysis*, *Fourier analysis* and *Neural Network* classification algorithms

7.6 Field Test

In-service pipeline from Figure 7-19 was used to bond artificial defects having various sizes and to compute the asymmetry coefficient from the measured data.

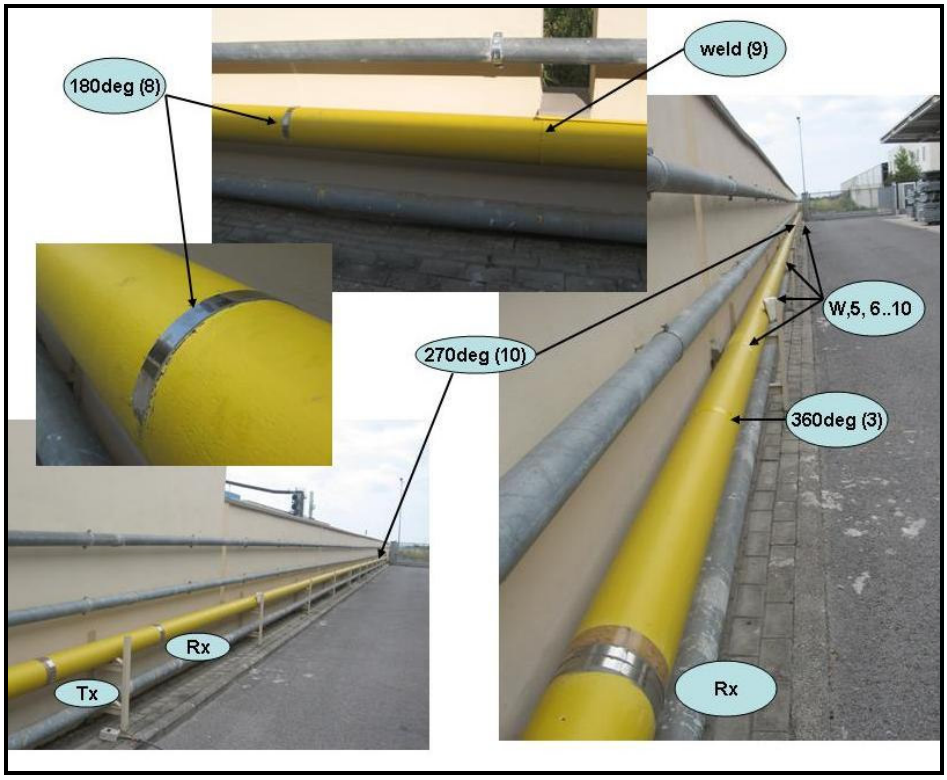

Figure 7-19 Features present on the 6" gas pipeline

Figure 7-20 illustrates the signal measured using the commercial MsS® Instrument. In both figures (RF and video signal), the geometrical discontinuities that were detected along the pipeline under test were labelled with numbers from 1 to 10. Among them there are artificial defects, having different radial and circumferential extensions, as well as symmetrical joints (welds) located at relatively regular distances (approx. 10meters). For instance the discontinuities labelled with numbers 3, 4 and 7 are located respectively at 2m, 5m and 14m. Considering the relative distances and magnitudes, 2 joints can be individuated as feature no.5 and no. 7. The other reflections can be considered as generated by defects, while around 25m, another joint is expected to be found. However, the low relative

distances between features 8, 9 and 10 and their similar magnitudes make defect individuation particularly difficult.

In this case, the asymmetry coefficient (AC) was calculated to classify the detected discontinuities. The values of the asymmetry coefficient corresponding to each discontinuity and the corresponding label are listed in the Table 7-1. Symbols S and NS stand for "*Symmetrical*" and "*Non-Symmetrical*" respectively.

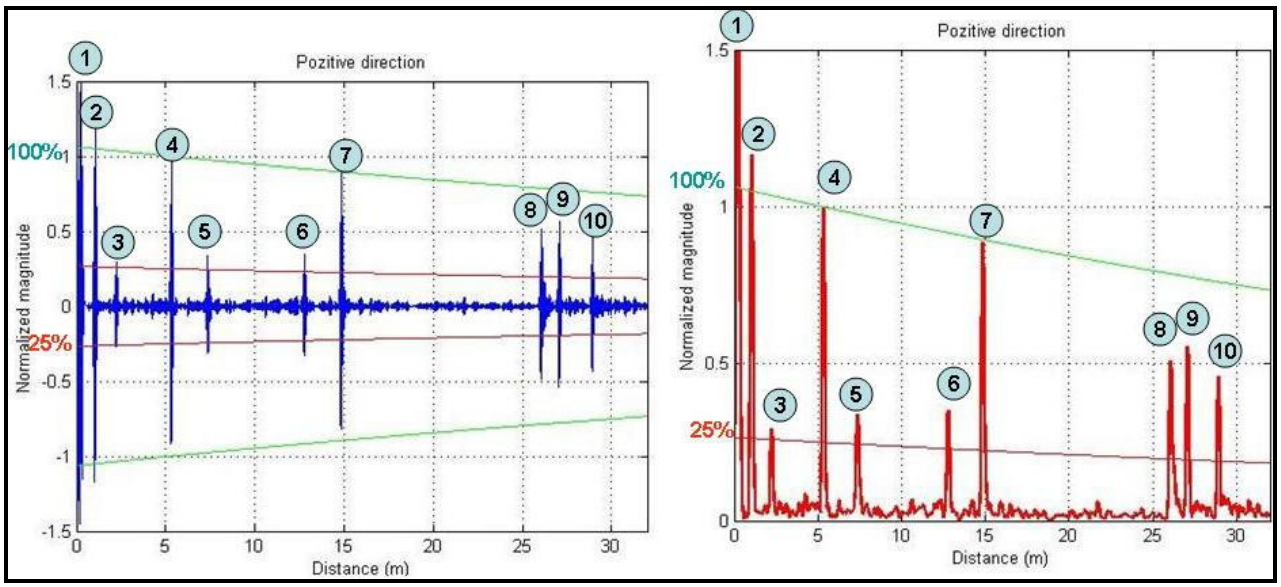

Figure 7-20 Features detected along the 6" gas pipeline using a 25% threshold – RF and video signal

Table 7-1 Classification of the features detected in Figure 7-20

Features detected	1	2	3	4	5	6	7	8	9	10
Asymmetry coefficient (%)	-	-	19.0	3.4	91.2	91.5	24.5	77.4	6.6	77.0
Feature type	Initial pulse	Transm. wave	360deg	weld	90deg	90deg	weld	180deg	weld	270deg
Classification	-	-	S	S	NS	NS	S	NS	S	NS
Distance from RX	0	1	2.2	5.3	7.3	12.7	14.8	26	27	28.9

The classification was made by considering the 50% threshold for the AC. The discontinuities having an AC value above 50% were classified as non-symmetrical, while, those having AC values under 50% were classified as symmetrical (joints).

A visual inspection could confirm a number of 4 symmetrical discontinuities and another 4 non-symmetrical, with the configuration described in Table 7-1.

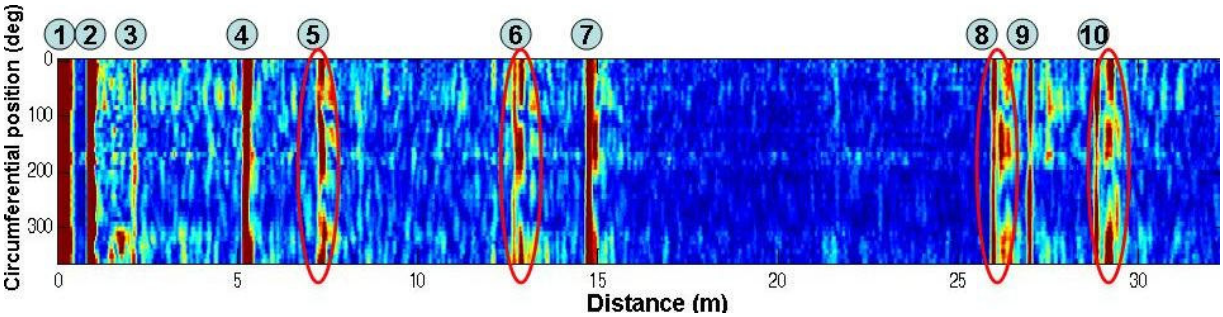

Figure 7-21 Colour map of the inspected in-service gas pipeline

The colour map representation of the test results (Figure 7-21) can also provide some information on the symmetry of the detected discontinuities. For instance, some circumferential discontinuity regarding the amplitude distribution can be noted at the reflections market with a red circle.

7.7 Conclusions

A GW detection system based on a single symmetrical transducer can hardly distinguish among symmetrical and asymmetrical discontinuities in pipelines or classify the detected echoes. The local transducer described in this chapter was capable to completely classify echoes that were due to symmetrical as well as asymmetrical discontinuities of a long in-service pipeline. The use of the above sensing system together with a colour map graphical representation, the use of the angular profile of phase and amplitude and computation of the asymmetry coefficient can bring to less false positives when inspecting long sections of pipeline by distinguishing the defects from joints or welds.

Furthermore, the use of Long Range Guided Waves generated by a magnetostrictive sensor for long-term condition monitoring of piping systems significantly improve efficiency and reduce costs of plant maintenance.

The last research results (discontinuities could be classified at distances up to 29 m from the transducer) have outlined the potential of long-range inspection with magnetostrictive sensors to perform cost-effective inspections reaching also a good sensitivity and a good defect sizing and classification with respect to conventional techniques thus potentially acting as a stand-alone technique.

CHAPTER 8 FURTHER DEVELOPMENTS

8.1 Pipeline monitoring applications

Although sensor's stability has been checked and some monitoring procedures exist already, research work is still in course to fully assess the monitoring capabilities of the MsS® technology.

The procedure implies coating removal on a small pipe segment, bonding of magnetostrictive strips onto the pipeline and coating replacement. An initial signal acquisition is performed and memorized into the database corresponding to the aforesaid pipeline. The sensor's strips would be left in place so that further inspections can be done with regularity.

Another possibility is the development of an independent inspection system that can be placed on the pipelines located in remote areas and left there for monitoring purposes. The system must be composed of the transducing system (magnetostrictive strips and coil), the signal generator with an independent power source and a transmitter antenna. The signal would be generated continuously and the results transmitted via satellite to a monitoring centre. The monitoring centre would gather the information from the various inspection locations and dedicated software together with an alarming system would inform the personnel about the early development of possible defects.

However, special software is to be developed that can perform signal processing in order to detect slight changes in the acquired signal with respect to the initial condition of the pipeline segment. By periodically examining the structure using the installed probes and comparing the acquired data, changes in the structural condition with time can be tracked cost effectively for assessing its safety and determining an appropriate course of action for operation and maintenance/inspection.

8.2 Extreme temperature applications

At present, the MsS® probes are used for relatively low temperature (≤65℃) applications. Some experiments have also been performed to test the stability of the MsS® sensor at changes in pipe temperature. Pipelines that were part of the heating system have been tested, with the temperature ranging from about 15^0C to 60^0C with good results.

Moreover, problems have been reported regarding the inspection of piping systems at very low temperatures (around -70^oC) in some chemical plants.

However, to apply the guided-wave SH mode on pipelines or pressure vessels at extreme temperatures, development of high-temperature (up to 400℃ – Nickel's Curie temperature) or low temperature MsS® probes is necessary, including the method for joining the ferromagnetic strip to the structure under test.

REFERENCES

1. J. P. Ellenberger, “Piping Systems & Pipeline: ASME code simplified”, McGraw-Hill Mechanical Engineering, 2005.
2. J. B. Nestleroth, “Pipeline In-line Inspection – Challenges to NDT”, Proceedings, ECNDT 2006, 9th European Conference on NDT, Berlin, Germany, September 25-29, 2006.
3. G. Acciani, F. Bertoncini, G. Brunetti, G. Fornarelli, M. Raugi, F. Turcu, “Classification of defects for Guided Waves Inspected Pipes by a Neural Network Approach”, Proceedings, OIPE, 2006.
4. J. B. Nestleroth, T. A. Bubenik, “Magnetic Flux Leakage (MFL) Technology For Natural Gas Pipeline Inspection”, Batelle, Columbus, OH, USA, February 1999. Document prepared for The Gas Research Institute Harvey Haines Project Manager; available to the U.S. Public through the National Technical Information Center.
5. Hegeon Kwun, Sang-Young Kim, and Glenn M. Light, “Magnetostrictive Sensor Guided-Wave Probes for Structural Health Monitoring of Pipelines and Pressure Vessels”, Sensor Systems and NDT Technology Department, Applied Physics Division, Southwest Research Institute, San Antonio, Texas, USA.
6. D. N. Alleyne, B. Pavlakovic, M. J. S. Lowe, P. Cawley, “Rapid Long range Inspection of Chemical Plant Pipework Using Guided Waves”, Proceedings, 15th WCNDT, Roma, Italy, 2000.
7. M. Beller, A. Barbina, D. Strack, “Combined In-Line Inspection of Pipelines for Metal Loss and Cracks”, Proceedings, ECNDT 2006, 9th European Conference on NDT, Berlin, Germany, September 25-29, 2006.
8. F. Bertoncini, M. Raugi, F. Turcu, “Long Range Guided Wave Inspection of Pipelines by a new Local Magnetostrictive Transducer”, Proceedings, IEEE Ultrasonics Symposium, New York, USA, October 2007.

9. K. Reber, A. Belanger, “Reliability of Flaw Size Calculation based on Magnetic Flux Leakage Inspection of Pipelines”, Proceedings, ECNDT 2006, 9th European Conference on NDT, Berlin, Germany, September 25-29, 2006.

10. R. Schmidt, “Unpiggable Pipelines – What a Challenge For In-Line Inspection!”, 3P Services, Lingen, Germany, 2004; web file http://www.ppsa-online.com/papers/2004-Aberdeen-7-Schmidt.pdf

11. P. Cawley, D. Alleyene, “Practical Long Range Guided Wave Inspection - Managing Complexity”, Review of Quantitative Nondestructive Evaluation, Vol. 22, 2003.

12. Viktorov, I.A., “Rayleigh and Lamb Waves--Physical Theory and Applications” (Plenum Press, New York, 1967).

13. J. L. Rose, "Ultrasonic Waves in Solid Media," (Cambridge University Press, 1999).

14. Myoung-Seon Choi, Sang-Young Kim and Hegeon Kwun, “An Equivalent Circuit Model of Magnetostrictive Transducers for Guided Wave Applications”, Journal of the Korean Physical Society, Vol. 47, No. 3, September 2005, pp. 454-462.

15. J. D. Achenbach, *Wave propagation in elastic solids*, North-Holland/ American Elsevier, The Netherlands, 1975.

16. A. E. Armenàkas, D. C. Gazis, G. Herrmann, “Free vibrations of circular cylindrical shells”, Pergamon press, Oxford, 1969

17. MsS training manual for long range guided wave pipe inspection, South-West Research Institute, San Antonio, Texas – February 2005

18. F. Bertoncini, A. Musolino, M. Raugi, F. Turcu, “Long range guided waves characterization of defects by two port equivalent”, WEAS Transactions on circuits and systems, Issue 10, Vol. 4, October 2005, pp. 1316-1322.

19. Alltran-Non destructive Testing Research, Consultancy & Equipement Manufacture, “Information Sheet: Compact Low Frequency Ultrasonic

Transducers", D. N. Alleyne, 565 Rayners Lane, Piner, Middlesex, HA5 5HP.

20. P. Mudge and P. Catton, "Monitoring of Engineering Assets using Ultrasonic Guided Waves", TWI, Cambridge, UK, *ECNDT 2006, 9th European Conference on NDT, Berlin, Germany, September 25-29, 2006.*

21. S. Lebsack , "Guided-wave Ultrasonic Inspection & Verification Studies of Buried Pipelines" , Proceedings, 16th WCNDT 2004 - World Conference on NDT Aug 30 - Sep 3, 2004 - Montreal, Canada

22. J. Heerings, N. Trimborn, A. den Herder, "Inspection Effectiveness and its Effect on the Integrity of Pipework", ECNDT 2006, 9th European Conference on NDT, Berlin, Germany, September 25-29, 2006.

23. Clark, A. E. Ferromagnetic Materials, vol 1, ed Wolfhart, E.P. (Amsterdam: North-Holland).

24. Brown, W. F., Magnetic Materials, Ch 8 in the Handbook of Chemistry and Physics, Condon and Odishaw, eds., McGraw-Hill, 1958.

25. Operating and technical instructions for magnetostrictive sensor (MSS) instrumentation system, model MsSR2020, MsSR2020D, prepared by Sensor Systems and NDE Technology Department, Applied Physics Division, South West Research Institute, San Antonio, Texas – December 2004.

26. User's manual for MsS data analysis and reporting software for piping inspection TM, prepared by Sensor Systems and NDE Technology Department, Applied Physics Division, South West Research Institute, San Antonio, Texas – December 2004.

27. Seung Hyun Cho, Chan Il Park, Yoon Young Kim, "Effects of the orientation of magnetostrictive nickel strip on torsional wave transduction efficiency of cylindrical waveguides", APPLIED PHYSICS LETTERS 86, 2005.

28. Jason A. Paulsen, Andrew P. Ring, Chester, C. H. Lo, John E. Snyder, and David C. Jiles, "New Magnetostrictive Materials for Use as a Magnetic

Stress Sensor for Nondestructive Evaluation", Review of Progress in Quantitative NDE Green Bay, Wisconsin July 27 – August 1, 2003.

29. F. Bertoncini, M. Raugi, "Analysis of Torsional Guided Waves for Inspection of Pipes", WSEAS Transactions on systems, no. 11, vol. 4, pp. 2001-2009, 2005.

30. J. Li and J. L. Rose, "Angular-Profile Tuning of Guided Waves in Hollow Cylinders Using a Circumferential Phased Array", IEEE Transactions on ultrasonics, ferroelectrics and frequency control", vol. 49, no. 12, pp. 1720-1729, December 2002.

31. B. Cannas, F. Cau, A. Fanni, A. Montisci, P. Testoni, M. Usai, "Neural NDT by means of Reflected Longitudinal and Torsional Wave Modes in Long and Inaccessible Pipes", Proceedings, WSEAS, Malta, 2005.

32. M. Raugi, F. O. Turcu, F. Bertoncini, G. Fornarelli, G. Brunetti, "Classification of Defects on Pipes by Ultrasonic Guided Waves Using a Neural Network Approach", IEEE International Ultrasonics Symposium, pp 382-387,2007.

33. P.S. Addison, "The illustrated wavelet transform handbook", IOP Publishing, 2002.

34. Stéphane Mallat, "A wavelet tour of signal processing", Academic Press, 1999.

35. A. Demma, P. Cawley, M. Lowe, A.G. Roosenbrand, "The reflection of Fundamental torsional mode from cracks and notches in pipes", The Journal of The Acoustical Society of America, no. 114 (2), pp. 611-625, August 2003.